Immune modulation by intravenous immune globulin: cross-talk between Fc gamma receptors and regulatory T cells in allergic inflammation

Gabriel Nathan Kaufman
Division of Experimental Medicine
McGill University, Montreal

December 2016

A thesis submitted to McGill University in partial fulfillment of the requirements of the degree of Doctor of Philosophy.

Abstract

Intravenous immune globulin (IVIg), a preparation of pooled human antibodies, has potent immunomodulatory properties as a treatment for inflammatory pathologies. The specific mechanisms of action are not completely understood, especially in the context of allergen-driven disease. We sought to characterize several facets of IVIg regulatory biology using an established murine model of allergic airways disease. We first examined the requirement for activating and inhibitory Fc gamma receptors for the anti-inflammatory actions of IVIg, concluding that the inhibitory Fc gamma receptor IIb expression on dendritic cells is necessary and sufficient for IVIg to tolerize the immune system.

Turning to the efferent end of the regulatory response, we studied the regulatory T cell compartment by selective depletion using cell-specific transgenic deletion mice. We demonstrated the absolute requirement for regulatory T cells in the IVIg-mediated anti-inflammatory response, and that IVIg generates a specific pool of regulatory T cells *de novo* from non-regulatory T cell precursors. We also characterized the gene expression profile of these IVIg-generated peripheral regulatory T cells, determining that they have a unique gene expression signature.

In related work, we investigated the gene expression of activated B cells in a simulated regulatory context *in vitro*, profiling the transcriptome and reporting a novel marker for memory B cells that appears to play a role in B cell regulatory function.

We complete this thesis with pertinent literature-review manuscripts and a supplemental review chapter on the roles of dendritic cells as activators of T cells.

Abrégé

L'immunoglobuline intraveineuse (IgIV), une préparation d'anticorps humains, possède des propriétés immunomodulatrices qui sont utilisées comme traitement pour les pathologies inflammatoires. Les mécanismes spécifiques de son action ne sont pas entièrement connus, spécialement dans le contexte des pathologies contrôlées par des antigènes. Nous avons caractérisé plusieurs aspects de la biologie régulatrice d'IgIV en utilisant un modèle murin établi de pathologie des voies aériennes. Nous avons premièrement examiné les conditions d'activation des récepteurs Fc gamma activateurs et inhibiteurs des actions anti-inflammatoires d'IgIV, en concluant que l'expression du récepteur inhibiteur Fc gamma IIb est nécessaire et suffisante pour que l'IgIV rende le système immunitaire tolérant.

Se concentrant sur le côté efférent de la réponse régulatrice, nous avons étudié le compartiment des cellules T régulatrices par déplétion ciblée, en utilisant des souris transgéniques de suppression cellulaire. Nous avons démontré le besoin absolu de la présence de cellules T régulatrices dans la réponse anti-inflammatoire médiée par l'IgIV, et que l'IgIV génère une population spécifique de cellules T régulatrices *de novo* à partir de cellules précurseures non-régulatrices. Nous avons aussi caractérisé le profil d'expression génique de ces cellules T régulatrices périphériques générées par l'IgIV, démontrant qu'elles ont une signature distincte d'expression génique.

Dans un travail connexe, nous avons étudié l'expression génique des cellules B activées dans un contexte régulateur *in vitro*, décrivant le profil du transcriptome. Nous décrivons un nouveau marqueur pour les cellules B mémoire qui parait jouer un rôle dans les fonctions régulatrices des cellules B.

Nous complétons cette thèse avec des manuscrits de revue de littérature pertinente et un chapitre de revue sur les rôles des cellules dendritiques comme activateurs des cellules T.

Preface and Contributions

The present work represents a series of explorations into the regulatory biology of the immune system. The author had started his PhD with an attempt to examine the effects of intravenous immune globulin (IVIg) on dendritic cell (DC) tolerogenic phenotype, but – like much scientific endeavour – found his research moving in other stimulating directions, allied to his original interests yet slightly different in focus. This thesis, written in partial fulfillment of the degree requirements for the PhD degree in McGill University's Division of Experimental Medicine, presents four scientific papers and an additional chapter representing an expansion on collaborative work towards a fourth publication. These contributions and the connections between them are detailed herein.

Growing out of a more than 30-year interest of our principal investigator Bruce D Mazer MD, dating back to his postgraduate fellowship in the 1990s (1), into the anti-inflammatory effects of IVIg, this author was involved – during undergraduate research internships in the years 2003, 2004, and 2007 – in the initial murine characterization of the anti-inflammatory actions of IVIg in a murine model of allergic airways disease (AAD). That work was finally published in 2011, with the present author credited with first authorship (2). Crucial finding of that work included that IVIg abrogated inflammatory responses to allergen challenge, modulated the phenotype of $CD11c^+$ DC, and induced $Foxp3^+$ Treg in local and systemic lymphoid tissues.

The author's former laboratory colleague Amir H Massoud PhD, who moved the IVIg work forward over the course of his extremely productive doctorate, demonstrated that DC were the primary target cell of IVIg in the murine AAD model, and that these DC were sufficient to induce Treg (3). We therefore wrote a review article examining the relationships between IVIg and the Treg compartment in the context of regulating immune-system responses to inflammation (4). That article, which constitutes the main portion of the literature review of this thesis, is presented here *in toto* in chapter 1.

The present author also provides a supplementary introduction chapter (chapter 2) as part of the literature review, which describes some of the more general lines of DC biology as it pertains to T cell activation. This topic was felt by the author to be crucial to the understanding of his thesis as a whole, but was not covered in sufficient detail in the manuscripts.

The second manuscript (chapter 3), which presents the author's investigation of a related facet of DC biology, was initially a side project designed to exclude a possibility in response to potential reviewer questions. Dr Massoud had demonstrated that IVIg ligates dendritic cell immunoreceptor (DCIR), a C-type lectin receptor on dendritic cells (5). We therefore wanted to exclude the effects of the canonical IgG receptor family, the Fc gamma receptors, by using knockout mouse strains. To our surprise, we found that while the activating Fc gamma receptors were dispensable for the anti-inflammatory actions of IVIg, the inhibitory Fc gamma receptor IIB (FcγRIIB) was required for the IVIg-mediated abrogation of AAD and the induction of Treg. Furthermore, we determined that this receptor's expression was specifically required on DC for Treg induction; DC deficient in FcγRIIB have deficient antigen uptake inhibition in response to IVIg treatment.

Our laboratory's work thus far had demonstrated that IVIg treatment of antigen-exposed mice was associated with a significant increase in Treg. We then proceeded to explore the absolute requirement of Treg for IVIg-mediated abrogation of AAD using a cell-specific Treg depletion model system, the DEREG mouse. We determined that IVIg generates peripherally-induced Foxp3^{+} Treg (pTreg) *de novo* from non-Treg precursors, and that these Treg are both necessary and sufficient for the inhibition of allergen-induced AAD. We further characterised the transcriptome of these IVIg-generated pTreg by gene expression microarray. This report is the third article included in this thesis (chapter 4), presently (December 2016) in revision for resubmission to *The Journal of Immunology*.

Concurrent with the work described above, our laboratory has had a long-standing interest in the regulatory potential of Th2-stimulated B cells. Given this author's experience with microarray

data analysis and interest in exploring an aspect of regulatory biology distinct from the DC:T cell axis, he became involved in the analysis of incompletely analyzed (circa 2005!) microarray data acquired under the rubric of a study designed to understand B cell activation and regulation in the inflammatory microenvironment. The main body of that work, reporting a novel marker for memory B cells that appears to play a role in B cell regulatory function, is published in *Frontiers in Immunology* (6); the present author is credited with third authorship on that paper. The third manuscript (chapter 5) presented in this thesis is an expanded investigation and discussion of commonly employed bioinformatics tools for gene expression analyses, which were used to provide a deeper understanding of the transcriptome of activated B cells in a regulatory context.

The reader will undoubtedly note that a methodology common to much of the author's work is the flexiVent small-animal respiratory physiology measurement system, which consists of a computer-controlled piston ventilator which executes forced oscillation measurements and transforms the acquired signal into respiratory physiology parameters (7). Presented as an excursus to the thesis, the present author wrote a brief introduction to the classic mathematical models of lung function, some of which are used by the flexiVent software to calculate and report respiratory physiology data. Since these mathematical models formed the basis for most of the studies that the present author undertook during the course of his doctorate, he wished to examine the basic principles behind his data. The author feels that an in-depth understanding of the background behind any data acquisition technique is of value to any scientist; he notes that such understanding has served him well in troubleshooting difficult protocols throughout his academic career.

The review articles presented in chapter 1 and in the excursus of this thesis, and the research results presented in chapters 3, 4, and 5 of this thesis are original scholarship and represent distinct contributions to knowledge. The present author's specific contributions are as follows:

Chapter 1: Revising first draft of review, significantly expanding content by surveying and reporting additional literature, writing the final version for submission, revising in response to reviewers, submitting final version for publication.

Chapter 2: Literature review written for thesis.

Chapter 3: Study design, method optimization, data generation for Figures 3 through 6, preparation of the flow-cytometry Supplement, writing the manuscript.

Chapter 4: Design of the microarray experiment, microarray data analysis, data generation for Figure 1D-E, Figure 8, Table I, and the Supplement; extensive revision of first draft of the manuscript, writing the final version for submission.

Chapter 5: Data generation for Figures 1 through 4, Table 1, Appendix II; microarray data analysis scripts in Appendix I, writing the manuscript.

Excursus: Original literature review.

The contributions of the present author's colleagues are as follows:

Chapter 1: Drawing of Figure 1, Amir H Massoud.

Chapter 3: Data generation for Figure 7, writing associated methods and results text, Marieme Dembele. Flow cytometric sample preparation and acquisition for Figure 4C, Marianne Béland.

Chapter 4: Study design, data generation for Figures 1 through 7, first draft of manuscript, Amir H Massoud. Microarray sample preparation and array scanning, McGill University and Génome Québec Innovation Centre gene expression analysis services platform.

Chapter 5: B cell culture and RNA isolation, Salem Al-Tememi. Microarray sample preparation and array scanning, McGill University and Génome Québec Innovation Centre gene expression analysis services platform.

References

1. Mazer BD, Gelfand EW. An open-label study of high-dose intravenous immunoglobulin in severe childhood asthma. *J Allergy Clin Immunol* (1991) **87**(5):976-83. PubMed PMID: 2026848.

2. Kaufman GN, Massoud AH, Audusseau S, Banville-Langelier AA, Wang Y, Guay J, et al. Intravenous immunoglobulin attenuates airway hyperresponsiveness in a murine model of

allergic asthma. *Clin Exp Allergy* (2011) **41**(5):718-28. doi: 10.1111/j.1365-2222.2010.03663.x. PubMed PMID: 21255135.

3. Massoud AH, Guay J, Shalaby KH, Bjur E, Ablona A, Chan D, et al. Intravenous immunoglobulin attenuates airway inflammation through induction of forkhead box protein 3-positive regulatory T cells. *J Allergy Clin Immunol* (2012) **129**(6):1656-65 e3. doi: 10.1016/j.jaci.2012.02.050. PubMed PMID: 22564681.

4. Kaufman GN, Massoud AH, Dembele M, Yona M, Piccirillo CA, Mazer BD. Induction of Regulatory T Cells by Intravenous Immunoglobulin: A Bridge between Adaptive and Innate Immunity. *Front Immunol* (2015) **6**:469. doi: 10.3389/fimmu.2015.00469. PubMed PMID: 26441974; PubMed Central PMCID: PMCPMC4566032.

5. Massoud AH, Yona M, Xue D, Chouiali F, Alturaihi H, Ablona A, et al. Dendritic cell immunoreceptor: a novel receptor for intravenous immunoglobulin mediates induction of regulatory T cells. *J Allergy Clin Immunol* (2014) **133**(3):853-63 e5. doi: 10.1016/j.jaci.2013.09.029. PubMed PMID: 24210883.

6. Xue D, Desjardins M, Kaufman GN, Béland M, Al-Tememi S, Ahmed E, et al. Semaphorin 4C: A Novel Component of B-Cell Polarization in Th2 Driven Immune Responses. *Frontiers in Immunology* (2016) **7**:558. doi: 10.3389/fimmu.2016.00558.

7. McGovern TK, Robichaud A, Fereydoonzad L, Schuessler TF, Martin JG. Evaluation of respiratory system mechanics in mice using the forced oscillation technique. *J Vis Exp* (2013) (75):e50172. doi: 10.3791/50172. PubMed PMID: 23711876; PubMed Central PMCID: PMCPMC3684007.

Acknowledgements

"Lift up your eyes on high, and behold Who has created these things"
-Isaiah 40:26

The author counts himself blessed at being given the privilege to explore the wonders of God's Creation as a career. Concurrently, he wishes to go on record in text (if not in print!) to thank all those who have helped him along the way to the successful completion of his doctorate.

Potḥim bi-ḵhevod ha-aḵhsania – we open with the honour of the house (cf. Babylonian Talmud Beraḵhot 63b). The author wishes to thank Bruce D Mazer MD for being an excellent lab director, study manager, mentor, scientific editor, kosher travel consultant, and student. The author notes that Dr Mazer offered him a PhD position even after having hosting him throughout his Bachelor's degree, and remains grateful for the *aḵhsania* (lit., "inn", Rashi to *op. cit.*) accorded to him at the Meakins-Christie Laboratories/Translational Research in Respiratory Diseases Program (TRR) to pursue his doctoral degree in optimal circumstances.

Marianne Béland MSc, research assistant extraordinaire, late of the Meakins-Christie Laboratories/Translational Research in Respiratory Diseases Program, was of invaluable help to the author, whether it be processing samples from all-night dissection sessions, discussing the finer points of flow cytometry, providing an often-needed house of sober second thought to discuss study plans, or indulging the author's shopping fetish as it extends to fine laboratory equipment and reagents. The author estimates that he is not alone in the realization that without Ms Béland's excellent assistance his PhD would not have come to fruition or to completion.

"No man is an Iland" (*Devotions upon Emergent Occasions*, John Donne, 1624). The author wishes to thank his past and present fellow lab-members for their collaboration, support, and uplifting *esprit de corps*, as well as for putting up with an often-grumpy and always-tired colleague. Modern science exists as a collaborative effort, and this spirit runs deep in the group of fellow-

travelers who have worked alongside, aided, and sometimes abetted (!) the author throughout his doctoral studies.

Aḥaronim aḥaronim ḥavivim – the last-mentioned are the dearest (cf. Bereishit Rabbah 78:8). The author wishes to thank his long-patient wife Carolyn Gehr for moral, emotional, physical, and pecuniary support, as well as her capable management of a busy household while working full-time; and his children Nahum Shmuel, Yosef Akiva, and Yishai Amram (Kaufman), for putting up with a largely absentee father for the past five years. It is the sincere hope of this author that the submission of this thesis will hasten the end of a 13-year odyssey towards the highest academic degree one can obtain, and will perhaps open a vista to an existence where he does not have to work *every* Sunday and vacation away from family and home!

The author acknowledges the financial support of graduate studentships from Canadian Blood Services (Feb 2011 – Dec 2011), Canadian Institutes of Health Research (Jan 2013 – Dec 2015), and Fonds de Recherche du Québec – Santé (awarded Feb 2012 but declined), as well as an entrance scholarship and travel support stipends from the McGill University Division of Experimental Medicine.

Chapter 1:

Induction of regulatory T cells by intravenous immunoglobulin: a bridge between adaptive and innate immunity

Gabriel N Kaufman[1], Amir H Massoud[1,2†], Marieme Dembele[1], Madelaine Yona[1], Ciriaco A Piccirillo[3] and Bruce D Mazer[1,4]*

[1] Translational Research in Respiratory Diseases (TRR) Program, The Research Institute of the McGill University Health Centre, Montreal, QC, Canada

[2] Laboratory of Cellular and Molecular Immunology, University of Montreal Hospital Research Centre, Montreal, QC, Canada

[3] Infectious Diseases and Immunity in Global Health (IGIDH) Program, The Research Institute of the McGill University Health Centre, Montreal, QC, Canada

[4] Department of Pediatrics, Faculty of Medicine, McGill University, Montreal, QC, Canada

[†] Present address: Division of Immunology Research, Boston Children's Hospital, Boston, MA, USA

*** Correspondence:** Dr Bruce D Mazer, Translational Research in Respiratory Diseases Program, The Research Institute of the McGill University Health Centre, Centre for Translational Biology (CTB) Room EM3.2219, 1001 Decarie Blvd. Montreal QC H4A 3J1, Canada. bruce.mazer@mcgill.ca

This chapter examines the relationships between IVIg and the Treg compartment in the context of regulating immune-system responses to inflammation. Previous work from our laboratory had demonstrated that IVIg treatment of antigen-exposed animals induced regulatory T cells in target organs (lung), along with local (thoracic lymph nodes) and systemic (spleen) lymphoid organs. We therefore chose to examine the published literature regarding Treg induction in response to IVIg treatment.

The specific contributions of the present author to this paper were: revision of the first draft of the review written by Amir H Massoud, significantly expanding the review's content by surveying and reporting additional literature, writing the final version for submission, revising in response to reviewers, and submitting final version for publication. Amir H Massoud drew Figure 1.

Abstract

IVIg is a polyclonal IgG preparation with potent immunomodulatory properties. The mode of action of IVIg has been investigated in multiple disease states, with various mechanisms described to account for its benefits. Recent data indicates that IVIg increases both the number and suppressive capacity of regulatory T cells, a subpopulation of T cells that are essential for immune homeostasis. IVIg alters dendritic cell function, cytokine and chemokine networks, and T lymphocytes, leading to development of regulatory T cells. The ability of IVIg to influence Treg induction has been shown both in animal models and in human diseases. In this review, we discuss data on the potential mechanisms contributing to the interaction between IVIg and the regulatory T cell compartment.

1. Introduction

1.1. Intravenous immunoglobulin

Intravenous immunoglobulin (IVIg) is prepared from polyclonal immunoglobulin G (IgG) purified from pooled plasma samples of several thousand healthy donors. IgG has been the standard treatment for primary immunodeficiency diseases since Bruton's identification of a patient with agammaglobulinemia in the early 1950's (1). However, Imbach, in the early 1980s, demonstrated that administration of high doses of human polyclonal IgG in children with immune deficiency who concomitantly suffered from immune thrombocytopenic purpura (ITP) had a dramatic increase in platelet counts (2). Since then, there has been a progressive increase in the use of IVIg in patients with a wide variety of autoimmune and inflammatory disorders. IVIg is used as a primary treatment for ITP, Kawasaki Syndrome (KS), Guillain-Barré Syndrome, myasthenia gravis, chronic inflammatory demyelinating polyneuropathy, systemic lupus erythematosus, and other autoimmune and neurologic disorders (3). IVIg is commonly used in the prevention or treatment of neonatal sepsis. Rationally, those infants who are premature or suffer from very low birth-weights should benefit from the immune supplementation provided by IVIg. However, large randomized clinical trials have failed to show consistent benefit in terms of prevention or

outcomes from septic episodes (4-6). Novel preparations enriched in IgM may have some promise but to date results are inconsistent (7, 8).

IVIg is now the most commonly prescribed plasma-based product worldwide (3, 9). This increased use raises questions regarding the long-term viability of this therapy. Considering the high cost and limited availability of this resource, it is imperative to investigate the underlying mechanisms of IVIg in order to tailor the anti-inflammatory response obtained by treatment, allowing for better therapies for inflammatory and autoimmune diseases. Furthermore, this can lead to the development of non-plasma-derived drugs with similar therapeutic benefits.

Many mechanisms explaining the immune-regulatory actions of IVIg have been postulated, including modulation of inhibitory Fc-gamma receptor (FcγR) expression, blockade of activating FcγR on antigen-presenting cells (APC), interference with cytokine production, inhibition of cell activation or induction of apoptosis in variety of immune cells, including dendritic cells (DC), macrophages, natural killer cells, and T and B lymphocytes (3, 9, 10). However, a key factor in immune modulation is the ability to counter inflammatory responses with regulatory cells. In this review we will explore the links between IVIg and regulatory T cell responses.

1.2. Regulatory T cells

Regulatory T cells (Treg) were initially described in the 1990s as a specialized subpopulation of T cells that maintain immune system homeostasis and tolerance to self-antigens (11, 12). The transcription factor forkhead box P3 (FOXP3) is considered the marker of choice for this cell (13). FOXP3 is a master-switch transcription factor: its expression modifies T cells towards a regulatory phenotype, enabling many of the anti-inflammatory functions of Treg (14). The fundamental property that defines Treg is their ability to transfer immune suppression *in vivo* from one animal to another, or *in vitro* from one cell culture to another (15). Based on their developmental or functional differences, Treg are categorized into two main populations: naturally-occurring Treg that are generated in the thymus (tTreg), and peripherally induced Treg (pTreg) generated in

peripheral lymphoid tissues from non-Treg precursor $CD4^+$ cells. While Treg are $CD4^+$ T effector cells with characteristic FOXP3 expression, this is not sufficient to define a cell population as Treg: single-cell flow cytometric sorting experiments have shown the importance of elevated expression of the high-affinity IL-2 receptor, CD25, as a hallmark of Treg (16). Other markers, including HLA-DR, GARP, and low CD127 expression, along with CTLA-4 and Helios, are not entirely consistent or reliable, and depend on the activation state of the cell (17). Recent work by Bin Dhuban et al. (18) has identified two cell-surface Treg markers: TIGIT, a novel CD28-related protein; and FCRL3, an Fc-receptor-like glycoprotein, which allow for high-consistency detection of Treg in human peripheral blood mononuclear cells (PBMC).

Pre-clinical studies have shown that freshly isolated or *ex vivo*-expanded Treg can confer immunological tolerance in subjects with autoimmune and inflammatory disorders (19, 20). However, human Treg infusion therapy has been difficult to implement, and relatively few clinical trials have been initiated (21). Therefore, developing new therapeutic approaches with the capability to modulate the immune system through activation and/or expansion of Treg has been the subject of many recent studies. Several therapeutic immunosuppressive compounds, including rapamycin (22) and glucocorticoids (23), have been identified as promoting the expansion or suppressive activity of Treg.

IVIg has been proposed as a treatment that can promote development or activation of Treg in autoimmune diseases (24). Herein, we provide an overview examining if IVIg indeed influences induction of Treg in the context of different inflammatory and autoimmune conditions, and discuss mechanisms underlying Treg induction by IVIg.

2. Evidence for the action of IVIg in the promotion of Treg in human clinical trials

An early clue suggesting regulatory effects of IVIg was the observation that T cells, purified from IVIg-treated individuals, had significant suppressive effects when cultured with proliferating T and B cells (25). Subsequent studies demonstrated that IVIg therapy was associated with enhanced mitogen-induced “suppressor T cell function” in rheumatoid arthritis (26), ITP (27), and

pediatric acquired immune deficiency syndrome (28). More recently, Kessel et al. (29) demonstrated *in vitro* culture of IVIg with peripheral T cells led to increases in intracellular TGF-β, IL-10, and FOXP3 expression, as well as improvement in their suppressive functions when co-cultured with effector T cells.

T cells from patients treated with IVIg have been examined for increases in Treg. In Guillain-Barré Syndrome, IVIg therapy increases expression of *FOXP3*, and the production of inhibitory cytokines in Treg (30). In systemic lupus erythematosus, IVIg-treated patients show significant increases in Treg numbers; moreover, IVIg appeared to convert naive $FOXP3^{-}CD25^{-}$ into activated $FOXP3^{+}CD25^{+}$ Treg (31). Consistently, IVIg therapy of EGPA patients increased $FOXP3^{+}$ Treg numbers and production of IL-10 in $CD4^{+}$ T cells (32). In mononeuritis multiplex, a peripheral neuropathy, steroid unresponsive patients treated with IVIg exhibit enhanced populations of Treg (33).

2.1. Mechanisms of action of IVIg in Kawasaki syndrome

Kawasaki syndrome (KS) is an acute systemic vascular inflammation, primarily affecting children. A single IVIg treatment is generally successful in reducing fever and associated disease manifestations (34). Extensive work has focused on characterizing the IVIg-induced Treg response in KS. Burns et al. (35) investigated the link between TNF-α and IVIg therapy in KS, hypothesizing that TNF-α inhibition may decrease cell activation. They determined that infliximab treatment does not interfere with Treg induction by IVIg, finding that the expansion of CD14+ CD86+ tolerogenic DC correlated with increased Treg after IVIg treatment. They postulate that the IVIg-induced Treg pool secretes IL-10 and responds to the Ig heavy-chain Fc region.

In a subsequent study from the same group, Franco et al. (36) investigated the specificity of IVIg-induced Treg in subacute KS patients. IVIg treatment induced a subset of Treg that expressed high levels of CTLA-4, and secreted IL-10, but not TGF-β. This Treg expansion appeared to be key to controlling vascular inflammation in KS. Cloned Treg expanded *ex vivo* only responded to soluble IgG Fc and not to $F(ab)'^{2}$ fragments, indicating that these Treg were Fc-specific, and that the mechanism was likely T cell receptor (TCR)-dependent. Co-culture

experiments revealed that the Fc region of IgG was presented in a major histocompatibility complex (MHC)-restricted, TCR-mediated manner by EBV-transformed B cells. Further investigation of the Fc peptide specificities of the tTreg population revealed similar profiles in both IVIg-treated KS patients and in healthy controls, suggesting that Treg responses are functionally inadequate in KS, and that this can be reversed by IVIg (37).

In KS patients, IVIg treatment enhances the expression of genes related to Treg activation, including *FOXP3*, *CTLA4*, *GITR* and *TGFB1*. The expression levels of these genes were significantly lower in KS patients prior to treatment than in healthy controls (38, 39). Ni et al. (40) examined the mechanisms of Treg dysfunction in KS, focusing on microRNAs (miR). While acute KS patients had lower Treg numbers and decreased Treg marker expression, IVIg treatment increased Treg numbers and *FOXP3*, *CTLA4*, and *GITR* gene expression. Treg from untreated KS have down-regulated miR-155 and miR-21 microRNAs; miR155 down-regulation leads to increased SOCS1 signaling, decreased STAT-5 signaling, and miR-31 microRNA overexpression. IVIg treatment reversed these effects, restoring the SOCS1/STAT5 balance and decreasing miR-31 expression. FOXP3-dependent miR-155 inhibited SOCS1, and STAT3 suppressed miR21, which down-regulated FOXP3. IVIg treatment of KS patients lowered elevated IL-6 and pSTAT3, restoring miR-21 levels, providing an explanation for the increase in Treg numbers following IVIg infusion.

3. Modulatory effects of IVIg in animal models of inflammatory disorders via Treg expansion and induction

3.1. Role of IVIg in experimental autoimmune encephalomyelitis

In experimental autoimmune encephalomyelitis (EAE), an antigen-driven murine model of multiple sclerosis, IVIg treatment reduced the disease severity scores, promoted the expansion of Treg and and enhanced their suppressive capacity, both *in vivo* and *in vitro* (39). Importantly, administration of IVIg failed to confer protection in EAE mice that were depleted of Treg prior to treatment, suggesting a critical role of endogenous Treg in conferring protection by IVIg. In line with these findings, Okuda et al. (41) replicated the effects of IVIg in EAE, and showed that sulfonated IVIg was effective in increasing the frequency of Treg.

A potential target for IVIg in EAE are natural killer (NK) cells. NK cells have a wide variety of immunomodulatory functions, interacting with B cells, DC, and Treg (42, 43). Chong et al. (44) hypothesized that in IVIg-treated subjects, NK cells suppress disease by regulating inflammatory T cell responses. Using an EAE model, they demonstrated that IVIg treatment blocks EAE development and reducing demyelination by diminishing IL-17 and IFN-γ. NK cell depletion by anti-asialo GM1 antibody resulted in the loss of IVIg-mediated protection, and adoptive transfer of IVIg-treated NK cells was as equally protective as IVIg treatment. IVIg-treated NK cells induced $CD4^+$ $Foxp3^+$ Treg in spleen and draining lymph nodes, which were suppressive to antigen-specific effector T cells in *ex vivo* proliferation assays. Upon further investigation using an *in vitro* co-culture system, Treg induction was determined to depend on IL-2 and TGF-β1 production by NK cells. Chong et al. posit that IVIg may promote redistribution of NK cells in peripheral tissues, depending on the inflammatory stimulus. Since NK cells modulate their chemokine receptor expression to facilitate migration to local and peripheral sites of inflammation (45), IVIg may increase NK cell homing to inflammatory microenvironments and secondary lymphoid organs, where they can induce Treg. NK cell costimulatory molecule expression may also drive Treg induction: IL-2 and plate-bound anti-CD16 treatment upregulate CD86 and OX40-ligand on NK cells *in vitro* (46). CD86 has been implicated in Treg generation (47) and OX40-ligand can deliver a survival signal to Treg (48).

3.2. Treg induction in allergen-driven and autoimmune models

We have recently demonstrated, using an ovalbumin-driven murine model of allergic airway disease, that therapeutic administration of IVIg attenuated airway hyper-reactivity (AHR) and alleviated airway inflammation. This was accompanied by induction of highly suppressive, antigen-specific Treg derived from pre-existing T-effector cells. Treg induction was dependent on the interaction of IVIg with $CD11c^+$ DC (49). Similarly, in a murine model of ITP, IVIg increased thymic and splenic Treg, accompanied by restoration of platelet counts (50).

Different dosing regimens have been employed for IVIg to increase Treg (51). Our laboratory, as well as most other groups, uses high-dose IVIg (2 g/kg), which is analogous to the immunomodulatory dose used in clinical practice (49). Other studies have employed typical

antibody-replacement doses of 400-800 mg/kg (52). Ramakrishna et al. (53) reported an anti-inflammatory effect using extremely low-dose IVIg (187.5 mg/kg) in a HSV-mediated encephalitis murine model, which was felt to be dependent on enhancement of Treg. This dose range is rarely used clinically, making this work difficult to apply to standard practice. In addition, work from our laboratory and others (38, 54) suggests that a minor fraction of IVIg is required for some, but not all immunomodulatory effects. This will be discussed in more detail below.

4. Mechanisms of action of IVIg in induction of Treg

The mechanisms by which IVIg induces Treg may involve direct interaction of IgG with T cells, or modulation of other cellular or molecular targets, particularly antigen-presenting cells such as DC and macrophages. IVIg can also interact with other cells, such as B cells or NK cells. In addition, IVIg can modulate the production of pro-inflammatory cytokines, which may play a role in maintaining T cell tolerance.

4.1. The effect of IVIg on dendritic cell activation

Induction of protective T cell responses requires naïve T cells to receive signals via the TCR, costimulatory molecules, and cytokine receptors. These signals, via cell-cell contact and through soluble mediators, are provided by professional APC, such as DC. While DC represent the most efficient APC in capturing, processing, and presenting antigens to T cells (55), DC also play an active role in maintaining immune tolerance, as constitutive DC ablation results in spontaneous fatal autoimmunity (56). Tolerogenic DC are characterized by decreased expression of costimulatory molecules (CD40, CD80, and CD86), decreased antigen presentation (due to reduced MHC class II expression), enhanced expression of co-inhibitory molecules (e.g PD-L1, CTLA-4, and OX-40), and enhanced inhibitory cytokine production (57, 58). This DC subset is essential for maintaining tolerance via extrathymic induction of pTreg, and maintenance of pre-existing tTreg (59-62).

Induction of tolerance is critically dependent on the maturation state of DC. An immature DC phenotype is associated with induction, expansion, or enhancement of the suppressive capacity of Treg (63). Direct cell-to-cell interaction of DC and T cells via TCR (64), induction of

indolamine-2,3-dioxygenase (IDO) (65) as well as secretion of IL-10, TGF-β, and retinoic acid by DC (66) are all implicated in the peripheral induction or expansion of Treg by DC.

Although both myeloid and plasmacytoid DC may be involved in maintaining peripheral tolerance (67), polyclonal human IgG appears to target $CD11c^+$ DC, rather than $CD11c^-$ plasmacytoid DC (49, 68). We have demonstrated that $CD11c^+$ DC from IVIg-treated mice are necessary and sufficient for peripheral induction of Treg in lung and draining thoracic lymph nodes (49). IVIg decreases CD80 and CD86 both *in vitro* and *in vivo*; in addition, adoptively transferred IVIg-treated DC can increase Treg in lungs of antigen-exposed and challenged mice (49, 69).

IVIg-exposed $CD11c^+$ DC are less competent in driving lymphocyte proliferation, potentially due to decreased MHC-II and CD80/CD86 expression (68, 70-72). Work from the group of Bazin suggests that internalized IVIg interferes with antigen presentation by competing with antigen peptides for loading on MHC-II molecules in the intracellular MHC-II compartment (MIIC) (73, 74). Inhibition of T cell responses by reducing antigen presentation may also interfere with the activation of auto-reactive pathogenic T cells. In addition, IVIg alters the pattern of DC cytokine production, including up-regulation of inhibitory cytokines such as IL-10, and down-regulation of pro-inflammatory cytokines such as IL-12 and IFN-γ (53, 71, 75).

Pro-inflammatory cytokines counteract Treg differentiation or decrease Treg suppressive effects. For example, IL-6 secretion from DC is known to abrogate Treg anergy, reverse Treg suppression, and skew Treg differentiation toward Th-17 (76, 77). In contrast, IVIg reduces the production of IL-6 and TNF-α by peripheral blood monocytes (78, 79); it can therefore maintain Treg homeostasis. In is conceivable that IVIg-generated Treg may attenuate DC maturation by anti-inflammatory cytokine production, expanding the inhibitory effects of IVIg by further tolerizing DC in a negative feedback loop.

How IVIg targets DC is still incompletely elucidated, and different mechanisms have been postulated. The effect of polyclonal IgG on DC appears to involve activating FcγR, by triggering immunoreceptor tyrosine-based activation motifs (ITAM) (80). However, both Fc and $F(ab')^2$

fragments of IgG have been shown to suppress DC maturation and modulate DC cytokine production (71). F(ab')2 fragments have been shown to inhibit LPS-induced phosphorylation of extracellular signal-regulated kinase (ERK1/2), an intracellular signaling molecule that mediates the inflammatory response induced by Toll-Like Receptor (TLR) ligation in DC (81).

Although a full discussion of IVIg-FcγR receptor biology is beyond the scope of this review, it is important to note that inhibitory FcγRIIB were required for the anti-inflammatory effects of IVIg in murine models of ITP (72), nephrotoxic nephritis (82), and epidermolysis bullosa acquisita (EBA) (54). Similarly, we have found that FcγRIIB is required for IVIg-mediated abrogation of allergic airways disease (Kaufman GN et al., in preparation). Up-regulation of FcγRIIB expression on DC, and on APC in general, likely plays a role in the suppression of DC activation, although no direct physical interaction between IVIg with this receptor has been reported (83).

De Groot et al. (84) proposed another DC-dependent mechanism by which IVIg promotes Treg expansion. They described promiscuous IgG-derived T cell epitope peptides (Tregitopes) containing epitopes from both Fc and Fab fragment of the IgG molecule, with the capability of activating $Foxp3^+$ Treg. They postulated that these Tregitopes are presented in the context of MHC-II by APC to Treg, and contribute to Treg activation and expansion (85, 86). This is consistent with the results from Franco et al (36) discussed earlier where B cells presented Fc regions of IgG in a MHC-restricted and TCR-mediated manner.

4.2. The anti-inflammatory effects of sialylated IgG and its relationship to Treg development

Human IgG therapy has two consistently used dosing regimens. Patients requiring immune supplementation for immune deficiency typically receive between 400-800 mg/kg monthly. After many years of using lower doses, these were deemed ineffective in cross-over studies. Individuals requiring immune modulation frequently receive infusion of IVIg containing 2-5 times the immune supplementation dose. It has therefore been hypothesized that minor fractions of IVIg provide molecules that provide the anti-inflammatory components needed for immune modulation. This has been demonstrated regarding specific neutralizing antibodies, anti-idiotypic antibodies or anti-apoptosis antibodies.

The Ravetch group developed the concept that the anti-inflammatory properties of IVIg were isolated to an IgG subset characterized by terminal α2,6 sialylation of the Fc glycan. Specifically, the Fc portion of the IgG molecule contained an N-linked glycan moiety covalently bound to a highly conserved glycosylation site at Asn297 (87, 88). In various clinical scenarios, lower serum levels of sialylated IgG were found in individuals with systemic lupus erythematosus or juvenile-onset rheumatoid arthritis, as compared to healthy controls (89-91). This sialylated fraction of IVIg (saIVIg), which makes up roughly 1-2% of the total IgG in pooled therapeutic preparations. In proof of concept studies, saIVIg was therapeutically effective in animal models of rheumatoid arthritis (92), ITP (93) and allergic airways disease (94) at doses 10 times lower than unfractionated IVIg.

The mechanism of action of saIVIg is still under investigation. Kaneko et al. (87) proposed that saIVIg interacts with DC-SIGN (dendritic cell-specific intercellular adhesion molecule-3 grabbing non-integrin) on human DC, or the murine ortholog SIGN-R1 (specific intracellular adhesion molecule-3 grabbing non-integrin homolog-related 1) on murine splenic macrophages. This triggers increased expression of the inhibitory Fc receptor FcγRIIB (88). This may contribute to the induction and expansion of Treg; FcγRIIB-deficient mice are incapable of generating Treg in a model of mucosal antigen tolerance (95). Guilliams et al. review the role of FcγRIIB in IVIg therapy and suggest that IVIg increases FcγRIIB expression in inflamed tissues during the effector phase of the immune response (96).

Using experimental models of multiple sclerosis (EAE) and serum-induced arthritis, Fiebiger et al. (97) recently reported that saIVIg Fc confers protective effects in T cell- and antibody-mediated diseases. They developed a mutated IgG Fc construct (F241A), which had a similar structure to saIVIg Fc, but displayed DC-SIGN binding independent of sialylation. Both saIVIg Fc and F241A IgG Fc alleviated arthritis and EAE by inducing Treg expansion and activation, up-regulating FcγRIIB on effector macrophages, and suppressing Th17 and Th1 responses. The anti-inflammatory responses required expression of DC-SIGN as well as secretion of IL-33 by macrophages.

Washburn et al. described a novel hyper-sialylated IgG derivative, tetra-Fc-sialylated IVIg (s4-IVIg), which was maximally sialylated but lacked advanced glycation end products (AGEs) that are hazardous to human health. s4-IVIg was efficacious in animal models of arthritis, ITP, and EBA (91). These results substantiate data obtained by Schwab et al. (54) who demonstrated requirements for IgG sialylation and FcγRIIB expression in their disease models.

As IVIg is a heterogeneous compound, it is not surprising that non-sialylated IgG is also biologically active. Othy et al. demonstrated effects of IVIg on Th17 and Treg cells independent of Fc sialylation (98). Similarly, there are studies using different murine models of ITP (99, 100) and rheumatoid arthritis (101), which did not require sialylated IgG. Differences in strains or induction of pathological conditions in various murine models are reasons for the discrepancies in the dependence on sialylation. To obtain more definitive results, it will be critical to evaluate the role of minor IgG fractions in subjects with inflammatory and autoimmune diseases.

4.3. IVIg binds C-type lectin receptors on dendritic cells

DC-SIGN and SIGN-R1 are C-type lectin receptors, which bind mannosylated and fucosylated structures, such as HIV envelope protein gp120 (102). While ligation of DC-SIGN by mannose-expressing pathogens stimulates pro-inflammatory cytokine secretion by DC, fucose-expressing pathogens or synthetic fucose-containing ligands inhibit LPS-induced production of IL-6 and IL-12, and stimulate the secretion of anti-inflammatory IL-10 by DC (103). Hence, ligation of these innate receptors by saIVIg may regulate cytokine production by DC, and therefore contribute to Treg homeostasis. Smits et al. (104) showed that binding of *Lactobacillus Reuteri* and *Lactobacillus Casei* bacteria to DC-SIGN on monocyte-derived DC drove the development of Treg. These Treg produced increased levels of IL-10 and were capable of inhibiting the proliferation of bystander T cells in an IL-10-dependent fashion.

Work from the group of Ravetch and other investigators suggests that the conformational changes in IgG molecules induced by sialylation lead to a reduction in binding affinity of IgG to FcγR by masking the FcγR binding site (105). Furthermore, sialylation exposes a binding site on IgG for carbohydrate-binding C-type lectin receptors such as DC-SIGN or SIGN-R1 (89, 97, 106).

In contrast, the group of Crispin were unable to reproduce these findings, claiming that sialylation of IgG does not result in conformational changes to the IgG molecule, nor to increases in binding affinity of IgG to DC-SIGN (107, 108). They suggest that cross-linking of sialic-acid-binding Siglecs (sialic acid binding Ig-like lectins), such as CD22, and direct binding of Fc receptors, induces inhibitory signaling through immunoreceptor tyrosine-based inhibition motif (ITIM) pathways. We have recently described that IVIg efficiently modifies dendritic cells to induce regulatory T cells in the absence of activating FcγR (94). It is worth noting that the sialylation of IgG is not restricted to the Fc fragment, and a high proportion of sialic acid residues on the $F(ab')^2$ fragments of IgG has been identified recently by Kasemann et al. (109).

In addition to DC-SIGN, other C-type lectin receptors may interact with IVIg and contribute to induction and/or expansion of Treg. We have recently reported (94) that saIVIg specifically interacts with the C-type lectin dendritic cell immunoreceptor (DCIR) on $CD11c^+$ DC. This appears to lead to internalization of IgG into DC and is associated with inhibitory signaling in ligated DC that consequently results in the peripheral induction of $Foxp3^+$ Treg. The contribution of $DCIR^+$ DC in the induction and expansion of Treg has been demonstrated in previous studies, although not in the context of IVIg therapy. Yamazaki et al. (110) showed that two subsets of $CD8^+CD205^+$ and $CD8^-DCIR^+$ DC differentiate peripheral $Foxp3^+$ Treg, in part through the endogenous production of TGF-β. These data indicate that multiple C-lectin receptors are implicated in the generation of tolerogenic DC by IVIg.

4.4. Interaction of IVIg with Treg

Direct interaction of polyclonal IgG with Treg may represent another mechanism by which IVIg can induce tolerance. Kessel et al. (29) demonstrated that IVIg increases expression of intracellular FOXP3, TGF-β, and IL-10 when added to culture with human $CD4^+$ T cells. IgG was shown to bind to both human and mouse Treg (39, 111) which increased FOXP3 expression, accompanied by augmented *ex vivo* suppressive function. IVIg stimulated phosphorylation of ZAP-70 in Treg (111), which is known to enhance suppressive activity (112).

Additionally, interaction of IgG with effector T cells can affect the balance of cytokine production, mainly by down-regulating pro-inflammatory cytokines such as IL-2, IFN-γ and TNF-α, and increasing inhibitory cytokines (113, 114). Early work (115) on cytokine networks elucidated that IVIg abrogated production of both Th1- and Th2-type pro-inflammatory cytokines from PBMC in culture. Maddur et al. (116) demonstrated the reciprocal enhancement of Treg differentiation compared to inhibition of Th17 differentiation in culture, in association with decreases in Th17 effector cytokines (IL-17A, IL-17F, IL-21, and CCL20). In clinical trials, two groups have investigated the effect of IVIg therapy on the profile of intracellular cytokine expression in T cells. In ITP patients who were responsive to IVIg therapy, there was increased production of IL-10 and TGF-β by CD4+ T cells, as well as decreased Th-1 cytokine production (117, 118).

Experiments from our laboratory could not confirm direct action of IVIg on T cells on the induction of Treg. We examined naïve $CD4^+$ $Foxp3^-$ T cells from Foxp3-GFP reporter mice in the absence of APC. Pre-treatment of these cells with IVIg, followed by co-culture with DC and a source of antigen, did not result in the induction of Foxp3 expression, whereas IVIg pretreatment of DC prior to co-culture induced Treg *ex vivo*. Further, (49) we found that, in allergic airways disease, Treg induction required $CD11c^+$ DC both *in vitro* and *in vivo*, suggesting that the DC compartment is main target of IVIg in our system. We therefore hypothesize that IVIg first tolerizes DC, which in turn induce Treg.

Modification of chemokine or chemokine receptors on circulating leukocytes is another potential mode of action of IVIg, which would lead to recruitment of cells to specific tissue sites. Evidence suggests that Treg compartmentalization and trafficking are tissue- or organ-specific, and that distinct chemokine receptor and integrin expression may contribute to selective trafficking of Treg to inflammatory microenvironments (119). For instance, expression of chemokine receptors CCR4 and CCR8 are required on Treg for tissue homing (120). Treg may switch their homing receptor expression profiles depending upon the direction of their trafficking. A majority of Treg found in secondary lymphoid tissues express CD62L and CCR7 (121). Moreover, while both effector and regulatory T cells might express similar patterns of chemokine

receptors, both subsets may compete for interaction with APC or access to the site of inflammation.

We have demonstrated, in a mouse model of ovalbumin-driven allergic airway disease that IVIg specifically increases the expression of CCR4 on the induced Treg population, suggesting their enhanced ability to recruit to the site of inflammation. Additionally, we found that expression of CD62L, which acts as a homing receptor for lymphocytes entering secondary lymphoid tissues, is decreased in Treg isolated from inflamed lung tissues (49). In a murine model of ITP, Treg compartmentalization was also modified by IVIg therapy (50), stressing the potential for action of IVIg on chemokine receptor expression. It is unclear if this action is direct or indirect, via signals from APC.

5. Conclusions

IVIg is an extremely complex preparation that contains a multitude of biologically active moieties: it likely achieves immunomodulation through a number of synergistic mechanisms, which provide positive therapeutic effects. The immune-regulatory effects of IVIg appear to be pleiotropic and involve different stages of the inflammatory cascade, with a complex interplay of IgG molecules with different cells and mediators.

In this review, we describe potential mechanisms behind the actions of IVIg in the generation and differentiation of Treg. Recent findings reinforce the efficacy of IVIg in the enhancement of Treg in various autoimmune disorders. The action of IVIg in the modulation of Treg, and the consequent maintenance of immune tolerance, provides a rationale for therapeutic approaches specifically targeting this axis of the immune system. This also renews interest in developing alternative treatments, such as Tregitopes or monoclonal antibodies, for refractory inflammatory and autoimmune diseases, which are often associated with deficiencies in Treg and are difficult to manage with conventional therapeutic approaches.

The effects of IVIg on the potentiation of Treg appear to involve the interaction of IgG with APC and potentially T cells, and are dependent on the modulation of cytokine networks

within different immune cell types. Based on our own studies and the conclusions of this review, we suggest a set of potential cellular mechanisms, which are summarized schematically in Figure 1. Initially, saIVIg binds C-type lectin receptors on dendritic cells (Figure 1A), which induces inhibitory FcγRIIB expression on DC or on effector macrophages (Figure 1B), thus potentiating the activation threshold of the adaptive arm of the immune system. The associated inhibitory receptor signaling renders the DC tolerogenic, reducing DC costimulatory molecule expression (Figure 1C) and pro-inflammatory cytokine secretion (Figure 1D). Anti-inflammatory cytokine and mediator production by both DC and Treg (Figure 1E), and presentation of IgG regulatory epitopes (Figure 1F) to Treg by DC decrease pro-inflammatory cytokine production in naïve effector T cells (Figure 1G) and generate Treg from non-Treg precursors (Figure 1H). These Treg inhibit effector Th1, Th2, and Th17 cell proliferation and activity (Figure 1I) in the inflammatory microenvironment, and secrete anti-inflammatory cytokines (Figure 1E) that tolerize DC. In addition, IVIg-mediated modulation of chemokine or chemokine receptor expression in T cell subsets might contribute to the homeostasis or regulation of trafficking of Treg, although proper functional characterization is needed. NK cells play a role in processing of innate antigens and have multiple known ITIM–linked receptors: IVIg may target NK cells to directly induce Treg by cytokine production or cell-cell contact (discussed above). IVIg-treated NK cells may also induce antibody-dependent cellular cytotoxicity of mature DC, which reduces antigen presentation and inhibits proinflammatory effector T cell function (122).

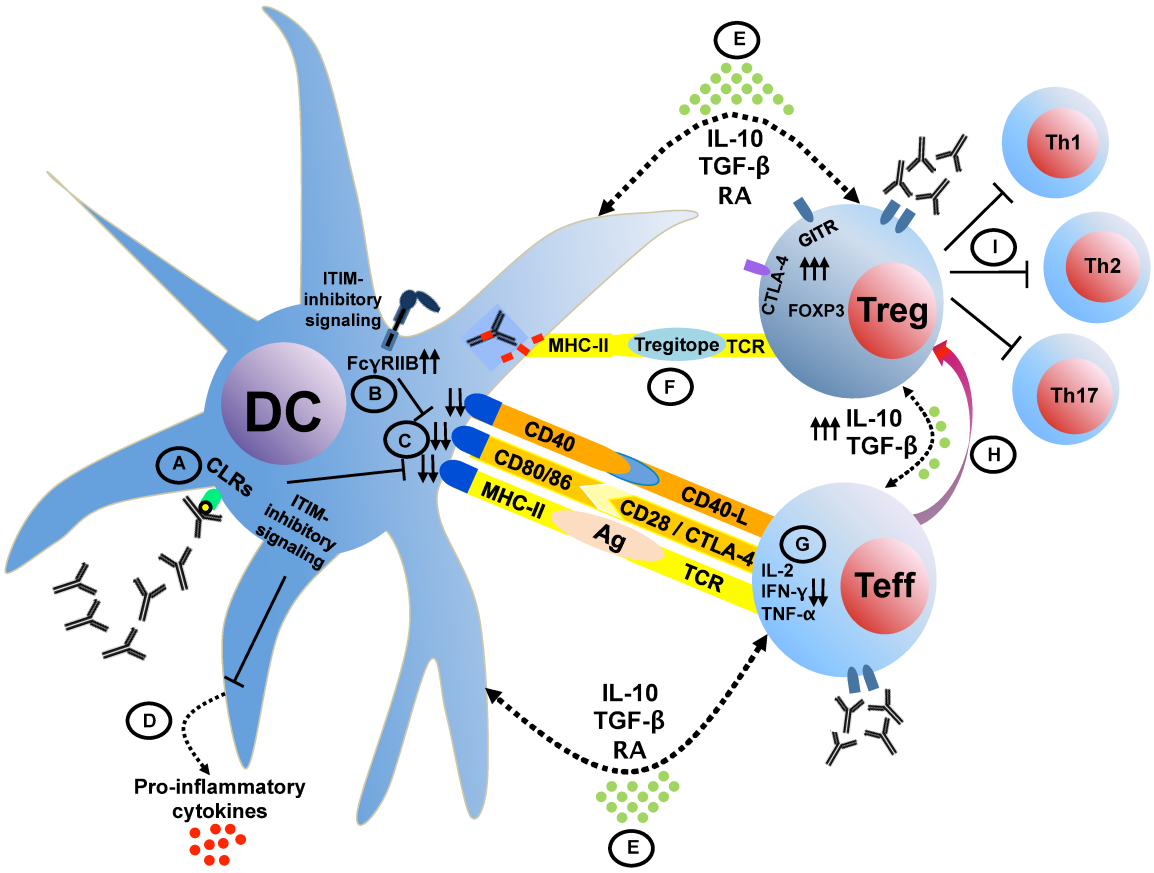

Figure 1: IVIg tolerizes DC, which interact with T cells to induce Treg. Sialylated IVIg ligates C-type lectin receptors on DC **(A)**, which induces FcγRIIB expression **(B)**, reduces costimulatory molecule expression **(C)** and pro-inflammatory cytokine secretion **(D)**. Anti-inflammatory cytokine and mediator production **(E)**, and presentation of IgG regulatory epitopes **(F)**, decreases pro-inflammatory cytokine production in naïve effector T cells **(G)** and generates Treg from non-Treg precursors **(H)**. These Treg inhibit effector Th1, Th2, and Th17 cell proliferation and activity **(I)** in the inflammatory microenvironment, and secrete anti-inflammatory cytokines **(E)** that tolerize DC. CLRs, C-type lectin receptors; GITR, glucocorticoid-induced TNFR family related gene; ITIM, immunoreceptor tyrosine-based inhibition motif; RA, retinoic acid.

Interaction of sialylated IgG with C-type lectin receptors trigger an inhibitory response in ligated cells that might consequently provide the required signals for maintaining immune tolerance. In this review, we bring evidence that shows the association of this interaction with the promotion of Treg. However, more investigation is still required to elucidate the beneficial effect of IVIg in modulation of Treg, particularly in clinical trials. Further avenues of research include identifying specific cellular markers or phenotypic patterns associated with DC tolerogenicity, as well as precise characterization of the IVIg-generated Treg population.

6. Conflict of interest

None of the authors has any potential financial conflict of interest related to this manuscript.

7. Author contributions

Surveyed the literature, wrote the article: GNK, AHM, MD, MY. Revised the article: GNK, CAP, BDM. All authors approved the final version of this article for publication, and accept responsibility for the integrity of the work.

8. Abbreviations

APC, antigen-presenting cell; CLRs, C-type lectin receptors; DC, dendritic cell; EAE, experimental autoimmune encephalitis; F(ab), fragment antibody-binding region; Fc, fragment crystallizable region; FcγR, Fc-gamma receptor; GFP, green fluorescent protein; IgG, immunoglobulin G; IVIg, intravenous immunoglobulin; ITAM, immunoreceptor tyrosine-based activation motif; ITIM, immunoreceptor tyrosine-based inhibition motif; ITP, immune thrombocytic purpura; KS, Kawasaki Syndrome; MHC, major histocompatibility complex; NK, natural killer; saIVIg, sialylated fraction of IVIg; TCR, T cell receptor; Treg, regulatory T cell.

9. Acknowledgements

We acknowledge the financial support of Talecris and Grifols Bioscience (Clinical Investigation Program), Canadian Institutes for Health Research (CIHR grants ISO115295 (BDM) and MOP67211 (CAP)), The Research Institute of the McGill University Health Centre (RI-MUHC), and

the Strauss Family Foundation. We thank Marylin Desjardins MD for her expert advice and critical comments. GNK is the recipient of a CIHR Canada Graduate Scholarships Doctoral Research Award. CAP holds a CIHR Canada Research Chair.

10. References

1. Bruton OC. Agammaglobulinemia. *Pediatrics* (1952) **9**(6):722-8. Epub 1952/06/01. PubMed PMID: 14929630.

2. Imbach P, Barandun S, Baumgartner C, Hirt A, Hofer F, Wagner HP. High-dose intravenous gammaglobulin therapy of refractory, in particular idiopathic thrombocytopenia in childhood. *Helvetica paediatrica acta* (1981) **36**(1):81-6. PubMed PMID: 6785258.

3. Nimmerjahn F, Ravetch JV. Anti-inflammatory actions of intravenous immunoglobulin. *Annual review of immunology* (2008) **26**:513-33. Epub 2008/03/29. doi: 10.1146/annurev.immunol.26.021607.090232. PubMed PMID: 18370923.

4. Group IC, Brocklehurst P, Farrell B, King A, Juszczak E, Darlow B, et al. Treatment of neonatal sepsis with intravenous immune globulin. *N Engl J Med* (2011) **365**(13):1201-11. doi: 10.1056/NEJMoa1100441. PubMed PMID: 21962214.

5. Ohlsson A, Lacy JB. Intravenous immunoglobulin for preventing infection in preterm and/or low birth weight infants. *Cochrane Database Syst Rev* (2013) **7**:CD000361. doi: 10.1002/14651858.CD000361.pub3. PubMed PMID: 23821390.

6. Ohlsson A, Lacy JB. Intravenous immunoglobulin for suspected or proven infection in neonates. *Cochrane Database Syst Rev* (2013) **7**:CD001239. doi: 10.1002/14651858.CD001239.pub4. PubMed PMID: 23821359.

7. Akdag A, Dilmen U, Haque K, Dilli D, Erdeve O, Goekmen T. Role of pentoxifylline and/or IgM-enriched intravenous immunoglobulin in the management of neonatal sepsis. *Am J Perinatol* (2014) **31**(10):905-12. doi: 10.1055/s-0033-1363771. PubMed PMID: 24515621.

8. Capasso L, Borrelli AC, Parrella C, Lama S, Ferrara T, Coppola C, et al. Are IgM-enriched immunoglobulins an effective adjuvant in septic VLBW infants? *Ital J Pediatr* (2013) **39**:63. doi: 10.1186/1824-7288-39-63. PubMed PMID: 24098953; PubMed Central PMCID: PMC3851812.

9. Kazatchkine MD, Kaveri SV. Immunomodulation of autoimmune and inflammatory diseases with intravenous immune globulin. *N Engl J Med* (2001) **345**(10):747-55. Epub 2001/09/08. doi: 10.1056/NEJMra993360. PubMed PMID: 11547745.

10. Gold R, Stangel M, Dalakas MC. Drug Insight: the use of intravenous immunoglobulin in neurology--therapeutic considerations and practical issues. *Nature clinical practice Neurology* (2007) **3**(1):36-44. Epub 2007/01/06. doi: 10.1038/ncpneuro0376. PubMed PMID: 17205073.

11. Sakaguchi S, Sakaguchi N, Asano M, Itoh M, Toda M. Immunologic self-tolerance maintained by activated T cells expressing IL-2 receptor alpha-chains (CD25). Breakdown of a single mechanism of self-tolerance causes various autoimmune diseases. *Journal of immunology (Baltimore, Md : 1950)* (1995) **155**(3):1151-64. Epub 1995/08/01. PubMed PMID: 7636184.

12. Tang Q, Bluestone JA. The Foxp3+ regulatory T cell: a jack of all trades, master of regulation. *Nature immunology* (2008) **9**(3):239-44. Epub 2008/02/21. doi: 10.1038/ni1572. PubMed PMID: 18285775; PubMed Central PMCID: PMCPmc3075612.

13. Piccirillo CA, Shevach EM. Naturally-occurring CD4+CD25+ immunoregulatory T cells: central players in the arena of peripheral tolerance. *Seminars in immunology* (2004) **16**(2):81-8. Epub 2004/03/24. doi: 10.1016/j.smim.2003.12.003. PubMed PMID: 15036231.

14. Hori S, Nomura T, Sakaguchi S. Control of regulatory T cell development by the transcription factor Foxp3. *Science* (2003) **299**(5609):1057-61. doi: 10.1126/science.1079490. PubMed PMID: 12522256.

15. Vigouroux S, Yvon E, Biagi E, Brenner MK. Antigen-induced regulatory T cells. *Blood* (2004) **104**(1):26-33. Epub 2004/03/18. doi: 10.1182/blood-2004-01-0182. PubMed PMID: 15026316.

16. d'Hennezel E, Yurchenko E, Sgouroudis E, Hay V, Piccirillo CA. Single-cell analysis of the human T regulatory population uncovers functional heterogeneity and instability within FOXP3+ cells. *Journal of immunology (Baltimore, Md : 1950)* (2011) **186**(12):6788-97. doi: 10.4049/jimmunol.1100269. PubMed PMID: 21576508.

17. Bin Dhuban K, Kornete M, E SM, Piccirillo CA. Functional dynamics of Foxp3(+) regulatory T cells in mice and humans. *Immunological reviews* (2014) **259**(1):140-58. doi: 10.1111/imr.12168. PubMed PMID: 24712464.

18. Bin Dhuban K, d'Hennezel E, Nashi E, Bar-Or A, Rieder S, Shevach EM, et al. Coexpression of TIGIT and FCRL3 Identifies Helios+ Human Memory Regulatory T Cells. *Journal of immunology (Baltimore, Md : 1950)* (2015) **194**(8):3687-96. doi: 10.4049/jimmunol.1401803. PubMed PMID: 25762785.

19. Pilat N, Baranyi U, Klaus C, Jaeckel E, Mpofu N, Wrba F, et al. Treg-therapy allows mixed chimerism and transplantation tolerance without cytoreductive conditioning. *American journal of transplantation : official journal of the American Society of Transplantation and the American Society of Transplant Surgeons* (2010) **10**(4):751-62. Epub 2010/02/13. doi: 10.1111/j.1600-6143.2010.03018.x. PubMed PMID: 20148810; PubMed Central PMCID: PMCPmc2856406.

20. Xu W, Lan Q, Chen M, Chen H, Zhu N, Zhou X, et al. Adoptive transfer of induced-Treg cells effectively attenuates murine airway allergic inflammation. *PloS one* (2012) **7**(7):e40314. Epub 2012/07/14. doi: 10.1371/journal.pone.0040314. PubMed PMID: 22792275; PubMed Central PMCID: PMCPmc3392250.

21. Riley JL, June CH, Blazar BR. Human T regulatory cell therapy: take a billion or so and call me in the morning. *Immunity* (2009) **30**(5):656-65. Epub 2009/05/26. doi: 10.1016/j.immuni.2009.04.006. PubMed PMID: 19464988; PubMed Central PMCID: PMCPmc2742482.

22. Battaglia M, Stabilini A, Roncarolo MG. Rapamycin selectively expands CD4+CD25+FoxP3+ regulatory T cells. *Blood* (2005) **105**(12):4743-8. doi: 10.1182/blood-2004-10-3932. PubMed PMID: 15746082.

23. Ray A, Khare A, Krishnamoorthy N, Qi Z, Ray P. Regulatory T cells in many flavors control asthma. *Mucosal Immunol* (2010) **3**(3):216-29. doi: 10.1038/mi.2010.4. PubMed PMID: 20164832; PubMed Central PMCID: PMC3039023.

24. Bayry J, Mouthon L, Kaveri SV. Intravenous immunoglobulin expands regulatory T cells in autoimmune rheumatic disease. *The Journal of rheumatology* (2012) **39**(2):450-1. Epub

2012/02/03. doi: 10.3899/jrheum.111123. PubMed PMID: 22298280; PubMed Central PMCID: PMCPmc3623090.

25. Durandy A, Fischer A, Griscelli C. Dysfunctions of pokeweed mitogen-stimulated T and B lymphocyte responses induced by gammaglobulin therapy. *The Journal of clinical investigation* (1981) **67**(3):867-77. Epub 1981/03/01. PubMed PMID: 6162859; PubMed Central PMCID: PMCPmc370638.

26. Sany J, Clot J, Bonneau M, Andary M. Immunomodulating effect of human placenta-eluted gamma globulins in rheumatoid arthritis. *Arthritis and rheumatism* (1982) **25**(1):17-24. Epub 1982/01/01. PubMed PMID: 7066033.

27. Delfraissy JF, Tchernia G, Laurian Y, Wallon C, Galanaud P, Dormont J. Suppressor cell function after intravenous gammaglobulin treatment in adult chronic idiopathic thrombocytopenic purpura. *British journal of haematology* (1985) **60**(2):315-22. Epub 1985/06/01. PubMed PMID: 2408658.

28. Gupta A, Novick BE, Rubinstein A. Restoration of suppressor T-cell functions in children with AIDS following intravenous gamma globulin treatment. *American journal of diseases of children (1960)* (1986) **140**(2):143-6. Epub 1986/02/01. PubMed PMID: 2936236.

29. Kessel A, Ammuri H, Peri R, Pavlotzky ER, Blank M, Shoenfeld Y, et al. Intravenous immunoglobulin therapy affects T regulatory cells by increasing their suppressive function. *Journal of immunology (Baltimore, Md : 1950)* (2007) **179**(8):5571-5. Epub 2007/10/04. PubMed PMID: 17911644.

30. Chi LJ, Wang HB, Zhang Y, Wang WZ. Abnormality of circulating CD4(+)CD25(+) regulatory T cell in patients with Guillain-Barre syndrome. *Journal of neuroimmunology* (2007) **192**(1-2):206-14. Epub 2007/11/13. doi: 10.1016/j.jneuroim.2007.09.034. PubMed PMID: 17997492.

31. Barreto M, Ferreira RC, Lourenco L, Moraes-Fontes MF, Santos E, Alves M, et al. Low frequency of CD4+CD25+ Treg in SLE patients: a heritable trait associated with CTLA4 and TGFbeta gene variants. *BMC immunology* (2009) **10**:5. Epub 2009/01/29. doi: 10.1186/1471-2172-10-5. PubMed PMID: 19173720; PubMed Central PMCID: PMCPmc2656467.

32. Tsurikisawa N, Saito H, Oshikata C, Tsuburai T, Akiyama K. High-dose intravenous immunoglobulin treatment increases regulatory T cells in patients with eosinophilic granulomatosis with polyangiitis. *The Journal of rheumatology* (2012) **39**(5):1019-25. Epub 2012/04/03. doi: 10.3899/jrheum.110981. PubMed PMID: 22467925.

33. Tsurikisawa N, Taniguchi M, Saito H, Himeno H, Ishibashi A, Suzuki S, et al. Treatment of Churg-Strauss syndrome with high-dose intravenous immunoglobulin. *Annals of allergy, asthma & immunology : official publication of the American College of Allergy, Asthma, & Immunology* (2004) **92**(1):80-7. Epub 2004/02/06. doi: 10.1016/s1081-1206(10)61714-0. PubMed PMID: 14756469.

34. Burns JC, Glodé MP. Kawasaki syndrome. *The Lancet* (2004) **364**(9433):533-44.

35. Burns JC, Song Y, Bujold M, Shimizu C, Kanegaye JT, Tremoulet AH, et al. Immune-monitoring in Kawasaki disease patients treated with infliximab and intravenous immunoglobulin. *Clinical and experimental immunology* (2013) **174**(3):337-44. doi: 10.1111/cei.12182. PubMed PMID: 23901839; PubMed Central PMCID: PMC3826300.

36. Franco A, Touma R, Song Y, Shimizu C, Tremoulet AH, Kanegaye JT, et al. Specificity of regulatory T cells that modulate vascular inflammation. *Autoimmunity* (2014) **47**(2):95-104. doi: 10.3109/08916934.2013.860524. PubMed PMID: 24490882.

37. Burns JC, Touma R, Song Y, Padilla RL, Tremoulet AH, Sidney J, et al. Fine specificities of natural regulatory T cells after IVIG therapy in patients with Kawasaki disease. *Autoimmunity* (2015) **48**(3):181-8. doi: 10.3109/08916934.2015.1027817. PubMed PMID: 25822882.

38. Anthony RM, Ravetch JV. A novel role for the IgG Fc glycan: the anti-inflammatory activity of sialylated IgG Fcs. *Journal of clinical immunology* (2010) **30 Suppl 1**:S9-14. Epub 2010/05/19. doi: 10.1007/s10875-010-9405-6. PubMed PMID: 20480216.

39. Ephrem A, Chamat S, Miquel C, Fisson S, Mouthon L, Caligiuri G, et al. Expansion of CD4+CD25+ regulatory T cells by intravenous immunoglobulin: a critical factor in controlling experimental autoimmune encephalomyelitis. *Blood* (2008) **111**(2):715-22. Epub 2007/10/13. doi: 10.1182/blood-2007-03-079947. PubMed PMID: 17932250.

40. Ni FF, Li CR, Li Q, Xia Y, Wang GB, Yang J. Regulatory T cell microRNA expression changes in children with acute Kawasaki disease. *Clinical and experimental immunology* (2014) **178**(2):384-93. doi: 10.1111/cei.12418. PubMed PMID: 25039241.

41. Okuda S, Kamei S, Harano S, Shinya N, Hayashida K, Sasaki T. [Enhancement of regulatory T cell induction by intravenous S-sulfonated Immunoglobulin during the treatment of experimental autoimmune encephalomyelitis]. *Yakugaku zasshi : Journal of the Pharmaceutical Society of Japan* (2012) **132**(2):243-9. Epub 2012/02/02. PubMed PMID: 22293707.

42. Bao Y, Han Y, Chen Z, Xu S, Cao X. IFN-alpha-producing PDCA-1+ Siglec-H- B cells mediate innate immune defense by activating NK cells. *European journal of immunology* (2011) **41**(3):657-68. doi: 10.1002/eji.201040840. PubMed PMID: 21287550.

43. Bergmann C, Wild CA, Narwan M, Lotfi R, Lang S, Brandau S. Human tumor-induced and naturally occurring Treg cells differentially affect NK cells activated by either IL-2 or target cells. *European journal of immunology* (2011) **41**(12):3564-73. doi: 10.1002/eji.201141532. PubMed PMID: 21905023.

44. Chong WP, Ling MT, Liu Y, Caspi RR, Wong WM, Wu W, et al. Essential role of NK cells in IgG therapy for experimental autoimmune encephalomyelitis. *PloS one* (2013) **8**(4):e60862. doi: 10.1371/journal.pone.0060862. PubMed PMID: 23577171; PubMed Central PMCID: PMC3618232.

45. Moretta A. Natural killer cells and dendritic cells: rendezvous in abused tissues. *Nat Rev Immunol* (2002) **2**(12):957-65.

46. Zingoni A, Sornasse T, Cocks BG, Tanaka Y, Santoni A, Lanier LL. Cross-talk between activated human NK cells and CD4+ T cells via OX40-OX40 ligand interactions. *Journal of immunology (Baltimore, Md : 1950)* (2004) **173**(6):3716-24. PubMed PMID: 15356117.

47. Liang S, Alard P, Zhao Y, Parnell S, Clark SL, Kosiewicz MM. Conversion of CD4+ CD25- cells into CD4+ CD25+ regulatory T cells in vivo requires B7 costimulation, but not the thymus. *J Exp Med* (2005) **201**(1):127-37. doi: 10.1084/jem.20041201. PubMed PMID: 15630140; PubMed Central PMCID: PMC2212775.

48. Griseri T, Asquith M, Thompson C, Powrie F. OX40 is required for regulatory T cell-mediated control of colitis. *J Exp Med* (2010) **207**(4):699-709. doi: 10.1084/jem.20091618. PubMed PMID: 20368580; PubMed Central PMCID: PMC2856021.

49. Massoud AH, Guay J, Shalaby KH, Bjur E, Ablona A, Chan D, et al. Intravenous immunoglobulin attenuates airway inflammation through induction of forkhead box protein 3-positive regulatory T cells. *The Journal of allergy and clinical immunology* (2012) **129**(6):1656-65.e3. Epub 2012/05/09. doi: 10.1016/j.jaci.2012.02.050. PubMed PMID: 22564681.

50. Aslam R, Hu Y, Gebremeskel S, Segel GB, Speck ER, Guo L, et al. Thymic retention of CD4+CD25+FoxP3+ T regulatory cells is associated with their peripheral deficiency and thrombocytopenia in a murine model of immune thrombocytopenia. *Blood* (2012) **120**(10):2127-32. Epub 2012/07/05. doi: 10.1182/blood-2012-02-413526. PubMed PMID: 22760780.

51. Kerr J, Quinti I, Eibl M, Chapel H, Spaeth PJ, Sewell WC, et al. Is dosing of therapeutic immunoglobulins optimal? – A review of a 3-decade long debate in Europe. *Frontiers in Immunology* (2014) **5**. doi: 10.3389/fimmu.2014.00629.

52. Roifman CM, Levison H, Gelfand EW. High-dose versus low-dose intravenous immunoglobulin in hypogammaglobulinaemia and chronic lung disease. *Lancet* (1987) **1**(8541):1075-7. PubMed PMID: 2883406.

53. Ramakrishna C, Newo AN, Shen YW, Cantin E. Passively administered pooled human immunoglobulins exert IL-10 dependent anti-inflammatory effects that protect against fatal HSV encephalitis. *PLoS pathogens* (2011) **7**(6):e1002071. Epub 2011/06/10. doi: 10.1371/journal.ppat.1002071. PubMed PMID: 21655109; PubMed Central PMCID: PMCPmc3107211.

54. Schwab I, Mihai S, Seeling M, Kasperkiewicz M, Ludwig RJ, Nimmerjahn F. Broad requirement for terminal sialic acid residues and FcgammaRIIB for the preventive and therapeutic activity of intravenous immunoglobulins in vivo. *European journal of immunology* (2014) **44**(5):1444-53. doi: 10.1002/eji.201344230. PubMed PMID: 24505033.

55. Cines DB, Blanchette VS. Immune thrombocytopenic purpura. *N Engl J Med* (2002) **346**(13):995-1008. Epub 2002/03/29. doi: 10.1056/NEJMra010501. PubMed PMID: 11919310.

56. Ohnmacht C, Pullner A, King SB, Drexler I, Meier S, Brocker T, et al. Constitutive ablation of dendritic cells breaks self-tolerance of CD4 T cells and results in spontaneous fatal autoimmunity. *J Exp Med* (2009) **206**(3):549-59. Epub 2009/02/25. doi: 10.1084/jem.20082394. PubMed PMID: 19237601; PubMed Central PMCID: PMCPmc2699126.

57. Adorini L. Tolerogenic dendritic cells induced by vitamin D receptor ligands enhance regulatory T cells inhibiting autoimmune diabetes. *Annals of the New York Academy of Sciences* (2003) **987**:258-61. PubMed PMID: 12727648.

58. Steinman RM, Hawiger D, Nussenzweig MC. Tolerogenic dendritic cells. *Annual review of immunology* (2003) **21**:685-711. doi: 10.1146/annurev.immunol.21.120601.141040. PubMed PMID: 12615891.

59. Kushwah R, Hu J. Role of dendritic cells in the induction of regulatory T cells. *Cell & bioscience* (2011) **1**(1):20. Epub 2011/06/30. doi: 10.1186/2045-3701-1-20. PubMed PMID: 21711933; PubMed Central PMCID: PMCPmc3125210.

60. Zou T, Caton AJ, Koretzky GA, Kambayashi T. Dendritic cells induce regulatory T cell proliferation through antigen-dependent and -independent interactions. *Journal of immunology (Baltimore, Md : 1950)* (2010) **185**(5):2790-9. Epub 2010/08/06. doi: 10.4049/jimmunol.0903740. PubMed PMID: 20686126.

61. Sun Y, Brown NK, Ruddy MJ, Miller ML, Lee Y, Wang Y, et al. B and T lymphocyte attenuator tempers early infection immunity. *Journal of immunology (Baltimore, Md : 1950)* (2009) **183**(3):1946-51. Epub 2009/07/10. doi: 10.4049/jimmunol.0801866. PubMed PMID: 19587015; PubMed Central PMCID: PMCPmc2895307.

62. Brandl C, Ortler S, Herrmann T, Cardell S, Lutz MB, Wiendl H. B7-H1-deficiency enhances the potential of tolerogenic dendritic cells by activating CD1d-restricted type II NKT cells. *PloS one* (2010) **5**(5):e10800. Epub 2010/06/04. doi: 10.1371/journal.pone.0010800. PubMed PMID: 20520738; PubMed Central PMCID: PMCPmc2875405.

63. Kubo T, Hatton RD, Oliver J, Liu X, Elson CO, Weaver CT. Regulatory T cell suppression and anergy are differentially regulated by proinflammatory cytokines produced by TLR-activated dendritic cells. *Journal of immunology (Baltimore, Md : 1950)* (2004) **173**(12):7249-58. Epub 2004/12/09. PubMed PMID: 15585847.

64. Bhattacharya P, Gopisetty A, Ganesh BB, Sheng JR, Prabhakar BS. GM-CSF-induced, bone-marrow-derived dendritic cells can expand natural Tregs and induce adaptive Tregs by different mechanisms. *Journal of leukocyte biology* (2011) **89**(2):235-49. Epub 2010/11/05. doi: 10.1189/jlb.0310154. PubMed PMID: 21048215; PubMed Central PMCID: PMCPmc3024903.

65. Loubaki L, Chabot D, Bazin R. Involvement of the TNF-alpha/TGF-beta/IDO axis in IVIg-induced immune tolerance. *Cytokine* (2015) **71**(2):181-7. doi: 10.1016/j.cyto.2014.10.016. PubMed PMID: 25461397.

66. Maldonado RA, von Andrian UH. How tolerogenic dendritic cells induce regulatory T cells. *Adv Immunol* (2010) **108**:111-65. doi: 10.1016/B978-0-12-380995-7.00004-5. PubMed PMID: 21056730; PubMed Central PMCID: PMC3050492.

67. Kuipers H, Lambrecht BN. The interplay of dendritic cells, Th2 cells and regulatory T cells in asthma. *Current opinion in immunology* (2004) **16**(6):702-8. Epub 2004/10/30. doi: 10.1016/j.coi.2004.09.010. PubMed PMID: 15511661.

68. Kaufman GN, Massoud AH, Audusseau S, Banville-Langelier AA, Wang Y, Guay J, et al. Intravenous immunoglobulin attenuates airway hyperresponsiveness in a murine model of allergic asthma. *Clinical and experimental allergy : journal of the British Society for Allergy and Clinical Immunology* (2011) **41**(5):718-28. Epub 2011/01/25. doi: 10.1111/j.1365-2222.2010.03663.x. PubMed PMID: 21255135.

69. Yamamoto M, Kobayashi K, Ishikawa Y, Nakata K, Funada Y, Kotani Y, et al. The inhibitory effects of intravenous administration of rabbit immunoglobulin G on airway inflammation are dependent upon Fcgamma receptor IIb on CD11c(+) dendritic cells in a murine model. *Clinical and experimental immunology* (2010) **162**(2):315-24. Epub 2010/09/08. doi: 10.1111/j.1365-2249.2010.04243.x. PubMed PMID: 20819092; PubMed Central PMCID: PMCPmc2996599.

70. Qian J, Zhu J, Wang M, Wu S, Chen T. Suppressive effects of intravenous immunoglobulin (IVIG) on human umbilical cord blood immune cells. *Pediatric allergy and immunology : official publication of the European Society of Pediatric Allergy and Immunology* (2011) **22**(2):211-20. Epub 2010/10/01. doi: 10.1111/j.1399-3038.2010.01049.x. PubMed PMID: 20880351.

71. Bayry J, Lacroix-Desmazes S, Carbonneil C, Misra N, Donkova V, Pashov A, et al. Inhibition of maturation and function of dendritic cells by intravenous immunoglobulin. *Blood* (2003) **101**(2):758-65. Epub 2002/10/24. doi: 10.1182/blood-2002-05-1447. PubMed PMID: 12393386.

72. Samuelsson A, Towers TL, Ravetch JV. Anti-inflammatory activity of IVIG mediated through the inhibitory Fc receptor. *Science* (2001) **291**(5503):484-6. Epub 2001/02/13. doi: 10.1126/science.291.5503.484. PubMed PMID: 11161202.

73. Trepanier P, Aubin E, Bazin R. IVIg-mediated inhibition of antigen presentation: predominant role of naturally occurring cationic IgG. *Clinical immunology (Orlando, Fla)* (2012) **142**(3):383-9. Epub 2012/01/28. doi: 10.1016/j.clim.2011.12.014. PubMed PMID: 22281428.

74. Aubin E, Lemieux R, Bazin R. Indirect inhibition of in vivo and in vitro T-cell responses by intravenous immunoglobulins due to impaired antigen presentation. *Blood* (2010) **115**(9):1727-34. Epub 2009/12/08. doi: 10.1182/blood-2009-06-225417. PubMed PMID: 19965673.

75. Ohkuma K, Sasaki T, Kamei S, Okuda S, Nakano H, Hamamoto T, et al. Modulation of dendritic cell development by immunoglobulin G in control subjects and multiple sclerosis patients. *Clinical and experimental immunology* (2007) **150**(3):397-406. Epub 2007/09/29. doi: 10.1111/j.1365-2249.2007.03496.x. PubMed PMID: 17900307; PubMed Central PMCID: PMCPmc2219369.

76. Veldhoen M, Hocking RJ, Atkins CJ, Locksley RM, Stockinger B. TGFbeta in the context of an inflammatory cytokine milieu supports de novo differentiation of IL-17-producing T cells. *Immunity* (2006) **24**(2):179-89. Epub 2006/02/14. doi: 10.1016/j.immuni.2006.01.001. PubMed PMID: 16473830.

77. Pasare C, Medzhitov R. Toll pathway-dependent blockade of CD4+CD25+ T cell-mediated suppression by dendritic cells. *Science* (2003) **299**(5609):1033-6. Epub 2003/01/18. doi: 10.1126/science.1078231. PubMed PMID: 12532024.

78. Andersson JP, Andersson UG. Human intravenous immunoglobulin modulates monokine production in vitro. *Immunology* (1990) **71**(3):372-6. Epub 1990/11/01. PubMed PMID: 2269476; PubMed Central PMCID: PMCPmc1384435.

79. Darville T, Tabor D, Simpson K, Jacobs RF. Intravenous immunoglobulin modulates human mononuclear phagocyte tumor necrosis factor-alpha production in vitro. *Pediatric research* (1994) **35**(4 Pt 1):397-403. Epub 1994/04/01. PubMed PMID: 8047375.

80. Clynes R. IVIG therapy: interfering with interferon-gamma. *Immunity* (2007) **26**(1):4-6. Epub 2007/01/24. doi: 10.1016/j.immuni.2007.01.006. PubMed PMID: 17241954.

81. Bayry J, Bansal K, Kazatchkine MD, Kaveri SV. DC-SIGN and alpha2,6-sialylated IgG Fc interaction is dispensable for the anti-inflammatory activity of IVIg on human dendritic cells. *Proceedings of the National Academy of Sciences of the United States of America* (2009) **106**(9):E24; author reply E5. Epub 2009/02/25. doi: 10.1073/pnas.0900016106. PubMed PMID: 19237553; PubMed Central PMCID: PMCPmc2651302.

82. Kaneko Y, Nimmerjahn F, Madaio MP, Ravetch JV. Pathology and protection in nephrotoxic nephritis is determined by selective engagement of specific Fc receptors. *The Journal of Experimental Medicine* (2006) **203**(3):789-97. doi: 10.1084/jem.20051900. PubMed PMID: PMC2118246.

83. Siragam V, Crow AR, Brinc D, Song S, Freedman J, Lazarus AH. Intravenous immunoglobulin ameliorates ITP via activating Fc gamma receptors on dendritic cells. *Nature medicine* (2006) **12**(6):688-92. Epub 2006/05/23. doi: 10.1038/nm1416. PubMed PMID: 16715090.

84. De Groot AS, Moise L, McMurry JA, Wambre E, Van Overtvelt L, Moingeon P, et al. Activation of natural regulatory T cells by IgG Fc-derived peptide "Tregitopes". *Blood* (2008) **112**(8):3303-11. Epub 2008/07/29. doi: 10.1182/blood-2008-02-138073. PubMed PMID: 18660382; PubMed Central PMCID: PMCPmc2569179.

85. Cousens LP, Najafian N, Mingozzi F, Elyaman W, Mazer B, Moise L, et al. In vitro and in vivo studies of IgG-derived Treg epitopes (Tregitopes): a promising new tool for tolerance induction and treatment of autoimmunity. *Journal of clinical immunology* (2013) **33 Suppl 1**:S43-9. Epub 2012/09/04. doi: 10.1007/s10875-012-9762-4. PubMed PMID: 22941509; PubMed Central PMCID: PMCPmc3538121.

86. Elyaman W, Khoury SJ, Scott DW, De Groot AS. Potential application of tregitopes as immunomodulating agents in multiple sclerosis. *Neurology research international* (2011)

2011:256460. Epub 2011/09/24. doi: 10.1155/2011/256460. PubMed PMID: 21941651; PubMed Central PMCID: PMCPmc3175387.

87. Kaneko Y, Nimmerjahn F, Ravetch JV. Anti-inflammatory activity of immunoglobulin G resulting from Fc sialylation. *Science* (2006) **313**(5787):670-3. Epub 2006/08/05. doi: 10.1126/science.1129594. PubMed PMID: 16888140.

88. Anthony RM, Wermeling F, Karlsson MC, Ravetch JV. Identification of a receptor required for the anti-inflammatory activity of IVIG. *Proceedings of the National Academy of Sciences of the United States of America* (2008) **105**(50):19571-8. Epub 2008/11/28. doi: 10.1073/pnas.0810163105. PubMed PMID: 19036920; PubMed Central PMCID: PMCPmc2604916.

89. Chen XX, Chen YQ, Ye S. Measuring decreased serum IgG sialylation: a novel clinical biomarker of lupus. *Lupus* (2015). doi: 10.1177/0961203315570686. PubMed PMID: 25672371.

90. Sondermann P, Pincetic A, Maamary J, Lammens K, Ravetch JV. General mechanism for modulating immunoglobulin effector function. *Proceedings of the National Academy of Sciences of the United States of America* (2013) **110**(24):9868-72. doi: 10.1073/pnas.1307864110. PubMed PMID: 23697368; PubMed Central PMCID: PMC3683708.

91. Washburn N, Schwab I, Ortiz D, Bhatnagar N, Lansing JC, Medeiros A, et al. Controlled tetra-Fc sialylation of IVIg results in a drug candidate with consistent enhanced anti-inflammatory activity. *Proceedings of the National Academy of Sciences of the United States of America* (2015) **112**(11):E1297-306. doi: 10.1073/pnas.1422481112. PubMed PMID: 25733881; PubMed Central PMCID: PMC4371931.

92. Anthony RM, Nimmerjahn F, Ashline DJ, Reinhold VN, Paulson JC, Ravetch JV. Recapitulation of IVIG anti-inflammatory activity with a recombinant IgG Fc. *Science* (2008) **320**(5874):373-6. Epub 2008/04/19. doi: 10.1126/science.1154315. PubMed PMID: 18420934; PubMed Central PMCID: PMCPmc2409116.

93. Schwab I, Biburger M, Kronke G, Schett G, Nimmerjahn F. IVIg-mediated amelioration of ITP in mice is dependent on sialic acid and SIGNR1. *European journal of immunology* (2012) **42**(4):826-30. doi: 10.1002/eji.201142260. PubMed PMID: 22278120.

94. Massoud AH, Yona M, Xue D, Chouiali F, Alturaihi H, Ablona A, et al. Dendritic cell immunoreceptor: a novel receptor for intravenous immunoglobulin mediates induction of regulatory T cells. *The Journal of allergy and clinical immunology* (2014) **133**(3):853-63 e5. doi: 10.1016/j.jaci.2013.09.029. PubMed PMID: 24210883.

95. Samsom JN, van Berkel LA, van Helvoort JM, Unger WW, Jansen W, Thepen T, et al. Fc gamma RIIB regulates nasal and oral tolerance: a role for dendritic cells. *Journal of immunology (Baltimore, Md : 1950)* (2005) **174**(9):5279-87. Epub 2005/04/22. PubMed PMID: 15843524.

96. Guilliams M, Bruhns P, Saeys Y, Hammad H, Lambrecht BN. The function of Fcgamma receptors in dendritic cells and macrophages. *Nat Rev Immunol* (2014) **14**(2):94-108. doi: 10.1038/nri3582. PubMed PMID: 24445665.

97. Fiebiger BM, Maamary J, Pincetic A, Ravetch JV. Protection in antibody- and T cell-mediated autoimmune diseases by antiinflammatory IgG Fcs requires type II FcRs. *Proceedings of the National Academy of Sciences of the United States of America* (2015) **112**(18):E2385-94. doi: 10.1073/pnas.1505292112. PubMed PMID: 25870292; PubMed Central PMCID: PMC4426441.

98. Othy S, Topcu S, Saha C, Kothapalli P, Lacroix-Desmazes S, Kasermann F, et al. Sialylation may be dispensable for reciprocal modulation of helper T cells by intravenous immunoglobulin. *European journal of immunology* (2014) **44**(7):2059-63. doi: 10.1002/eji.201444440. PubMed PMID: 24700174.

99. Guhr T, Bloem J, Derksen NI, Wuhrer M, Koenderman AH, Aalberse RC, et al. Enrichment of sialylated IgG by lectin fractionation does not enhance the efficacy of immunoglobulin G in a murine model of immune thrombocytopenia. *PloS one* (2011) **6**(6):e21246. doi: 10.1371/journal.pone.0021246. PubMed PMID: 21731683; PubMed Central PMCID: PMC3121734.

100. Leontyev D, Katsman Y, Ma XZ, Miescher S, Kasermann F, Branch DR. Sialylation-independent mechanism involved in the amelioration of murine immune thrombocytopenia using intravenous gammaglobulin. *Transfusion* (2012) **52**(8):1799-805. doi: 10.1111/j.1537-2995.2011.03517.x. PubMed PMID: 22257295.

101. Campbell IK, Miescher S, Branch DR, Mott PJ, Lazarus AH, Han D, et al. Therapeutic effect of IVIG on inflammatory arthritis in mice is dependent on the Fc portion and independent of sialylation or basophils. *Journal of immunology (Baltimore, Md : 1950)* (2014) **192**(11):5031-8. doi: 10.4049/jimmunol.1301611. PubMed PMID: 24760152; PubMed Central PMCID: PMC4025610.

102. Geijtenbeek TB, Gringhuis SI. Signalling through C-type lectin receptors: shaping immune responses. *Nat Rev Immunol* (2009) **9**(7):465-79. Epub 2009/06/13. doi: 10.1038/nri2569. PubMed PMID: 19521399.

103. Gringhuis SI, den Dunnen J, Litjens M, van der Vlist M, Geijtenbeek TB. Carbohydrate-specific signaling through the DC-SIGN signalosome tailors immunity to Mycobacterium tuberculosis, HIV-1 and Helicobacter pylori. *Nature immunology* (2009) **10**(10):1081-8. Epub 2009/09/01. doi: 10.1038/ni.1778. PubMed PMID: 19718030.

104. Smits HH, Engering A, van der Kleij D, de Jong EC, Schipper K, van Capel TM, et al. Selective probiotic bacteria induce IL-10-producing regulatory T cells in vitro by modulating dendritic cell function through dendritic cell-specific intercellular adhesion molecule 3-grabbing nonintegrin. *The Journal of allergy and clinical immunology* (2005) **115**(6):1260-7. Epub 2005/06/09. doi: 10.1016/j.jaci.2005.03.036. PubMed PMID: 15940144.

105. Anthony RM, Wermeling F, Ravetch JV. Novel roles for the IgG Fc glycan. *Annals of the New York Academy of Sciences* (2012) **1253**:170-80. Epub 2012/02/01. doi: 10.1111/j.1749-6632.2011.06305.x. PubMed PMID: 22288459.

106. Pincetic A, Bournazos S, DiLillo DJ, Maamary J, Wang TT, Dahan R, et al. Type I and type II Fc receptors regulate innate and adaptive immunity. *Nature immunology* (2014) **15**(8):707-16. doi: 10.1038/ni.2939. PubMed PMID: 25045879.

107. Crispin M, Yu X, Bowden TA. Crystal structure of sialylated IgG Fc: implications for the mechanism of intravenous immunoglobulin therapy. *Proceedings of the National Academy of Sciences of the United States of America* (2013) **110**(38):E3544-6. doi: 10.1073/pnas.1310657110. PubMed PMID: 23929778; PubMed Central PMCID: PMC3780870.

108. Yu X, Vasiljevic S, Mitchell DA, Crispin M, Scanlan CN. Dissecting the molecular mechanism of IVIg therapy: the interaction between serum IgG and DC-SIGN is independent of

antibody glycoform or Fc domain. *Journal of molecular biology* (2013) **425**(8):1253-8. doi: 10.1016/j.jmb.2013.02.006. PubMed PMID: 23416198.

109. Kasermann F, Boerema DJ, Ruegsegger M, Hofmann A, Wymann S, Zuercher AW, et al. Analysis and functional consequences of increased Fab-sialylation of intravenous immunoglobulin (IVIG) after lectin fractionation. *PloS one* (2012) **7**(6):e37243. Epub 2012/06/08. doi: 10.1371/journal.pone.0037243. PubMed PMID: 22675478; PubMed Central PMCID: PMCPmc3366990.

110. Yamazaki S, Dudziak D, Heidkamp GF, Fiorese C, Bonito AJ, Inaba K, et al. CD8+ CD205+ splenic dendritic cells are specialized to induce Foxp3+ regulatory T cells. *Journal of immunology (Baltimore, Md : 1950)* (2008) **181**(10):6923-33. Epub 2008/11/05. PubMed PMID: 18981112; PubMed Central PMCID: PMCPmc2814590.

111. Tha-In T, Metselaar HJ, Bushell AR, Kwekkeboom J, Wood KJ. Intravenous immunoglobulins promote skin allograft acceptance by triggering functional activation of CD4+Foxp3+ T cells. *Transplantation* (2010) **89**(12):1446-55. Epub 2010/05/14. doi: 10.1097/TP.0b013e3181dd6bf1. PubMed PMID: 20463648.

112. Becker C, Kubach J, Wijdenes J, Knop J, Jonuleit H. CD4-mediated functional activation of human CD4+CD25+ regulatory T cells. *European journal of immunology* (2007) **37**(5):1217-23. Epub 2007/04/05. doi: 10.1002/eji.200636480. PubMed PMID: 17407195.

113. Pashov A, Bellon B, Kaveri SV, Kazatchkine MD. A shift in encephalitogenic T cell cytokine pattern is associated with suppression of EAE by intravenous immunoglobulins (IVIg). *Multiple sclerosis (Houndmills, Basingstoke, England)* (1997) **3**(2):153-6. Epub 1997/04/01. PubMed PMID: 9291172.

114. Pashov A, Dubey C, Kaveri SV, Lectard B, Huang YM, Kazatchkine MD, et al. Normal immunoglobulin G protects against experimental allergic encephalomyelitis by inducing transferable T cell unresponsiveness to myelin basic protein. *European journal of immunology* (1998) **28**(6):1823-31. Epub 1998/06/30. doi: 10.1002/(sici)1521-4141(199806)28:06<1823::aid-immu1823>3.0.co;2-f. PubMed PMID: 9645363.

115. Andersson U, Bjork L, Skansen-Saphir U, Andersson J. Pooled human IgG modulates cytokine production in lymphocytes and monocytes. *Immunological reviews* (1994) **139**:21-42. Epub 1994/06/01. PubMed PMID: 7927412.

116. Maddur MS, Vani J, Hegde P, Lacroix-Desmazes S, Kaveri SV, Bayry J. Inhibition of differentiation, amplification, and function of human TH17 cells by intravenous immunoglobulin. *The Journal of allergy and clinical immunology* (2011) **127**(3):823-30.e1-7. Epub 2011/02/02. doi: 10.1016/j.jaci.2010.12.1102. PubMed PMID: 21281961.

117. Cooper N, Heddle NM, Haas M, Reid ME, Lesser ML, Fleit HB, et al. Intravenous (IV) anti-D and IV immunoglobulin achieve acute platelet increases by different mechanisms: modulation of cytokine and platelet responses to IV anti-D by FcgammaRIIa and FcgammaRIIIa polymorphisms. *British journal of haematology* (2004) **124**(4):511-8. Epub 2004/02/27. PubMed PMID: 14984503.

118. Mouzaki A, Theodoropoulou M, Gianakopoulos I, Vlaha V, Kyrtsonis MC, Maniatis A. Expression patterns of Th1 and Th2 cytokine genes in childhood idiopathic thrombocytopenic purpura (ITP) at presentation and their modulation by intravenous immunoglobulin G (IVIg) treatment: their role in prognosis. *Blood* (2002) **100**(5):1774-9. Epub 2002/08/15. PubMed PMID: 12176899.

119. Wei S, Kryczek I, Zou W. Regulatory T-cell compartmentalization and trafficking. *Blood* (2006) **108**(2):426-31. Epub 2006/03/16. doi: 10.1182/blood-2006-01-0177. PubMed PMID: 16537800; PubMed Central PMCID: PMCPmc1895488.

120. Iellem A, Mariani M, Lang R, Recalde H, Panina-Bordignon P, Sinigaglia F, et al. Unique chemotactic response profile and specific expression of chemokine receptors CCR4 and CCR8 by CD4(+)CD25(+) regulatory T cells. *J Exp Med* (2001) **194**(6):847-53. Epub 2001/09/19. PubMed PMID: 11560999; PubMed Central PMCID: PMCPmc2195967.

121. Matsushima H, Takashima A. Bidirectional homing of Tregs between the skin and lymph nodes. *The Journal of clinical investigation* (2010) **120**(3):653-6. Epub 2010/02/25. doi: 10.1172/jci42280. PubMed PMID: 20179349; PubMed Central PMCID: PMCPmc2827968.

122. Tha-In T, Metselaar HJ, Tilanus HW, Groothuismink ZM, Kuipers EJ, de Man RA, et al. Intravenous immunoglobulins suppress T-cell priming by modulating the bidirectional

interaction between dendritic cells and natural killer cells. *Blood* (2007) **110**(9):3253-62. doi: 10.1182/blood-2007-03-077057. PubMed PMID: 17673603.

Chapter 2:

Dendritic cells as activators of effector T cell function

Gabriel N Kaufman

This chapter covers some of the pertinent background information which provides the larger context for the research articles presented in chapters 3 and 4 of this thesis. The history, current clinical use, and potential mechanisms of action of IVIg, along with the relationships between IVIg and regulatory T cell (Treg) responses, are discussed in the review paper that we present in its entirety in chapter 1. As we discuss in our research manuscripts (chapters 3 and 4), dendritic cells (DC) are the target cell for IVIg in our model. We therefore present here some general lines of dendritic cell (DC) biology, focusing on effector T cell activation, since tolerizing T cells and shifting the effector T cell balance from proinflammatory to regulatory represents a crucial mechanism of action of IVIg in allergic airways disease. (DC also interact directly with B cells: this is beyond the scope of the present author's research work, and therefore not covered in this overview.)

T cell activation

As reviewed by Thaiss et al. (1), T cells require three signals for immune-response functional activation. The first signal defines specificity, the second signal causes immunogenicity, and the third signal modulates the function of the activated T cell. The molecular correlates of this three-signal model are (1) antigen presentation; (2) costimulation; and (3) secretion of cytokines. This contributes to T cell polarization, which is the restriction of an activated T cell to a defined cytokine production pattern (2). For example, T helper cells are divided into differently polarised subsets: Th1 cells are characterized by IL-12 and IFN-γ secretion, Th2 by IL-4 and IL-10 secretion,

and Th17 by secretion of IL-17 family cytokines. We discuss these functions as performed by dendritic cells.

Dendritic cells

Phenotype

As a former mentor of this author once said, “An immunologist’s definition of a cell is very approximate: if it expresses enough markers, we call it ‘cell type X’ ” (Jörg H Fritz, personal communication). We therefore open with a brief discussion of DC phenotype.

Dendritic cells are divided into two main types: conventional (cDC) and plasmacytoid (pDC). Plasmacytoid dendritic cells were initially described as being associated with high endothelial venules (HEVs) (3) and displaying morphology similar to plasma cells. They express B220 (CD54R), blood dendritic cell antigen (BDCA)-2 (CD303) and ILT7 (immunoglobulin-like transcript 7), along with low levels of CD11c, major histocompatibility complex (MHC) class II (MHC-II), and costimulatory molecules in the steady state. Their main function is the production of Type I interferons upon recognition of non-self nucleic acids, after which they become activated and present antigen (4). We do not discuss them further in this overview, because our previous work has shown the importance of conventional DC for the actions of IVIg, to the exclusion of murine pDC (author’s unpublished observations using anti-mPDCA selection kits for murine DC).

The first cell-surface marker of cDC was determined to be CD11c integrin (5). Since that report, cDC have been extensively characterized since the advent of multi-parameter flow cytometry and transcriptional profiling. cDC constitutively express CD45 and MHC-II. However, macrophages also express these markers, compounding the difficulty of identifying distinct cell populations. Some investigators have used autofluorescence as a discriminating parameter, with AF-high cells being designated as macrophages. Transcriptional profiling has revealed several unique DC markers, including Flt3 (25, 26), c-kit, CCR7 (27), and the zinc-finger transcription factor zbtb46 (28, 29). Merad et al. (6), in an excellent review of DC phenotype and function, recommend to

include autofluorescence, as well as macrophage markers such as CSF1R (CD115), FcγRI (CD64), and F4/80 in the mouse, when assaying for dendritic cells by flow cytometry.

History

DC, the professional antigen-presenting cell (APC) of the immune system, represent the bridge between innate and adaptive immunity. First described in 1973 as an "accessory cell" in the population of splenic lymphocytes (7), they were named for their tree-like processes (*dendreon* is Greek for "tree"). DC were shown to express high levels of MHC-II (8). These cells strongly stimulated the mixed-lymphocyte reaction, with hundred-fold efficiency over whole-splenocyte preparations (9). DC were formally characterized as APC by their ability to present the trinitrophenol antigen (10). *In vitro* antibody production assays revealed that DC activated $CD4^+$ helper T cells, which would then help B cells produce antibody (11, 12). Similarly, DC stimulated the differentiation and activation of $CD8^+$ cytotoxic T cells in mixed-culture *in vitro* assays (13, 14). Immunohistochemical examination of peripheral lymphoid organs showed that MHC-II-expressing DC were found in T cell areas, suggesting an *in vivo* role for DC in initiating T cell responses (15).

Antigen uptake and presentation

DC express many receptors that aid in antigen uptake, mostly calcium-dependent or C-type lectin receptors (16). These pattern-recognition receptors (PPR) recognize pathogen-associated molecular patterns (PAMP) on microbes, largely glycosyl residues. (Due to the reality that not all PPR ligands are indeed pathogen-associated, some investigators (17) have recommended the term MAMP, or microbe-associated molecular patterns. The present author notes that these molecular patterns can also be found on entities besides microbes, and would humbly suggest that perhaps a different acronym is called for!) DC PPR function to mediate endocytosis, sometimes in association with other signalling molecules such as Toll-like receptors (TLRs),

trafficking to distinct antigen-processing compartments depending on cytoplasmic receptor domains.

Different routes of endocytosis are employed by DC depending on the type of antigen and the required presentation strategy. Antigens produced intracellularly, mostly peptides from viral infection or cytosolic bacteria, are presented in MHC class I (MHC-I). MHC-I cross-presentation can also occur after virus phagocytosis or micropinocytosis. MHC-I, expressed by all nucleated cells, presents peptide antigens to effector $CD8^+$ cytotoxic T cells, which leads to T-cell-mediated killing of the target cell. Antigens presented in MHC-II, which is a characteristic of professional APC, are generally of extracellular origin, such as from microbes or soluble antigens – including allergens. These are endocytosed by phagocytosis or micropinocytosis, processed in acidified endocytic vesicles, and are presented as peptides in the context of MHC-II to effector $CD4^+$ helper T cells. The interaction between processed antigen in MHC and the antigen-specific T cell receptor (TCR) provides “Signal 1” in effector T cells (18).

Costimulation

Subsequent to the MHC:peptide signal, DC provide co-stimulation, which correlates with “Signal 2” in T cells. This antigen-nonspecific co-stimulation, or the provision of context to antigen presentation, determines the type of effector cell response. The pattern of DC costimulatory molecule expression, along with the differentiation state of the receiving T cell and the cytokine milieu, affects the balance of immunogenicity versus tolerance (19).

Jenkins and Schwartz (20) provided the initial evidence for the requirement of a second signalling event from DC to T cells, in that T cells activated by TCR engagement alone became anergic. Later reports delineated the main costimulatory molecule CD80 or B7-1 (21) as the ligand for the T cell surface molecule CD28 (22), which is responsible for activating and polarizing T cells. CD86 or B7-2 was also identified as a ligand for CD28 (23). CD28 ligation allows T cells to proliferate and secrete IL-2 and other cytokines (24), and increase their glucose metabolism (25). CD80/86-CD28

interactions are also important in promoting tolerance: CD28 stimulation of double-positive thymocytes induces Foxp3 expression and Treg differentiation (26). CD80 and CD86 also bind to the CD28 homolog CTLA-4, which, in contrast, inhibits T cell proliferation, cell cycle progression, and IL-2 synthesis (27). Furthermore, CTLA-4 binding of DC CD80/CD86 increases the activity of the immunomodulatory enzyme indoleamine 2,3-dioxygenase (IDO) in DC (28). This provides a negative feedback loop for DC-mediated activation of T cells (29, 30).

T cells also express inducible T cell co-stimulator (ICOS), which is ligated by ICOS ligand (ICOSL or B7-H2) expressed on APC (31). ICOS ligation amplifies effector T cell responses, regardless of polarization (32). ICOSL/ICOS interactions are also required for IL10 production by Treg; this is blocked by CD28 signalling subsequent to CD80/CD86 ligation (33), providing another negative feedback loop.

DC express a pair of ligands for the programed cell death-1 (PD-1) receptor on T cells. PD-L1 is constitutively expressed on resting DC, among other hematopoietic and non-hematopoietic cells (34) while PD-L2 is only expressed on APC (35). These are upregulated in response to activating stimuli such as LPS, anti-CD40, GM-CSF, IL-4, IFN-γ, and IL-12 (36). Ligation of PD-1 leads to inhibition of the PI3K/AKT pathway: in the presence of TGF-β this biases naïve T cells towards Treg development and survival (37).

OX40 ligand (OX40L), a tumor necrosis factor family molecule, is expressed on professional APC such as DC, macrophages, and B cells, activated T cells, as well as on many other immune and non-immune cell types (38, 39). OX40L:OX40 interactions are required for primary and memory Th2 responses (40). Ito et al. (41) showed that OX40L inhibited Treg differentiation from naïve T cell precursors, as well as Treg IL-10 production. Additionally, Vu et al. (42) demonstrated that OX40 is a negative regulator of Treg differentiation, inhibiting Foxp3 expression and Treg suppressive abilities.

Cytokine production

T cells require cytokine stimulation, termed "Signal 3," for functional expansion and differentiation (43). The particular pattern of cytokine stimulation provided by the APC will influence the final functional differentiation of the target T cell. (Although autocrine and paracrine T cell cytokine stimulation does play an important role in T cell proliferation and differentiation – primarily via interleukin (IL)-2 secretion and response – we concentrate here on the DC:T cell stimulation axis.) $CD8^+$ T cells require IL-12 and type I interferons (IFN-α, IFN-β) in order to stage a productive effector response (44). IL-12 leads to expression of the T-bet transcription factor, which leads to an enforcer phenotype (45). These inflammatory cytokines and IL-2 shift the balance to short-lived effector responses, while IL-21 is beneficial, if not absolutely required, for the development and maintenance of a pool of central memory cytotoxic T cells (46, 47).

$CD4^+$ T cells differentiate into several distinct effector populations, divided by function. T helper cells are divided into Th1, Th2, Th17, and Tfh (T follicular helper) cells based on the patterns of cytokines that they secrete. They are required for virtually all adaptive immune responses. For example, Th1 cells activate macrophages to kill intracellular pathogens, Th2 cells recruit granulocytes and promote mucosal immunity, Th17 cells recruit neutrophils, and Tfh cells help lymphoid follicular B cells to produce specific antibody classes. $CD4^+$ T cells also differentiate into Treg, which suppress T cell activity and prevent autoimmune responses. These varied effector functions are specified by different Signal 3 cytokine stimuli from the APC, as well as T cell master-regulator expression and and cytokine production. It must be noted at this juncture that significant Th plasticity exists, and that cells can change effector function depending on combinations of master-regulator expression (48).

IL-1 is able to act on $CD4^+$ T cells to initiate an effector response and to support the generation of a memory population, even though its absolute requirement is not established (49). The cytokines that drive Th1 development are IFN-γ and IL-12, which stimulate the JAK-STAT pathway in order to activate STAT1 which induces T-bet expression, and STAT4 which promotes expansion

and differentiation of the committed Th1 population. Th1 cells also secrete IFN-γ in an autocrine manner in response to encountering antigen (50). Th2 cells are triggered by IL-4 secretion by APC, which activates STAT6, promoting GATA3 expression. GATA3 is the master regulator of Th2 cytokine gene expression; it also represses Th1-associated STAT4, IL-12 receptor β2, and Runx3 (51). Th17 cells, named for their characteristic secretion of IL-17 family cytokines, are differentiated in the presence of IL-6 and TGF-β (52). Tfh cells require IL-6 from APC, which induces autocrine IL-21 production. These cytokines stimulate the expression of the Tfh master transcription factor Bcl6, which is required for the expression of the CXCR5 receptor, the homing receptor for CXCL13 produced by follicular stromal cells (53). Treg are induced by a tolerogenic cytokine environment: initial IL-10, TNF-α, TGF-β secretion in the absence of IL-6 leads to peripherally-induced Treg (pTreg), which produce IL-10 and TGF-β themselves. As detailed by Kornete and Piccirillo (54), DC secrete the inflammatory mediators retinoic acid, vitamin D, and thymic stromal lymphopoietin (TSLP), that all play roles in Treg differentiation. Additionally, Treg express cell-surface markers that promote DC tolerogenicity: LAG-3 decreases antigen presentation, NRP-1 prolongs Treg:DC interactions, and LFA-1 promotes the formation of T cell aggregates around immature DC.

References

1. Thaiss CA, Semmling V, Franken L, Wagner H, Kurts C. Chemokines: a new dendritic cell signal for T cell activation. *Front Immunol* (2011) **2**:31. doi: 10.3389/fimmu.2011.00031. PubMed PMID: 22566821; PubMed Central PMCID: PMCPMC3342358.

2. Swain SL. T-cell subsets. Who does the polarizing? *Curr Biol* (1995) **5**(8):849-51. PubMed PMID: 7583138.

3. Facchetti F, de Wolf-Peeters C, van den Oord JJ, de Vos R, Desmet VJ. Plasmacytoid monocytes (so-called plasmacytoid T-cells) in Kikuchi's lymphadenitis. An immunohistologic study. *Am J Clin Pathol* (1989) **92**(1):42-50. PubMed PMID: 2787597.

4. Reizis B, Bunin A, Ghosh HS, Lewis KL, Sisirak V. Plasmacytoid dendritic cells: recent progress and open questions. *Annu Rev Immunol* (2011) **29**:163-83. doi: 10.1146/annurev-immunol-031210-101345. PubMed PMID: 21219184; PubMed Central PMCID: PMCPMC4160806.

5. Metlay JP, Witmer-Pack MD, Agger R, Crowley MT, Lawless D, Steinman RM. The distinct leukocyte integrins of mouse spleen dendritic cells as identified with new hamster monoclonal antibodies. *J Exp Med* (1990) **171**(5):1753-71. PubMed PMID: 2185332; PubMed Central PMCID: PMCPMC2187889.

6. Merad M, Sathe P, Helft J, Miller J, Mortha A. The dendritic cell lineage: ontogeny and function of dendritic cells and their subsets in the steady state and the inflamed setting. *Annu Rev Immunol* (2013) **31**:563-604. doi: 10.1146/annurev-immunol-020711-074950. PubMed PMID: 23516985; PubMed Central PMCID: PMCPMC3853342.

7. Steinman RM, Cohn ZA. Identification of a novel cell type in peripheral lymphoid organs of mice. I. Morphology, quantitation, tissue distribution. *J Exp Med* (1973) **137**(5):1142-62. PubMed PMID: 4573839; PubMed Central PMCID: PMCPMC2139237.

8. Steinman RM, Kaplan G, Witmer MD, Cohn ZA. Identification of a novel cell type in peripheral lymphoid organs of mice. V. Purification of spleen dendritic cells, new surface markers, and maintenance in vitro. *J Exp Med* (1979) **149**(1):1-16. PubMed PMID: 762493; PubMed Central PMCID: PMCPMC2184752.

9. Steinman RM, Witmer MD. Lymphoid dendritic cells are potent stimulators of the primary mixed leukocyte reaction in mice. *Proc Natl Acad Sci U S A* (1978) **75**(10):5132-6. PubMed PMID: 154105; PubMed Central PMCID: PMCPMC336278.

10. Nussenzweig MC, Steinman RM, Gutchinov B, Cohn ZA. Dendritic cells are accessory cells for the development of anti-trinitrophenyl cytotoxic T lymphocytes. *J Exp Med* (1980) **152**(4):1070-84. PubMed PMID: 6968335; PubMed Central PMCID: PMCPMC2185968.

11. Inaba K, Steinman RM. Resting and sensitized T lymphocytes exhibit distinct stimulatory (antigen-presenting cell) requirements for growth and lymphokine release. *J Exp Med* (1984) **160**(6):1717-35. PubMed PMID: 6239901; PubMed Central PMCID: PMCPMC2187515.

12. Inaba K, Steinman RM. Protein-specific helper T-lymphocyte formation initiated by dendritic cells. *Science* (1985) **229**(4712):475-9. PubMed PMID: 3160115.

13. Inaba K, Young JW, Steinman RM. Direct activation of CD8+ cytotoxic T lymphocytes by dendritic cells. *J Exp Med* (1987) **166**(1):182-94. PubMed PMID: 2955069; PubMed Central PMCID: PMCPMC2188638.

14. Young JW, Steinman RM. Dendritic cells stimulate primary human cytolytic lymphocyte responses in the absence of CD4+ helper T cells. *J Exp Med* (1990) **171**(4):1315-32. PubMed PMID: 2139102; PubMed Central PMCID: PMCPMC2187833.

15. Witmer-Pack MD, Olivier W, Valinsky J, Schuler G, Steinman RM. Granulocyte/macrophage colony-stimulating factor is essential for the viability and function of cultured murine epidermal Langerhans cells. *J Exp Med* (1987) **166**(5):1484-98. PubMed PMID: 2445889; PubMed Central PMCID: PMCPMC2189651.

16. Steinman RM, Hemmi H. Dendritic cells: translating innate to adaptive immunity. *Curr Top Microbiol Immunol* (2006) **311**:17-58. PubMed PMID: 17048704.

17. Didierlaurent A, Simonet M, Sirard JC. Innate and acquired plasticity of the intestinal immune system. *Cell Mol Life Sci* (2005) **62**(12):1285-7. doi: 10.1007/s00018-005-5032-4. PubMed PMID: 15971103; PubMed Central PMCID: PMCPMC1865479.

18. Guermonprez P, Valladeau J, Zitvogel L, Thery C, Amigorena S. Antigen presentation and T cell stimulation by dendritic cells. *Annu Rev Immunol* (2002) **20**:621-67. doi: 10.1146/annurev.immunol.20.100301.064828. PubMed PMID: 11861614.

19. Hubo M, Trinschek B, Kryczanowsky F, Tuettenberg A, Steinbrink K, Jonuleit H. Costimulatory molecules on immunogenic versus tolerogenic human dendritic cells. *Front Immunol* (2013) **4**:82. doi: 10.3389/fimmu.2013.00082. PubMed PMID: 23565116; PubMed Central PMCID: PMCPMC3615188.

20. Jenkins MK, Schwartz RH. Pillars article: antigen presentation by chemically modified splenocytes induces antigen-specific T cell unresponsiveness in vitro and in vivo. J. Exp. Med. 1987. 165: 302-319. *J Immunol* (2009) **183**(7):4150-67. PubMed PMID: 19767565.

21. Freeman GJ, Freedman AS, Segil JM, Lee G, Whitman JF, Nadler LM. B7, a new member of the Ig superfamily with unique expression on activated and neoplastic B cells. *J Immunol* (1989) **143**(8):2714-22. PubMed PMID: 2794510.

22. Linsley PS, Clark EA, Ledbetter JA. T-cell antigen CD28 mediates adhesion with B cells by interacting with activation antigen B7/BB-1. *Proc Natl Acad Sci U S A* (1990) **87**(13):5031-5. PubMed PMID: 2164219; PubMed Central PMCID: PMCPMC54255.

23. Azuma M, Ito D, Yagita H, Okumura K, Phillips JH, Lanier LL, et al. B70 antigen is a second ligand for CTLA-4 and CD28. *Nature* (1993) **366**(6450):76-9. doi: 10.1038/366076a0. PubMed PMID: 7694153.

24. Linsley PS, Brady W, Grosmaire L, Aruffo A, Damle NK, Ledbetter JA. Binding of the B cell activation antigen B7 to CD28 costimulates T cell proliferation and interleukin 2 mRNA accumulation. *J Exp Med* (1991) **173**(3):721-30. PubMed PMID: 1847722; PubMed Central PMCID: PMCPMC2118836.

25. Frauwirth KA, Riley JL, Harris MH, Parry RV, Rathmell JC, Plas DR, et al. The CD28 signaling pathway regulates glucose metabolism. *Immunity* (2002) **16**(6):769-77. PubMed PMID: 12121659.

26. Tai X, Cowan M, Feigenbaum L, Singer A. CD28 costimulation of developing thymocytes induces Foxp3 expression and regulatory T cell differentiation independently of interleukin 2. *Nat Immunol* (2005) **6**(2):152-62. doi: 10.1038/ni1160. PubMed PMID: 15640801.

27. Walunas TL, Bakker CY, Bluestone JA. CTLA-4 ligation blocks CD28-dependent T cell activation. *J Exp Med* (1996) **183**(6):2541-50. PubMed PMID: 8676075; PubMed Central PMCID: PMCPMC2192609.

28. Fallarino F, Grohmann U, Hwang KW, Orabona C, Vacca C, Bianchi R, et al. Modulation of tryptophan catabolism by regulatory T cells. *Nat Immunol* (2003) **4**(12):1206-12. doi: 10.1038/ni1003. PubMed PMID: 14578884.

29. Greene JL, Leytze GM, Emswiler J, Peach R, Bajorath J, Cosand W, et al. Covalent dimerization of CD28/CTLA-4 and oligomerization of CD80/CD86 regulate T cell costimulatory interactions. *J Biol Chem* (1996) **271**(43):26762-71. PubMed PMID: 8900156.

30. Carreno BM, Bennett F, Chau TA, Ling V, Luxenberg D, Jussif J, et al. CTLA-4 (CD152) can inhibit T cell activation by two different mechanisms depending on its level of cell surface expression. *J Immunol* (2000) **165**(3):1352-6. PubMed PMID: 10903737.

31. Yoshinaga SK, Whoriskey JS, Khare SD, Sarmiento U, Guo J, Horan T, et al. T-cell co-stimulation through B7RP-1 and ICOS. *Nature* (1999) **402**(6763):827-32. doi: 10.1038/45582. PubMed PMID: 10617205.

32. Wassink L, Vieira PL, Smits HH, Kingsbury GA, Coyle AJ, Kapsenberg ML, et al. ICOS expression by activated human Th cells is enhanced by IL-12 and IL-23: increased ICOS expression

enhances the effector function of both Th1 and Th2 cells. *J Immunol* (2004) **173**(3):1779-86. PubMed PMID: 15265908.

33. Tuettenberg A, Huter E, Hubo M, Horn J, Knop J, Grimbacher B, et al. The role of ICOS in directing T cell responses: ICOS-dependent induction of T cell anergy by tolerogenic dendritic cells. *J Immunol* (2009) **182**(6):3349-56. doi: 10.4049/jimmunol.0802733. PubMed PMID: 19265111.

34. Yamazaki T, Akiba H, Iwai H, Matsuda H, Aoki M, Tanno Y, et al. Expression of programmed death 1 ligands by murine T cells and APC. *J Immunol* (2002) **169**(10):5538-45. PubMed PMID: 12421930.

35. Zhong X, Tumang JR, Gao W, Bai C, Rothstein TL. PD-L2 expression extends beyond dendritic cells/macrophages to B1 cells enriched for V(H)11/V(H)12 and phosphatidylcholine binding. *Eur J Immunol* (2007) **37**(9):2405-10. doi: 10.1002/eji.200737461. PubMed PMID: 17683117.

36. Loke P, Allison JP. PD-L1 and PD-L2 are differentially regulated by Th1 and Th2 cells. *Proc Natl Acad Sci U S A* (2003) **100**(9):5336-41. doi: 10.1073/pnas.0931259100. PubMed PMID: 12697896; PubMed Central PMCID: PMCPMC154346.

37. Francisco LM, Sage PT, Sharpe AH. The PD-1 pathway in tolerance and autoimmunity. *Immunol Rev* (2010) **236**:219-42. doi: 10.1111/j.1600-065X.2010.00923.x. PubMed PMID: 20636820; PubMed Central PMCID: PMCPMC2919275.

38. Croft M, So T, Duan W, Soroosh P. The significance of OX40 and OX40L to T-cell biology and immune disease. *Immunol Rev* (2009) **229**(1):173-91. doi: 10.1111/j.1600-065X.2009.00766.x. PubMed PMID: 19426222; PubMed Central PMCID: PMCPMC2729757.

39. Webb GJ, Hirschfield GM, Lane PJ. OX40, OX40L and Autoimmunity: a Comprehensive Review. *Clin Rev Allergy Immunol* (2016) **50**(3):312-32. doi: 10.1007/s12016-015-8498-3. PubMed PMID: 26215166.

40. Jenkins SJ, Perona-Wright G, Worsley AG, Ishii N, MacDonald AS. Dendritic cell expression of OX40 ligand acts as a costimulatory, not polarizing, signal for optimal Th2 priming and memory induction in vivo. *J Immunol* (2007) **179**(6):3515-23. PubMed PMID: 17785785.

41. Ito T, Wang YH, Duramad O, Hanabuchi S, Perng OA, Gilliet M, et al. OX40 ligand shuts down IL-10-producing regulatory T cells. *Proc Natl Acad Sci U S A* (2006) **103**(35):13138-43. doi: 10.1073/pnas.0603107103. PubMed PMID: 16924108; PubMed Central PMCID: PMCPMC1559766.

42. Vu MD, Xiao X, Gao W, Degauque N, Chen M, Kroemer A, et al. OX40 costimulation turns off Foxp3+ Tregs. *Blood* (2007) **110**(7):2501-10. doi: 10.1182/blood-2007-01-070748. PubMed PMID: 17575071; PubMed Central PMCID: PMCPMC1988917.

43. Curtsinger JM, Schmidt CS, Mondino A, Lins DC, Kedl RM, Jenkins MK, et al. Inflammatory cytokines provide a third signal for activation of naive CD4+ and CD8+ T cells. *J Immunol* (1999) **162**(6):3256-62. PubMed PMID: 10092777.

44. Mescher MF, Curtsinger JM, Agarwal P, Casey KA, Gerner M, Hammerbeck CD, et al. Signals required for programming effector and memory development by CD8+ T cells. *Immunol Rev* (2006) **211**:81-92. doi: 10.1111/j.0105-2896.2006.00382.x. PubMed PMID: 16824119.

45. Joshi NS, Cui W, Chandele A, Lee HK, Urso DR, Hagman J, et al. Inflammation directs memory precursor and short-lived effector CD8(+) T cell fates via the graded expression of T-bet transcription factor. *Immunity* (2007) **27**(2):281-95. doi: 10.1016/j.immuni.2007.07.010. PubMed PMID: 17723218; PubMed Central PMCID: PMCPMC2034442.

46. Kaka AS, Shaffer DR, Hartmaier R, Leen AM, Lu A, Bear A, et al. Genetic modification of T cells with IL-21 enhances antigen presentation and generation of central memory tumor-specific cytotoxic T-lymphocytes. *J Immunother* (2009) **32**(7):726-36. doi: 10.1097/CJI.0b013e3181ad4071. PubMed PMID: 19561536; PubMed Central PMCID: PMCPMC2790367.

47. Cox MA, Harrington LE, Zajac AJ. Cytokines and the inception of CD8 T cell responses. *Trends Immunol* (2011) **32**(4):180-6. doi: 10.1016/j.it.2011.01.004. PubMed PMID: 21371940; PubMed Central PMCID: PMCPMC3074938.

48. O'Shea JJ, Paul WE. Mechanisms underlying lineage commitment and plasticity of helper CD4+ T cells. *Science* (2010) **327**(5969):1098-102. doi: 10.1126/science.1178334. PubMed PMID: 20185720; PubMed Central PMCID: PMCPMC2997673.

49. Ben-Sasson SZ, Hu-Li J, Quiel J, Cauchetaux S, Ratner M, Shapira I, et al. IL-1 acts directly on CD4 T cells to enhance their antigen-driven expansion and differentiation. *Proc Natl Acad Sci U S A* (2009) **106**(17):7119-24. doi: 10.1073/pnas.0902745106. PubMed PMID: 19359475; PubMed Central PMCID: PMCPMC2678417.

50. Szabo SJ, Sullivan BM, Peng SL, Glimcher LH. Molecular mechanisms regulating Th1 immune responses. *Annu Rev Immunol* (2003) **21**:713-58. doi: 10.1146/annurev.immunol.21.120601.140942. PubMed PMID: 12500979.

51. Yagi R, Zhu J, Paul WE. An updated view on transcription factor GATA3-mediated regulation of Th1 and Th2 cell differentiation. *Int Immunol* (2011) **23**(7):415-20. doi: 10.1093/intimm/dxr029. PubMed PMID: 21632975; PubMed Central PMCID: PMCPMC3123974.

52. Weaver CT, Harrington LE, Mangan PR, Gavrieli M, Murphy KM. Th17: an effector CD4 T cell lineage with regulatory T cell ties. *Immunity* (2006) **24**(6):677-88. doi: 10.1016/j.immuni.2006.06.002. PubMed PMID: 16782025.

53. Johnston RJ, Poholek AC, DiToro D, Yusuf I, Eto D, Barnett B, et al. Bcl6 and Blimp-1 are reciprocal and antagonistic regulators of T follicular helper cell differentiation. *Science* (2009) **325**(5943):1006-10. doi: 10.1126/science.1175870. PubMed PMID: 19608860; PubMed Central PMCID: PMCPMC2766560.

54. Kornete M, Piccirillo CA. Functional crosstalk between dendritic cells and Foxp3(+) regulatory T cells in the maintenance of immune tolerance. *Front Immunol* (2012) **3**:165. doi: 10.3389/fimmu.2012.00165. PubMed PMID: 22737152; PubMed Central PMCID: PMCPMC3381230.

Chapter 3:

Intravenous immune globulin requires the inhibitory Fc gamma receptor IIb, but not activating Fc gamma receptors, to ameliorate murine allergic airways disease

Gabriel N Kaufman[1], Marieme Dembele[1], Amir H Massoud[1*], Marianne Béland[1], Bruce D Mazer[1,2]

1 Translational Research in Respiratory Diseases (TRR) Program, The Research Institute of the McGill University Health Centre, Montreal, Quebec, H4A 3J1, Canada

2 Department of Pediatrics, McGill University Faculty of Medicine, Montreal, Quebec, H4A 3J1, Canada

* Present address: Division of Immunology Research, Boston Children's Hospital, Boston, Massachusetts, 02115, USA.

Corresponding author:
Bruce D Mazer MD
1001 Decarie Blvd
Mail stop EM3.2219
Montreal, Quebec
Canada H4A 3J1

Phone: 514-934-1934 ext 76447
Fax: 514-933-3962
Email: bruce.mazer@mcgill.ca

The following chapter presents an investigation into the requirement for IgG Fc receptors on DC for the tolerogenic effects of IVIg. Previous work from our laboratory had shown that IVIg binds to dendritic cell immunoreceptor (DCIR), a C-type lectin receptor on DC. We therefore wanted to exclude the effects of the canonical IgG receptor family, the Fc gamma receptors, by using knockout mouse strains. To our surprise, we found that while the activating Fc gamma receptors were dispensable for the anti-inflammatory actions of IVIg, the inhibitory Fc gamma receptor IIb (FcγRIIb) was required for the IVIg-mediated abrogation of AAD and the induction of Treg. Furthermore, we determined that this receptor's expression was specifically required on DC for Treg induction; DC deficient in FcγRIIb have deficient antigen uptake inhibition in response to IVIg treatment.

The present author's contributions to this paper consisted of study design, method optimization, data generation for Figures 3 through 6, and writing the manuscript. His colleagues' contributions were as follows: data generation for Figure 7, writing associated methods and results text, Marieme Dembele; flow cytometric sample preparation and acquisition for Figure 4C, Marianne Béland.

Introduction

Intravenous immune globulin (IVIg) is a polyclonal IgG preparation from pooled human serum. Classically administered as an antibody-replacement therapy, IVIg has anti-inflammatory properties when administered at high doses. The biological mechanisms of IVIg-mediated immunomodulation are not completely characterized, with several potential explanations proposed (1). A major area of investigation is the relationship of IVIg and Fc gamma receptors (FcγRs): several lines of evidence point to their role as canonical IgG receptors in the anti-inflammatory effects of IVIg (2). Studies from autoimmune disease models suggest a particular role for the inhibitory receptor FcγRIIb.

Fc gamma receptors

The fragment-crystallizable (Fc) portion of an antibody molecule is the tail portion of the antibody that is released by papain digestion. Fc receptors are the cell-surface receptors that bind the antibody Fc portion (3). They are expressed on a wide variety of cells, including many cell types from the lymphoid and myeloid lineages (Table 1) (4). Fc receptors are specific for immunoglobulin classes, with receptor affinity determined by immunoglobulin heavy chain. Specific Fc receptors exist for IgE, IgM, and IgA, as well as for IgG – receptor nomenclature uses the Greek letter for the specific heavy chain, which matches the specific α chain of the Fc receptor. (We limit our discussion here to the IgG Fc receptors).

Fc receptor	**Major isoforms expressed**	**Allotype**	**Specificity for human Ig**	**Cellular distribution**
FcγRI (CD64)	FcγRIa	---	IgG1=3>4 IgG2 does not bind	Monocytes, macrophages, neutrophils (IFN-γ stimulated),

Fc receptor	Major isoforms expressed	Allotype	Specificity for human Ig	Cellular distribution
				eosinophils (IFN-γ stimulated)
FcγRII (CD32)	FcγRIIa	Low responder	IgG3≥1=2 IgG4 doesn't bind	Monocytes, macrophages, neutrophils, platelets and Langerhans cells
	FcγRIIa	High responder	IgG3≥1>>>2 IgG4 doesn't bind	Monocytes, macrophages, neutrophils, platelets and Langerhans cells
	FcγRIIb	---	IgG3≥1>>2>4	Monocytes, macrophages, and B cells
	FcγRIIc	---	Not determined	Monocytes, macrophages, neutrophils, and B cells
FcγRIII (CD16)	FcγRIIIa	---	Not determined	Macrophages, NK cells, γδ T cells, and some monocytes
	FcγRIIIb	Neutrophil antigen 1, neutrophil antigen 2	IgG1=3>>>2=4	Neutrophils (IFN-γ stimulated), and eosinophils (IFN-γ stimulated)

Fc receptor	Major isoforms expressed	Allotype	Specificity for human Ig	Cellular distribution
FceRI	FceRI	---	IgE	Mast cells, basophils, Langerhans cells, and activated monocytes
FcεRII (CD23)	FcεRIIa	---	IgE	B cells
	FcεRIIb	---	IgE	B cells, T cells, monocytes, eosinophils, and macrophages
FcαRI (CD89)	FcαRIa	---	Serum IgA1=2, secretory IgA1=secretory IgA2	Neutrophils, monocytes, some macrophages, eosinophils, Kupffer cells, and some DCs

Table 1. Fc receptor expression on human leukocytes. Adapted from Woof et al (4).

Fc gamma receptors (FcγRs), the receptor family for IgG, typically bind IgG in the form of an immune complex (IC) with antigen, due to the relatively low binding affinities of individual IgG molecules for the FcγRs. The physiological reason behind this low binding affinity is to ensure that circulating monomeric IgG does not lead to inappropriate FcγR ligation (5). The only exception to this rule is the high-affinity FcγRI (6), which binds human IgG1 and IgG3, or IgG2a in the mouse. The first functions ascribed to FcγRs were elicited by studies of murine knockout models, where it was determined that FcγRs mediate IC-triggered inflammatory responses (7-9). IgG FC were also shown to inhibit B cell responses *in vitro* (10); later receptor characterization led to the identification of the inhibitory FcγRIIb.

Currently, FcγRs are known to be the main initiators of antibody-mediated cellular responses, thus playing a crucial role in effector cell activation. Furthermore, FcγRs are a prime example of balanced immunoreceptors, where the ratio of activating and inhibitory receptor expression on a given cell type establish the activation threshold and type of cellular response (11, 12). This activation/inhibition index, or threshold model of activation, allows for balancing of the immune-system activation state (13). FcγRs can modulate both afferent and efferent responses in either activation or inhibition contexts, ranging from shaping antibody repertoire to controlling APC immunogenicity to maintaining peripheral immune tolerance (5).

Canonical FcγRs, typically type I transmembrane glycoproteins, can be broadly divided into two categories based on their intracellular signaling domains. Activating FcγRs, which are composed of at least one common γ chain and a variant α chain, contain immunoreceptor tyrosine-based activation motifs (ITAM) linked to the γ chain(s). The inhibitory FcγRIIb, composed of only one α chain, contains an immunoreceptor tyrosine-based inhibitory motif (ITIM) (14) (Figure 1). Non-canonical FcγRs, such as the C-type lectin receptors, contain neither ITAM nor ITIM (5).

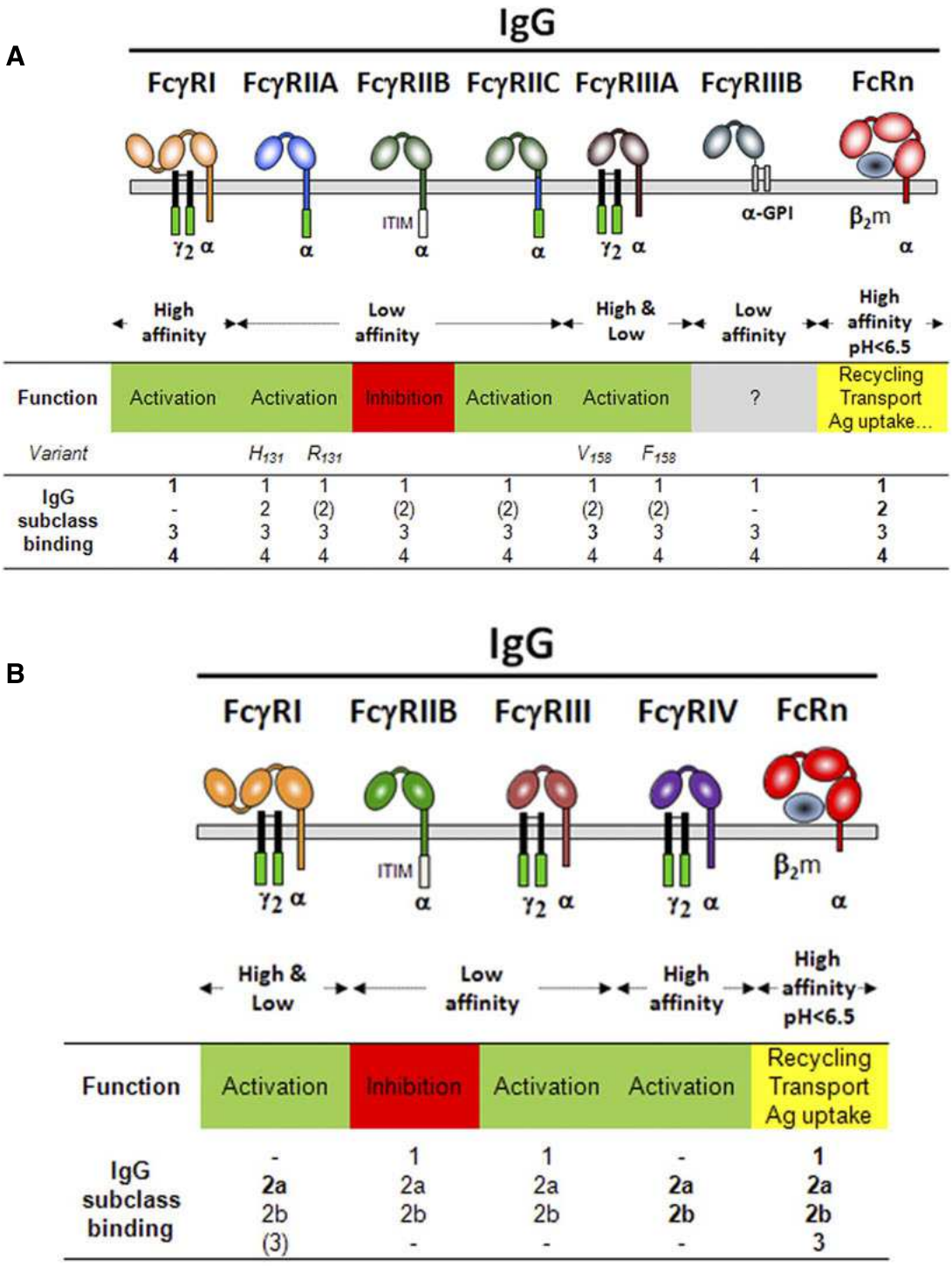

Figure 1: Schematics of FcγRs and IgG subclass binding in humans and mice.

Human (A) and mouse (B) IgG receptors, represented at the cell membrane (grey bar). ITAM, green box; ITIM, white box. From Bruhns (14).

FcγR signaling

The ITAM-containing activating FcγRs signal via Src family kinase phosphorylation of the two tyrosine residues in the ITAM and recruitment and activation of Syk family kinases, which bind to the phosphorylated ITAM via their tandem SH2 domains. Downstream events from Syk activation include PI3K recruitment and phosphorylation, which allows PIP3 production. PH-domain-containing molecules such as Btk and PLCγ are thereby recruited to the membrane, resulting in calcium flux and cellular activation (15). The ITIM-containing inhibitory FcγRIIb, which is expressed by most hemaopoietic cells, functions to modulate activation thresholds and maintain immune tolerance (16). This receptor signals via Src family kinase phosphorylation of the tyrosine residue in the ITIM and recruitment of the inhibitory phosphatase SHIP, which binds to the phosphorylated ITIM via its SH2 domain. SHIP catalyzes the conversion of PIP3 into PIP2, blocking Btk and PLCγ membrane recruitment, thus inhibiting calcium release and reducing cell activation (17) (Figure 2).

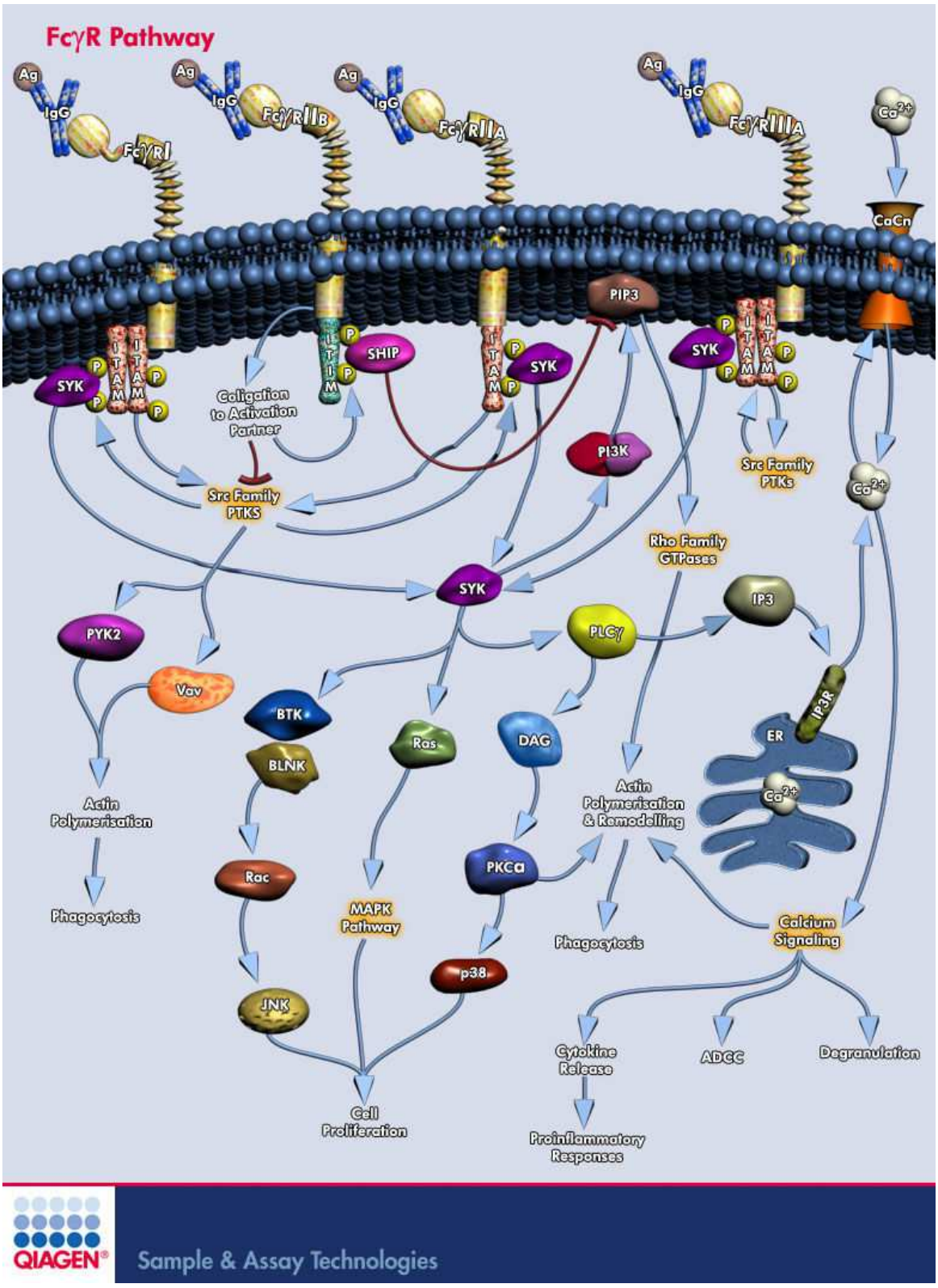

Figure 2: FcγR signalling pathway. From Qiagen GeneGlobe database (18).

IVIg and FcγRIIb

It has been postulated that IVIg upregulates FcγRIIb on effector cells such as dendritic cells or macrophages, which leads to tolerogenicity and immunomodulation. Schwab and Nimmerjahn (19) have extensively reviewed the evidence behind this theory, which has dominated much of the animal work on the mechanism of action of IVIg for the last 15 years. Most of these studies focused on murine models of autoimmunity, but there has been limited exploration of other inflammatory pathologies, such as allergic disease. It is unclear whether IVIg interacts directly with FcγRIIb or with other receptors. Zhuang et al. demonstrated that at least for human B lymphocytes, IVIg did not directly bind FcγRIIb or induce negative signaling (20). Moreover, we have demonstrated that a sialylated fraction of IVIg binds the C-type lectin receptor DCIR and is internalized in dendritic cells (21). Furthermore, Pincetic et al. (22) have proposed a novel theory of IgG conformational targeting, whereby the sialylation state of the IgG molecule affects its conformation and thus its target receptor, switching from classical (Type I) FcγRs in the open conformation, to C-type lectin receptors (Type II FcγRs) in the closed conformation, brought about by 2,6-sialylation of the IgG hinge region.

In the present study, we investigated the requirement of FcγRs for the anti-inflammatory actions of IVIg in a murine model of allergic airways disease (AAD). We determined that the activating FcγRs were dispensable, but the inhibitory FcγRIIb was required for IVIg-mediated abrogation of airway hyper-responsiveness and lung histopathology, along with Treg induction. Furthermore, we showed that FcγRIIb-deficient dendritic cells were unable to confer tolerance by adoptive transfer and displayed reduced antigen uptake efficiency.

Methods

Animal studies

All animal studies were conducted according to procedures reviewed and approved by the Faculty of Medicine's Faculty Animal Care Committee (FACC) at McGill University, in compliance with Canadian Council on Animal Care (CCAC) guidelines.

Mouse strains

All animals were purchased from Taconic and maintained in specific pathogen-free conditions in the vivarium of The Research Institute of the McGill University Health Centre. B6 wild-type (WT) mice were used as the control strain, and was the background for the knockout (ko) strains. Fcer1g ko mice (23), which lack the common γ chain subunit of ITAM-containing Fc gamma receptors and do not express FcγRI, FcγRIV, or FcγRIIA, were used as experimental strain 1. Fcgr2b ko mice (24), which lack the specific α chain of the ITIM-containing FcγRIIb and do not express FcγRIIb, were used as experimental strain 2. Both male and female mice were used at 6-8 weeks of age.

Allergic airways disease model

Mice were sensitized and challenged to OVA as previously described (25, 26). Animals were instilled with 10 µL in each nostril of a 10 mg/mL ovalbumin (OVA, Grade V, Sigma-Aldrich) solution in phosphate-buffered saline (PBS), or vehicle control, under gentle restraint without anaesthesia. Sensitization occurred on days 1-10, antigen re-exposure occurred at day 21, and challenge occurred on days 29-33. One day prior to antigen challenge (day 28), mice were treated by intraperitoneal injection (i.p.) with 2 g/kg IVIg (Grifols) or an equal volume of 5% human serum albumin (HSA) (Bayer) as control. Animals were used for airway hyper-responsiveness measurements on day 34.

Adoptive transfer of bone-marrow-derived dendritic cells

Dendritic cells were derived from bone marrow of naïve WT, Fcer1g ko, and Fcgr2b ko mice as per the protocol of Lutz et al. (27). Isolated bone marrow stromal cells were differentiated by GM-CSF treatment (20 ng/mL) in complete RPMI 1640 medium (2.5 mM L-glutamine, 10% FBS, Pen/Strep, 15 mM HEPES, 1 mM sodium pyruvate, and 50 µM 2-mercaptoethanol) for 6 days. Subsequently, bone-marrow-derived dendritic cells (BMDC) were washed, loaded with 1 mg/mL OVA and treated with 10 mg/mL IVIg for 24 hours (21). 1 million treated BMDC per mouse were extensively washed and adoptively transferred by intratracheal instillation (28) into recipient WT mice to induce AAD, as per the protocol of Koya et al. (29). Recipient WT mice were subjected to intranasal

challenge, as described above, on days 6-8 post-transfer, and used for airway hyper-responsiveness measurements on day 9.

Airway hyper-responsiveness to methacholine

Airway hyper-responsiveness was measured as described previously (26, 30) using the flexiVent small-animal ventilation system (SCIREQ). Mice were sedated with 10 mg/kg xylazine hydrochloride i.p., anaesthetized with 50 mg/kg sodium pentobarbital i.p., tracheotomised with an 18G Luer-stub cannula, and connected to the Y-adapter of the ventilator. Animals were subsequently paralyzed with 1.5 mg/kg rocuronium bromide i.p. and mechanically ventilated for the duration of the experiment. Methacholine (0-250 mg/mL in saline) was aerosolized into the inspiratory stream (4-second pulse), and lung resistance and elastance was measured after each dose by the forced-oscillation technique (31). Values reported are the mean of peak resistance and elastance for each methacholine instillation. Animals were euthanized by pentobarbital overdose following flexiVent measurements.

Histological analysis

Lungs from a subset of mice were fixed post-mortem by inflation with 10% neutral buffered formalin, processed, and embedded in paraffin using standard protocols. 5-micron sections were stained with hematoxylin and eosin (H&E) and examined by light microscopy.

Preparation of lung and spleen cell suspensions

Lungs and spleens from a subset of mice were dissected and digested with collagenase D (0.15 Wünsch U/mL) and DNAse I (0.1 mg/mL) (both from Roche Life Science) in phosphate-buffered saline, with 0.9 mM calcium chloride, 0.5 mM magnesium chloride hexahydrate, and 15 mM HEPES. Lungs were inflated with digestion enzyme solution before dissection. Red blood cells were lysed by ammonium chloride treatment. Single-cell suspensions were obtained by filtering through 40-µm mesh and resuspended in PBS without calcium or magnesium for flow cytometric analyses.

Flow cytometric analysis of Treg

Cell staining for flow cytometry was performed as described previously (21, 30). Cells were stained with a fixable protein-binding dye to assess viability (FVD; fixable viability dye), and Fc receptor binding was blocked using anti-CD16/32 antibody (Clone 93, BioLegend). Cells were subsequently incubated with appropriate fluorochrome-labeled antibodies for 30 minutes at 4°C in 100 µL PBS with 0.2% (w/v) bovine serum albumin (BSA). Cells were fixed and permeabilized using transcription-factor buffers (eBioscience) for intranuclear Foxp3 detection. Antibody concentrations were determined by titration for optimal signal-to-noise ratio. Samples were acquired on a BD LSR II or FACSCanto II flow cytometer using FACSDiva 6.0.3 software. Data analysis was performed offline using FlowJo v10.0.8 software (Treestar). Hierarchical gating strategies were specified manually for each cell population of interest as per the published gating strategy of d'Hennezel and Piccirillo (32).

Antigen uptake in BMDC

BMDC from WT, Fcer1g ko, and Fcgr2b ko mice, differentiated as described above, were treated with HSA or IVIg for 3 hours. They were then incubated with 10 ug/mL of OVA conjugated with AlexaFluor647 (OVA-Alexa647) (Thermo Fisher Scientific) for 1 hour at 37°C. Cells were harvested and processed for flow cytometry. Antigen uptake was assessed by gating on viable $CD11c^+$ cells and quantifying the median fluorescence intensity (MFI) of Alexa647. An uptake inhibition index was calculated as the ratio of the difference in MFI for OVA-Alexa647 between IVIg-treated and HSA-treated BMDC relative to the MFI of HSA-treated BMDC for cells from each mouse strain. The formula used was:

$$\text{Uptake inhibition index} = \frac{\text{MFI IVIg - MFI HSA}}{\text{MFI HSA}}$$

Statistics

Data analyses were performed using the R statistical environment (33). One or two-way analysis of variance (ANOVA) with Tukey post-hoc testing was used to determine statistical differences compared to control groups. flexiVent data was analyzed by repeated-measures ANOVA with

Tukey HSD (honest significant differences) post-hoc testing. Data represent at least two independent experiments per result. $P<0.05$ was considered statistically significant.

Results

IVIg requires the inhibitory FcγRIIb to abrogate allergic airways disease

To ascertain the requirement of FcγRIIb for the anti-inflammatory action of IVIg in an antigen-driven disease context, we subjected WT, Fcer1g ko, and Fcgr2b ko mice to OVA sensitization and challenge. All strains displayed increased AHR to inhaled methacholine, relative to vehicle controls, after OVA sensitization and challenge (Figure 3). IVIg treatment 24 h prior to challenge was sufficient to lower antigen-induced airway hyper-responsiveness to inhaled aerosol methacholine in both WT mice (Figure 3A-B) and Fcer1g ko mice (Figure 3C-D); they displayed lower overall lung resistance and elastance compared to sham-treated controls. Conversely, IVIg treatment was unable to block OVA-induced increased airway resistance and elastance in Fcrg2b ko mice (Figure 3E-F).

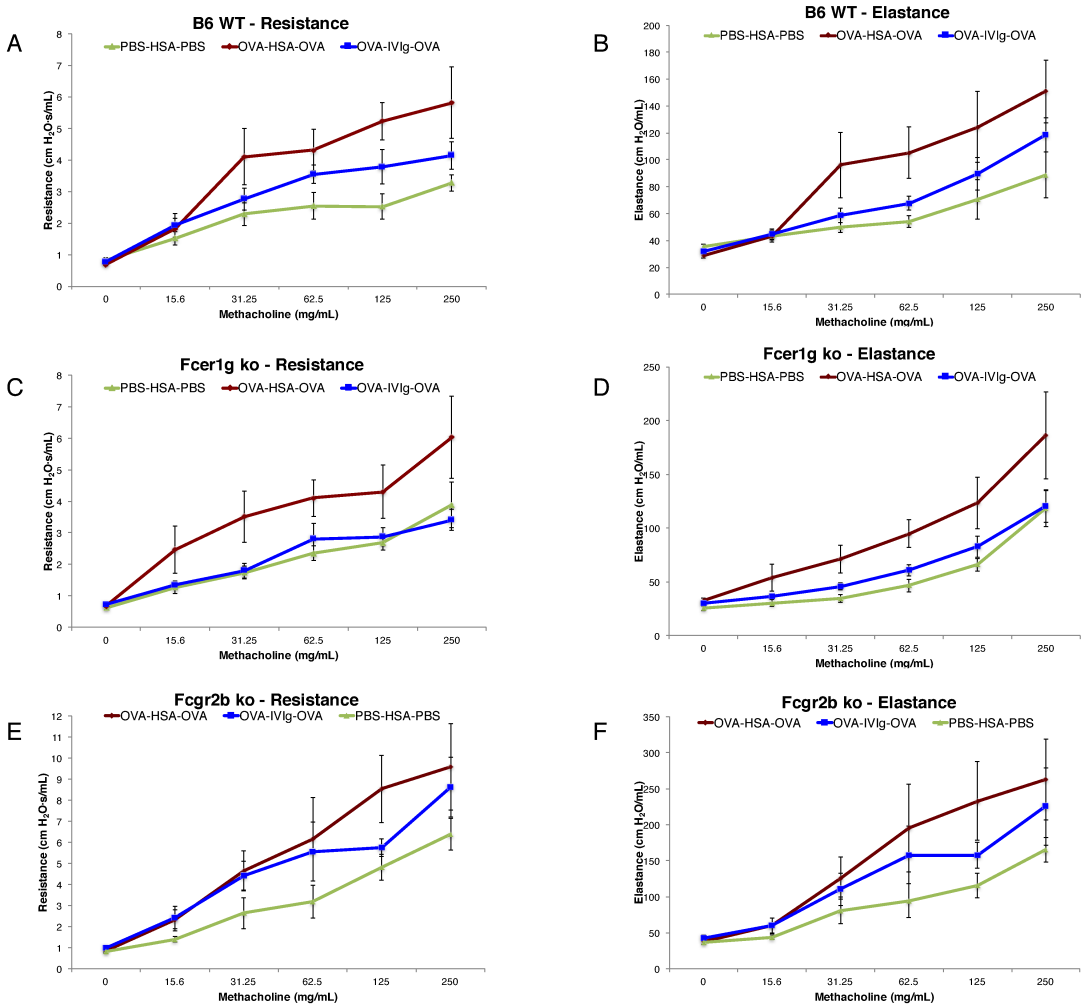

Figure 3: Resistance (A, C, E) and elastance (B, D, F) measurements from WT (A, B), Fcer1g ko (C, D), and Fcgr2b ko (E, F) mice. Graphs present mean ± SEM of measured parameters for dose of aerosolized methacholine administered. n=6-8 mice per group.

When examining lung sections, OVA-exposed animals from all strains show brush border disruption, goblet cell hyperplasia, and increased lymphocytic infiltration (Figure 4B,E,H). IVIg treatment ameliorates this histopathology in WT and Fcer1g ko mice (Figure 4C,F), but not in Fcgr2b mice (Figure 4I). These results suggest that IVIg is ineffective at protecting against OVA-induced airway hyper-responsiveness and lung histopathology when the inhibitory FcγRIIb is absent.

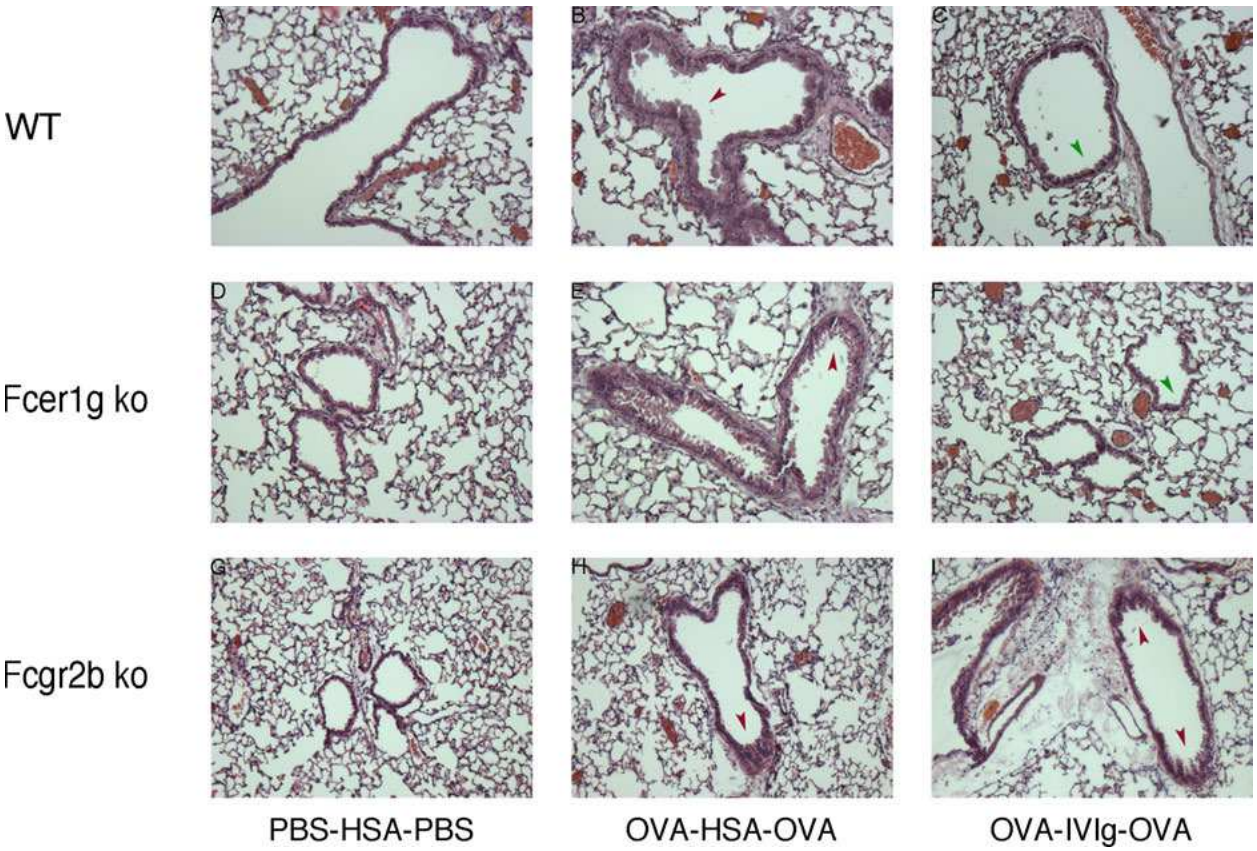

Figure 4. Representative photomicrographs of H&E-stained lung sections from WT (A, B, C), Fcer1g ko (D, E, F), and Fcgr2b ko (G, H, I) mice. Original magnification 100x. Red arrows, brush border disruption and lymphocyte infiltration. Green arrows, inflammation resolution in IVIg-treated animals.

IVIg does not induce a local or systemic Treg response in the absence of FcγRIIb

We have previously shown (30) that IVIg treatment of OVA-exposed B6 mice induces local and systemic Treg. In the present study, lung and spleen Treg were assayed post-mortem to verify if Fcgr2b ko animals could raise a similar response. As opposed to WT mice, Fcgr2b ko mice do not display statistically significant differences in Treg in both lung (Figure 5A) or spleen (Figure 5B) subsequent to IVIg treatment, suggesting that their allergic airways disease may be poorly controlled due to insufficient induction of regulatory cell populations.

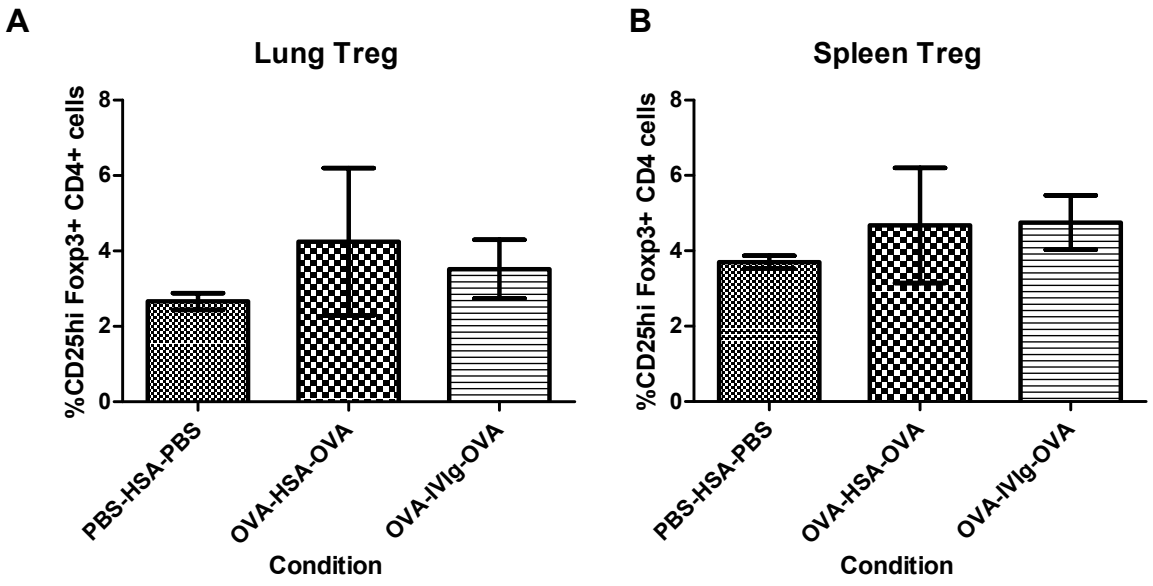

Figure 5. Treg in lung (A) and spleen (B) from Fcgr2b ko mice subjected to 34-day AAD protocol. Graphs present mean ± SEM % CD25hi Foxp3+ cells out of CD4+ cells. Gating strategy was viable $CD4^{+}$ $CD25^{hi}$ $Foxp3^{+}$ cells.

Fcgr2b ko dendritic cells are unable to tolerize recipient mice to antigen challenge

We have demonstrated that in the allergic airways disease model, the main cellular target of IVIg is the DC (26, 30). Furthermore, we have shown that adoptive transfer of $CD11c^{+}$ DC from OVA/IVIg-treated WT animals (30), and BMDC from WT or Fcer1g ko animals (21) recapitulates the protective effects of IVIg treatment, and induces regulatory T cells in local and systemic lymphoid tissues. In the present work, we therefore sought to examine the tolerogenic potential of IVIg-treated BMDC from Fcgr2b ko mice.

WT animals receiving OVA/IVIg-treated BMDC from Fcgr2b ko mice did not have appreciable decreases in lung resistance or elastance, relative to OVA-loaded DC (Figure 6A-B). Furthermore, while OVA/IVIg-treated DC from WT or Fcer1g ko mice were able to induce Treg in WT recipient lungs, treated DC from Fcgr2b ko DC were unable to induce Treg (Figure 6C), suggesting that these DC are unable to generate tolerance responses.

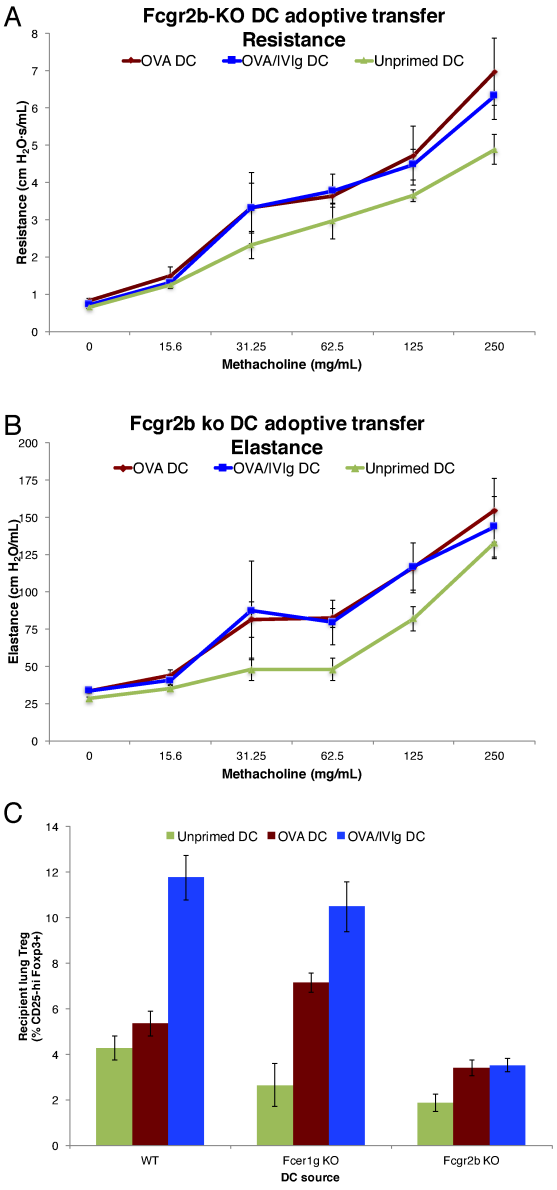

Figure 6. Resistance (A) and elastance (B) measurements from WT recipients of Fcgr2b ko DC. Graphs present mean ± SEM of measured parameters for dose of aerosolized methacholine administered. n=6-8 mice per group. No statistically significant differences observed. C, Lung Treg in WT recipients of DC from WT, Fcer1g ko, or Fcgr2b ko mice. Gating strategy was viable $CD4^{+}$ $CD25^{hi}$ $Foxp3^{+}$ cells.

Fcgr2b ko DC have deficient antigen uptake

We have previously shown (30) that the IVIg-mediated Treg response requires previous antigen exposure, and is antigen-specific. Thus, antigen presentation by DC is likely required for the recruitment and generation of Treg.

IVIg induced a modest but statistically significant decrease in antigen uptake in Fcgr2b-ko-derived BMDC, while reducing antigen uptake by approximately 2-fold in WT and Fcer1g-ko-derived BMDC (Figure 7A-B). The uptake inhibition index of IVIg in WT and Fcer1g-ko-derived BMDC were comparable, while it was significantly reduced in Fcgr2b ko BMDC (Figure 7C). Thus, the efficiency of IVIg to block antigen uptake by DC is impaired in the absence of FcγRIIb, suggesting that these DC are restricted to pro-inflammatory functions.

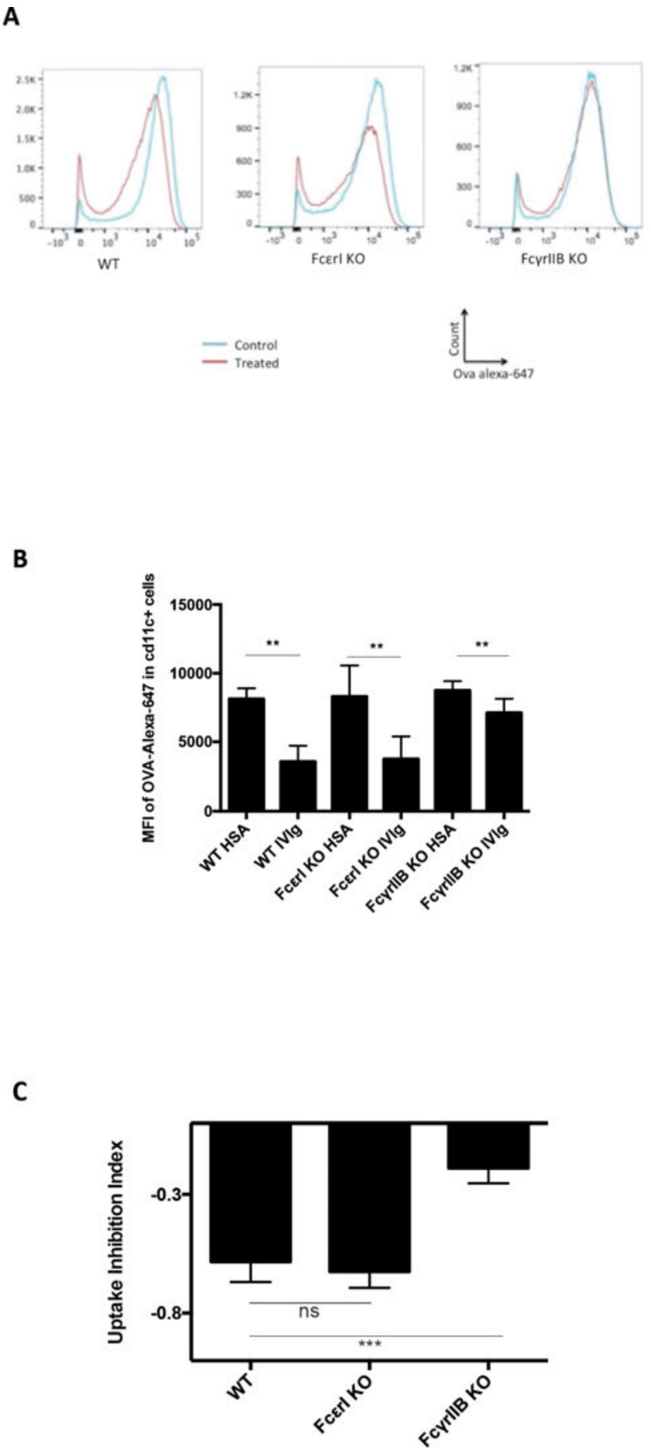

Figure 7. Representative flow cytometric histograms of OVA-Alexa 647 MFI shift (A), MFI values (B), and uptake inhibition index (C) for BMDC from WT, Fcer1g ko, and Fcgr2b ko mice. **, P < 0.01; ***, P < 0.001 ; NS, not statistically significant. Gating strategy was viable CD11c+ cells.

Discussion

IVIg and FcγRIIb

In the present work, we provide multiple lines of evidence that the anti-inflammatory action of IVIg requires the inhibitory ITIM-containing FcγRIIb. This is suggested by the failure of IVIg to resolve AHR and lung histopathology in Fcgr2b ko mice, along with the inability of these mice to generate Treg in response to IVIg treatment. Finally, IVIg-treated FcγRIIb-deficient DC are unable to attenuate AHR or induce Treg in an adoptive-transfer context.

These findings agree with other reports in murine autoimmune models, where FcγRIIb is required for the IVIg-mediated amelioration of idiopathic thrombocytopenic purpura (ITP) (34), nephrotoxic nephritis (NN) (35), and epidermolysis bullosa acquisita (EBA) (36). The parallels between our findings and those reported for autoimmune disease models suggest common mechanisms of action. In particular, FcγRIIb upregulation on myeloid cells and/or recruitment of effector cells expressing FcγRIIb are critical events for IVIg function (34, 35, 37). Furthermore, human chronic inflammatory demyelinating polyneuropathy (CIDP) patients show reduced FcγRIIb expression on $CD14^{hi}$ $CD16^{-}$ monocytes, along with naïve and memory B cells: IVIg treatment partially restores this deregulated expression (38, 39). It must be noted that this model is not universally accepted: Tjon et al. (40) review several of the discrepancies of the working model of IVIg upregulation of FcγRIIb, and discuss the difficulties of extrapolating from mouse to human mechanisms.

Treg are necessary for the control of AAD by IVIg

A major component of the anti-inflammatory actions of IVIg appears to be the development and/or activation of Treg (41). This paradigm has been mostly supported by evidence from autoimmune disease models such as ITP (42) and EAE (43), as well as in clinical studies of rheumatic disease (44). Previous findings from our laboratory (30) have extended these findings to antigen-driven allergic disease, in that IVIg treatment of OVA-exposed B6 mice induces local and systemic Treg. These Treg are necessary and sufficient to control all aspects of AAD. Selective depletion experiments using IVIg-treated Foxp3-DTR (DEREG) mice and adoptive transfer

replenishment strategies have demonstrated the absolute requirement for Treg in this disease model (Massoud et al., under review – presented in Chapter 4). In the present work, we determined that Fcgr2b ko mice are unable to raise a Treg response subsequent to IVIg treatment, and that DC lacking FcγRIIb are unable to confer tolerance or induce Treg by adoptive transfer. These findings suggest that FcγRIIb is required for the Treg-driven control of AAD.

Deficient DC are defective Treg inducers

While Treg appear to be the effector cell of IVIg-mediated abrogation of AAD, the target cell in this system is the dendritic cell. Our laboratory demonstrated this by adoptive transfer of IVIg-treated *ex vivo* purified CD11c+ DC as well as with *in vitro* differentiated BMDC, with both recapitulating the protective effects of whole-animal IVIg treatment (21, 30). We have postulated a model whereby sialylated IgG present in IVIg ligates a C-type lectin receptor on DC, thereby modulating the DC to generate a tolerogenic phenotype. These tolerogenic DC recruit effector T cells in turn and drive the differentiation of Treg (41). This model is supported by data from other groups: Misra et al. (45) reviewed work from their group demonstrating that IVIg inhibits DC activation and differentiation at therapeutic concentrations, and Othy et al. (46) have presented evidence that IVIg inhibited uptake and processing of fluorescently labelled OVA in human monocyte-derived DC. Here, we demonstrate that FcγRIIb is required for the IVIg-mediated antigen uptake inhibition in murine BMDC. This may be indicative of defective recruitment or retention of naïve T cells by FcγRIIb-deficient IVIg-treated DC, resulting in pro-inflammatory rather than tolerogenic effector cell activation (47, 48). As well, there may be tolerogenic signaling overlap between FcγRIIb and DCIR. Ligation of DCIR by sialylated IgG induces phosphorylation of the inhibitory phosphatases SHIP-1 and SHP-2 (21) which are also implicated in FcγRIIb signaling.

Differences between mice and humans

A well-recognized limitation of murine IVIg research is that effects are heavily influenced by the type of disease model and by the mouse strain. In the case of ITP, the disease phenotype is not rescued by IVIg in the *op/op* mouse strain (37), which is deficient in CSF-1. These mice do not express the C-type lectin receptor SIGN-R1 on marginal zone macrophages, thereby removing a

primary receptor for sialylated IgG (49). More broadly, the requirement of FcγRIIb for the protective effects of IVIg is only observed in Fcgr2b ko mice on a B6 background, but not in the identical ko strain on a Balb/c background (50). This is perhaps due to strain-specific differences in patterns and ratios of baseline expression of FcγRs on antigen-presenting cells. Strains of mice prone to autoimmune disease, such as NZB, NOD, BXSB, SB/Le, and MRL, have reduced FcγRIIb expression on activated B cells. This phenotype is associated with known polymorphisms in the promoter region of murine FcγRIIb that may affect gene transcription in a strain-dependent manner (51, 52). Of note, our laboratory's initial report of IVIg-mediated rescue of AAD was performed in Balb/c mice (26).

The present work is also limited by species. Human FcγRs are not all direct orthologs of mouse FcγRs and exhibit different biology (53). While the inhibitory FcγRIIb does behave in a similar manner in both murine and human myeloid cells, the ratios of expression to activating FcγRs differ, in part due to receptors only present on human cells such as FcγRIIA on DC, monocytes, and neutrophils; or FcγRIIIb on neutrophils (15). Furthermore, human and mouse FcγRs have different binding affinities to human IgG subclasses (54), making direct receptor-kinetic comparisons challenging. For these reasons, several investigators have suggested a humanized FcγR mouse approach, whereby mice deficient in murine FcγRs express transgenic human FcγRs. These "knock-in" mouse strains represent the latest tool set for *in vivo* investigation of human and humanized IgG antibodies, which have become increasingly important therapeutic options (55). It will be interesting to examine correlates of the present work in human cells *in vitro* and using humanized FcγR mice, which will undoubtedly provide further insights into the cellular and molecular mechanisms involved in the anti-inflammatory actions of IVIg in allergic disease.

Author contributions

GNK, MD, AHM and MB performed the experiments. GNK and MD wrote the paper. BDM revised the paper. BDM conceived the study, supervised the research group, and takes responsibility for the content of this paper.

Acknowledgements

Financial support for this study was from the Canadian Institutes of Health Research (grant to BDM; studentship to GNK) and Canadian Blood Services (studentship to GNK). MD held a McGill University Faculty of Medicine studentship. We thank the Fonds de Recherche du Québec – Santé and The Research Institute of the McGill University Health Centre for infrastructure support.

Conflict of interest

The authors declare that no conflict of interest, financial or otherwise, exists.

References

1. Matucci A, Maggi E, Vultaggio A. Mechanisms of Action of Ig Preparations: Immunomodulatory and Anti-Inflammatory Effects. *Frontiers in Immunology* (2015) **5**(690). doi: 10.3389/fimmu.2014.00690.

2. Nagelkerke SQ, Kuijpers TW. Immunomodulation by IVIg and the Role of Fc-Gamma Receptors: Classic Mechanisms of Action after all? *Frontiers in Immunology* (2015) **5**(674). doi: 10.3389/fimmu.2014.00674.

3. Paraskevas F, Lee ST, Orr KB, Israels LG. A receptor for Fc on mouse B-lymphocytes. *J Immunol* (1972) **108**(5):1319-27. PubMed PMID: 4555113.

4. Woof JM, Burton DR. Human antibody-Fc receptor interactions illuminated by crystal structures. *Nat Rev Immunol* (2004) **4**(2):89-99. doi: 10.1038/nri1266. PubMed PMID: 15040582.

5. Ravetch JV, Nimmerjahn F. Fc Receptors and Their Role in Immune Regulation and Inflammation In: Paul WE, editor. *Fundamental Immunology*. 7th ed. Philadelphia: Lippincott Williams & Wilkins (2012).

6. van der Poel CE, Spaapen RM, van de Winkel JG, Leusen JH. Functional characteristics of the high affinity IgG receptor, FcgammaRI. *J Immunol* (2011) **186**(5):2699-704. doi: 10.4049/jimmunol.1003526. PubMed PMID: 21325219.

7. Sylvestre DL, Ravetch JV. Fc receptors initiate the Arthus reaction: redefining the inflammatory cascade. *Science* (1994) **265**(5175):1095-8. PubMed PMID: 8066448.

8. Ravetch JV, Clynes RA. Divergent roles for Fc receptors and complement in vivo. *Annu Rev Immunol* (1998) **16**:421-32. doi: 10.1146/annurev.immunol.16.1.421. PubMed PMID: 9597136.

9. Nimmerjahn F, Ravetch JV. Divergent immunoglobulin g subclass activity through selective Fc receptor binding. *Science* (2005) **310**(5753):1510-2. doi: 10.1126/science.1118948. PubMed PMID: 16322460.

10. Nicholas R, Sinclair SC. Regulation of the immune response. I. Reduction in ability of specific antibody to inhibit long-lasting IgG immunological priming after removal of the Fc fragment. *J Exp Med* (1969) **129**(6):1183-201. PubMed PMID: 5305714; PubMed Central PMCID: PMCPMC2138663.

11. Ravetch JV, Bolland S. IgG Fc receptors. *Annu Rev Immunol* (2001) **19**:275-90. doi: 10.1146/annurev.immunol.19.1.275. PubMed PMID: 11244038.

12. Nimmerjahn F, Ravetch JV. Fc-receptors as regulators of immunity. *Adv Immunol* (2007) **96**:179-204. doi: 10.1016/S0065-2776(07)96005-8. PubMed PMID: 17981207.

13. Billadeau DD, Leibson PJ. ITAMs versus ITIMs: striking a balance during cell regulation. *J Clin Invest* (2002) **109**(2):161-8. doi: 10.1172/JCI14843. PubMed PMID: 11805126; PubMed Central PMCID: PMCPMC150845.

14. Bruhns P. Properties of mouse and human IgG receptors and their contribution to disease models. *Blood* (2012) **119**(24):5640-9. doi: 10.1182/blood-2012-01-380121. PubMed PMID: 22535666.

15. Nimmerjahn F, Ravetch JV. Fcgamma receptors as regulators of immune responses. *Nat Rev Immunol* (2008) **8**(1):34-47. doi: 10.1038/nri2206. PubMed PMID: 18064051.

16. Li F, Smith P, Ravetch JV. Inhibitory Fcgamma receptor is required for the maintenance of tolerance through distinct mechanisms. *J Immunol* (2014) **192**(7):3021-8. doi: 10.4049/jimmunol.1302934. PubMed PMID: 24563255; PubMed Central PMCID: PMCPMC3967505.

17. Scharenberg AM, Humphries LA, Rawlings DJ. Calcium signalling and cell-fate choice in B cells. *Nat Rev Immunol* (2007) **7**(10):778-89. doi: 10.1038/nri2172. PubMed PMID: 17853903; PubMed Central PMCID: PMCPMC2743935.

18. Qiagen GeneGlobe. Fc-GammaR Pathway [Web page]. (2016) [cited 2016 August 12]. Available from: https://www.qiagen.com/us/shop/genes-and-pathways/pathway-details/?pwid=178.

19. Schwab I, Nimmerjahn F. Intravenous immunoglobulin therapy: how does IgG modulate the immune system? *Nat Rev Immunol* (2013) **13**(3):176-89. doi: 10.1038/nri3401. PubMed PMID: 23411799.

20. Zhuang Q, Bisotto S, Fixman ED, Mazer B. Suppression of IL-4- and CD40-induced B-lymphocyte activation by intravenous immunoglobulin is not mediated through the inhibitory IgG receptor FcgammaRIIb. *J Allergy Clin Immunol* (2002) **110**(3):480-3. PubMed PMID: 12209098.

21. Massoud AH, Yona M, Xue D, Chouiali F, Alturaihi H, Ablona A, et al. Dendritic cell immunoreceptor: a novel receptor for intravenous immunoglobulin mediates induction of regulatory T cells. *J Allergy Clin Immunol* (2014) **133**(3):853-63 e5. doi: 10.1016/j.jaci.2013.09.029. PubMed PMID: 24210883.

22. Pincetic A, Bournazos S, DiLillo DJ, Maamary J, Wang TT, Dahan R, et al. Type I and type II Fc receptors regulate innate and adaptive immunity. *Nat Immunol* (2014) **15**(8):707-16. doi: 10.1038/ni.2939. PubMed PMID: 25045879.

23. Takai T, Li M, Sylvestre D, Clynes R, Ravetch JV. FcR gamma chain deletion results in pleiotrophic effector cell defects. *Cell* (1994) **76**(3):519-29. PubMed PMID: 8313472.

24. Takai T, Ono M, Hikida M, Ohmori H, Ravetch JV. Augmented humoral and anaphylactic responses in Fc gamma RII-deficient mice. *Nature* (1996) **379**(6563):346-9. doi: 10.1038/379346a0. PubMed PMID: 8552190.

25. McCusker C, Chicoine M, Hamid Q, Mazer B. Site-specific sensitization in a murine model of allergic rhinitis: role of the upper airway in lower airways disease. *J Allergy Clin Immunol* (2002) **110**(6):891-8. PubMed PMID: 12464956.

26. Kaufman GN, Massoud AH, Audusseau S, Banville-Langelier AA, Wang Y, Guay J, et al. Intravenous immunoglobulin attenuates airway hyperresponsiveness in a murine model of allergic asthma. *Clin Exp Allergy* (2011) **41**(5):718-28. doi: 10.1111/j.1365-2222.2010.03663.x. PubMed PMID: 21255135.

27. Lutz MB, Kukutsch N, Ogilvie AL, Rossner S, Koch F, Romani N, et al. An advanced culture method for generating large quantities of highly pure dendritic cells from mouse bone marrow. *J Immunol Methods* (1999) **223**(1):77-92. PubMed PMID: 10037236.

28. Rayamajhi M, Redente EF, Condon TV, Gonzalez-Juarrero M, Riches DW, Lenz LL. Non-surgical intratracheal instillation of mice with analysis of lungs and lung draining lymph nodes by flow cytometry. *J Vis Exp* (2011) (51). doi: 10.3791/2702. PubMed PMID: 21587154; PubMed Central PMCID: PMCPMC3280633.

29. Koya T, Matsuda H, Matsubara S, Miyahara N, Dakhama A, Takeda K, et al. Differential effects of dendritic cell transfer on airway hyperresponsiveness and inflammation. *Am J Respir Cell Mol Biol* (2009) **41**(3):271-80. doi: 10.1165/rcmb.2008-0256OC. PubMed PMID: 19151321; PubMed Central PMCID: PMCPMC2742748.

30. Massoud AH, Guay J, Shalaby KH, Bjur E, Ablona A, Chan D, et al. Intravenous immunoglobulin attenuates airway inflammation through induction of forkhead box protein 3-positive regulatory T cells. *J Allergy Clin Immunol* (2012) **129**(6):1656-65 e3. doi: 10.1016/j.jaci.2012.02.050. PubMed PMID: 22564681.

31. Schuessler TF, Bates JH. A computer-controlled research ventilator for small animals: design and evaluation. *IEEE Trans Biomed Eng* (1995) **42**(9):860-6. doi: 10.1109/10.412653. PubMed PMID: 7558060.

32. d'Hennezel E, Piccirillo CA. Analysis of human FOXP3+ Treg cells phenotype and function. *Methods Mol Biol* (2011) **707**:199-218. doi: 10.1007/978-1-61737-979-6_13. PubMed PMID: 21287337.

33. R Core Team. *R: A language and environment for statistical computing.* Vienna, Austria: R Foundation for Statistical Computing (2016).

34. Samuelsson A, Towers TL, Ravetch JV. Anti-inflammatory activity of IVIG mediated through the inhibitory Fc receptor. *Science* (2001) **291**(5503):484-6. doi: 10.1126/science.291.5503.484. PubMed PMID: 11161202.

35. Kaneko Y, Nimmerjahn F, Madaio MP, Ravetch JV. Pathology and protection in nephrotoxic nephritis is determined by selective engagement of specific Fc receptors. *J Exp Med* (2006)

203(3):789-97. doi: 10.1084/jem.20051900. PubMed PMID: 16520389; PubMed Central PMCID: PMCPMC2118246.

36. Schwab I, Mihai S, Seeling M, Kasperkiewicz M, Ludwig RJ, Nimmerjahn F. Broad requirement for terminal sialic acid residues and FcgammaRIIb for the preventive and therapeutic activity of intravenous immunoglobulins in vivo. *Eur J Immunol* (2014) **44**(5):1444-53. doi: 10.1002/eji.201344230. PubMed PMID: 24505033.

37. Bruhns P, Samuelsson A, Pollard JW, Ravetch JV. Colony-stimulating factor-1-dependent macrophages are responsible for IVIG protection in antibody-induced autoimmune disease. *Immunity* (2003) **18**(4):573-81. PubMed PMID: 12705859.

38. Quast I, Cueni F, Nimmerjahn F, Tackenberg B, Lunemann JD. Deregulated Fcgamma receptor expression in patients with CIDP. *Neurol Neuroimmunol Neuroinflamm* (2015) **2**(5):e148. doi: 10.1212/NXI.0000000000000148. PubMed PMID: 26380354; PubMed Central PMCID: PMCPMC4547878.

39. Tackenberg B, Jelcic I, Baerenwaldt A, Oertel WH, Sommer N, Nimmerjahn F, et al. Impaired inhibitory Fcgamma receptor IIb expression on B cells in chronic inflammatory demyelinating polyneuropathy. *Proc Natl Acad Sci U S A* (2009) **106**(12):4788-92. doi: 10.1073/pnas.0807319106. PubMed PMID: 19261857; PubMed Central PMCID: PMCPMC2660764.

40. Tjon AS, van Gent R, Geijtenbeek TB, Kwekkeboom J. Differences in Anti-Inflammatory Actions of Intravenous Immunoglobulin between Mice and Men: More than Meets the Eye. *Front Immunol* (2015) **6**:197. doi: 10.3389/fimmu.2015.00197. PubMed PMID: 25972869; PubMed Central PMCID: PMCPMC4412134.

41. Kaufman GN, Massoud AH, Dembele M, Yona M, Piccirillo CA, Mazer BD. Induction of Regulatory T Cells by Intravenous Immunoglobulin: A Bridge between Adaptive and Innate Immunity. *Front Immunol* (2015) **6**:469. doi: 10.3389/fimmu.2015.00469. PubMed PMID: 26441974; PubMed Central PMCID: PMCPMC4566032.

42. Aslam R, Hu Y, Gebremeskel S, Segel GB, Speck ER, Guo L, et al. Thymic retention of CD4+CD25+FoxP3+ T regulatory cells is associated with their peripheral deficiency and

thrombocytopenia in a murine model of immune thrombocytopenia. *Blood* (2012) **120**(10):2127-32. doi: 10.1182/blood-2012-02-413526. PubMed PMID: 22760780.

43. Koutrolos M, Berer K, Kawakami N, Wekerle H, Krishnamoorthy G. Treg cells mediate recovery from EAE by controlling effector T cell proliferation and motility in the CNS. *Acta Neuropathol Commun* (2014) **2**:163. doi: 10.1186/s40478-014-0163-1. PubMed PMID: 25476447; PubMed Central PMCID: PMCPMC4268825.

44. Bayry J, Mouthon L, Kaveri SV. Intravenous immunoglobulin expands regulatory T cells in autoimmune rheumatic disease. *J Rheumatol* (2012) **39**(2):450-1. doi: 10.3899/jrheum.111123. PubMed PMID: 22298280; PubMed Central PMCID: PMCPMC3623090.

45. Misra N, Bayry J, Dasgupta S, Ephrem A, Huyen JP, Delignat S, et al. Intravenous immunoglobulin and dendritic cells. *Clin Rev Allergy Immunol* (2005) **29**(3):201-5. PubMed PMID: 16391394.

46. Othy S, Bruneval P, Topcu S, Dugail I, Delers F, Lacroix-Desmazes S, et al. Effect of IVIg on human dendritic cell-mediated antigen uptake and presentation: role of lipid accumulation. *J Autoimmun* (2012) **39**(3):168-72. doi: 10.1016/j.jaut.2012.05.013. PubMed PMID: 22704540.

47. Rothoeft T, Gonschorek A, Bartz H, Anhenn O, Schauer U. Antigen dose, type of antigen-presenting cell and time of differentiation contribute to the T helper 1/T helper 2 polarization of naive T cells. *Immunology* (2003) **110**(4):430-9. PubMed PMID: 14632640; PubMed Central PMCID: PMCPMC1783073.

48. Ruedl C, Bachmann MF, Kopf M. The antigen dose determines T helper subset development by regulation of CD40 ligand. *Eur J Immunol* (2000) **30**(7):2056-64. doi: 10.1002/1521-4141(200007)30:7<2056::AID-IMMU2056>3.0.CO;2-S. PubMed PMID: 10940895.

49. Anthony RM, Wermeling F, Karlsson MC, Ravetch JV. Identification of a receptor required for the anti-inflammatory activity of IVIG. *Proc Natl Acad Sci U S A* (2008) **105**(50):19571-8. doi: 10.1073/pnas.0810163105. PubMed PMID: 19036920; PubMed Central PMCID: PMCPMC2604916.

50. Leontyev D, Katsman Y, Branch DR. Mouse background and IVIG dosage are critical in establishing the role of inhibitory Fcgamma receptor for the amelioration of experimental ITP. *Blood* (2012) **119**(22):5261-4. doi: 10.1182/blood-2012-03-415695. PubMed PMID: 22508937.

51. Jiang Y, Hirose S, Abe M, Sanokawa-Akakura R, Ohtsuji M, Mi X, et al. Polymorphisms in IgG Fc receptor IIb regulatory regions associated with autoimmune susceptibility. *Immunogenetics* (2000) **51**(6):429-35. PubMed PMID: 10866109.

52. Pritchard NR, Cutler AJ, Uribe S, Chadban SJ, Morley BJ, Smith KG. Autoimmune-prone mice share a promoter haplotype associated with reduced expression and function of the Fc receptor FcgammaRII. *Curr Biol* (2000) **10**(4):227-30. PubMed PMID: 10704418.

53. Nagelkerke SQ, Kuijpers TW. Immunomodulation by IVIg and the Role of Fc-Gamma Receptors: Classic Mechanisms of Action after all? *Front Immunol* (2014) **5**:674. doi: 10.3389/fimmu.2014.00674. PubMed PMID: 25653650; PubMed Central PMCID: PMCPMC4301001.

54. Lux A, Nimmerjahn F. Of mice and men: the need for humanized mouse models to study human IgG activity in vivo. *J Clin Immunol* (2013) **33 Suppl 1**:S4-8. doi: 10.1007/s10875-012-9782-0. PubMed PMID: 22948744.

55. Smith P, DiLillo DJ, Bournazos S, Li F, Ravetch JV. Mouse model recapitulating human Fcgamma receptor structural and functional diversity. *Proc Natl Acad Sci U S A* (2012) **109**(16):6181-6. doi: 10.1073/pnas.1203954109. PubMed PMID: 22474370; PubMed Central PMCID: PMCPMC3341029.

Chapter 4:

Peripherally Generated Foxp3^{+} Regulatory T Cells Mediate the Immunomodulatory Effects of Intravenous Immunoglobulin in Allergic Airways Disease[1]

Amir H Massoud[*†2], Gabriel N Kaufman[*], Di Xue[*], Marianne Béland[*], Marieme Dembele[*], Ciriaco A Piccirillo[‡], Walid Mourad[†], Bruce D Mazer[*]

* Translational Research in Respiratory Diseases (TRR) Program, The Research Institute of the McGill University Health Centre, Montreal, Quebec, H4A 3J1, Canada

† Cellular and Molecular Immunology Laboratory, University of Montreal Hospital Research Centre, Montreal, Quebec, H2X 0A9, Canada

‡ Infectious Diseases and Immunity in Global Health (IDIGH) Program, The Research Institute of the McGill University Health Centre, Montreal, Quebec, H4A 3J1, Canada

[1] Financial support for this work was from Grifols Bioscience (Clinical Investigation Program), Canadian Institutes for Health Research (CIHR) grants ISO115295 (to BDM) and MOP67211 (to CAP), the Research Institute of the McGill University Health Centre (RI-MUHC), and the Strauss Family Foundation.

[2] Present address: Division of Immunology Research, Boston Children's Hospital, Boston, Massachusetts, 02115, USA.

Corresponding author:

Bruce D Mazer MD
Phone: 514-934-1934 ext 73675
Fax: 514-933-3962
Email: bruce.mazer@mcgill.ca

This chapter presents our investigation into the efferent end of the IVIg-mediated immunomodulatory response. Previous work from our laboratory had demonstrated that IVIg treatment of antigen-exposed mice was associated with a significant increase in Treg in target organs, along with local and systemic lymphoid tissues. We therefore examined the absolute requirement for Treg in the IVIg-mediated abrogation of AAD using a cell-specific Treg depletion model system. We demonstrated that IVIg generates peripherally-induced $Foxp3^+$ Treg (pTreg) de novo from non-Treg precursors, and that these Treg are both necessary and sufficient for the inhibition of allergen-induced AAD.

The specific contributions of the present author to this paper were: design of the microarray experiment, microarray data analysis, data generation for Figure 1D-E, Figure 8, Table I, and the Supplement; extensive revision of Amir H Massoud's first draft of the manuscript, writing the final version for submission. His colleagues' contributions were as follows: study design, data generation for Figures 1 through 7, first draft of manuscript, Amir H Massoud; microarray sample preparation and array scanning; data generation for Figure 8E, Di Xue; McGill University and Génome Québec Innovation Centre gene expression analysis services platform.

Abstract:

Intravenous Immunoglobulin (IVIg) is widely used as an immunomodulatory therapy. We have recently demonstrated that IVIg protects against airway hyper-reactivity (AHR) and inflammation in mouse models of allergic airway disease (AAD), associated with induction of Foxp3+ regulatory T cells (Treg). Using mice carrying a DTR/EGFP transgene under the control of the Foxp3 promoter (DEREG), we demonstrate that IVIg generates a de novo population of peripheral Treg (pTreg) in the absence of endogenous Treg. IVIg-generated pTreg were sufficient for inhibition of OVA-induced AHR in an antigen-driven murine model of AAD. In the absence of endogenous Treg, IVIg failed to confer protection against AHR and airway inflammation. Adoptive transfer of purified IVIg-generated pTreg prior to antigen challenge effectively prevented airway inflammation and AHR in an antigen-specific manner. Microarray gene expression profiling of IVIg-generated pTreg revealed upregulation of genes associated with cell cycle, chromatin, cytoskeleton/motility, immunity, and apoptosis. These data demonstrate the importance of Treg in regulating AAD and show that IVIg-generated pTreg are necessary and sufficient for inhibition of allergen-induced AAD. The ability of IVIg to generate pure populations of highly antigen-specific pTreg represents a new avenue to study peripheral Treg, the cross talk between humoral and cellular immunity, and regulation of the inflammatory response to antigens.

Introduction

Regulatory T cells (Treg) are specialized subsets of T lymphocytes that express the forkhead box P3 (Foxp3) transcription factor and play a non-redundant role in maintaining immunological tolerance (1, 2), as illustrated by the severe autoimmune disease that develops in Foxp3-deficient neonatal mice and humans (3, 4).

Treg play an essential role in immune homeostasis. In particular, the presence of Treg in the lung is crucial for assuring normal lung health. In the steady state, antigen-presenting cells such as tissue-resident macrophages appear to be programmed to interact with T cells, ensuring that

inhalation of common particulate substances induces Treg responses, and minimizing the inflammatory potential associated with elimination of these substances (5). In situations where an inflammatory response is required, such as in viral infections, the presence of Treg is required to ensure that the necessary host response does not lead to overt destruction of lung tissue (6). Treg diminishing cell proliferation and inflammatory cytokine production, thereby minimizing the damage caused by the anti-viral response.

The mechanisms behind the induction of a Treg response and Treg-mediated suppression of inflammatory diseases are not entirely established. In allergic disease, individuals who are tolerant to inhaled allergens have higher peripheral blood Treg than symptomatic asthmatic individuals (7), suggesting that a lack of Treg may play a role in the aberrant responses to allergens in asthma. Few human studies have directly characterized lung Treg, and this data is highly variable, mainly due to the ubiquitous use of corticosteroids in symptomatic asthmatics (8-11). In murine studies, infusion of Treg can inhibit allergen driven allergic airways disease, and Treg induction may be an important part of abrogating allergic inflammation (Kaufman Massoud et al Frontiers) Therefore, in allergen-driven diseases such as asthma, strategies to boost Tregs are an important focus of research for development of novel Treg-based therapies (12).

We have demonstrated that intravenous immunoglobulin (IVIg) is able to attenuate airway hyper-responsiveness (AHR) and pulmonary inflammation following sensitization and challenge to ovalbumin (OVA) or ragweed (RW) in BALB/cJ (13) and C57BL/6J (14) mice. The action of IVIg is associated with a significant increase in highly suppressive Treg, and appears to be dependent on CD11c+ dendritic cells. This finding concurs with the work of Trinath et al (15). Treg generated following IVIg administration appear to be antigen-specific, but it is not known if this property is important in the action of IVIg in attenuating murine allergic airways disease (AAD). In addition, it is not clear if Treg generated by IVIg require the presence of thymic Treg (tTreg), or can be peripherally differentiated solely from pre-existing CD4+CD25-Foxp3- T cells.

In the present study, we have utilized mice carrying a DTR/EGFP transgene under the control of the Foxp3 promoter (DEREG), allowing for selective depletion of Foxp3+ Treg following injection

of diphtheria toxin (DT). We demonstrate that in the complete absence of Treg following multiple DT doses, IVIg failed to attenuate AHR and alleviate airway inflammation. However, when pre-established Treg were depleted before, but not following IVIg treatment, mice exhibited induction of Foxp3+ Treg following IVIg therapy, and did not develop AHR and airway inflammation after allergen challenge. Using a heterologous antigen model, IVIg-generated pTreg controlled allergic responses when adoptively transferred, in an antigen-specific manner. Thus, we have demonstrated that antigen-specific Treg can be induced from pre-existing CD4+ effector T cells, in the absence of tTreg. IVIg-generated antigen-specific Treg suppress all aspects of antigen-driven airway inflammation. We further characterized these IVIg-generated pTreg by gene expression microarray. Gene expression profiling revealed that IVIg-generated pTreg upregulate genes associated with cell cycle, chromatin, cytoskeleton/motility, immunity, and apoptosis. This suggests that IVIg-generated pTreg are a metabolically/transcriptionally active and phenotypically plastic population, actively responding to inflammation by dampening the immune response.

Methods

Animal studies

All animal studies were conducted according to procedures reviewed and approved by the Faculty of Medicine's Animal Care Committee at McGill University, in compliance with Canadian Council on Animal Care guidelines.

Mouse strains

C57BL/6 Foxp3-DTR/EGFP mice, expressing enhanced green fluorescent protein (EGFP) and diphtheria toxin receptor (DTR) under control of the forkhead box P3 (*Foxp3*) promoter, were kindly provided by A. Y. Rudensky (Memorial Sloan-Kettering Cancer Centre), and were used to track and/or deplete Foxp3+ Treg (16, 17). OT-II transgenic mice expressing an MHC class II-restricted, ovalbumin (OVA)-specific Vα2/Vβ5.1 T-cell receptor (18) were mated to Foxp3EGFP reporter mice (19) to produce transgenic mice with OVA-specific Foxp3EGFP Treg. Founder

Foxp3EGFP and OT-II strains on C57BL/6J backgrounds were obtained from Jackson Laboratories. Male and female mice were bred and maintained in a specific pathogen-free vivarium at the Research Institute-McGill University Health Centre and used at 6-8 weeks of age.

Allergic airways disease models and depletion of Treg

Mice were sensitized and challenged to OVA (13, 14) or RW (20) as previously described. One day prior to antigen challenge (day 28), mice were treated by intraperitoneal injection (i.p) with 2 g/kg IVIg (Grifols, Chapel Hill, NC) or an equal volume of 5% human serum albumin (HSA) (Grifols). Foxp3+ Treg depletion was achieved by i.p. injection of 40 ng/g diphtheria toxin (DT) to DEREG mice as described (16).

Flow cytometric analyses

Cell staining for flow cytometry was performed as described previously (14). Cells were stained with a protein-binding dye to assess viability (FVD eFluor780, eBioscience), and Fc receptor binding was blocked using anti-CD16/32 antibodies (clone 93, BioLegend). Cells were subsequently incubated with appropriate fluorochrome-labeled antibodies for 30 minutes at 4°C in 100 µL PBS with 0.2% (w/v) bovine serum albumin (BSA). Antibody clones, fluorochrome conjugations, and suppliers are specified in the flow-cytometry supplemental Table. Antibody concentrations were determined by titration for optimal signal-to-noise ratio. Some samples were fixed and permeabilized with Cytofix/Cytoperm (BD Biosciences) or transcription-factor buffers (eBioscience) for intracellular cytokine and/or intranuclear transcription factor detection. Samples were acquired on a BD LSR II or FACSCanto II flow cytometer using FACSDiva 6.0.3 software. Data analysis was performed offline using FlowJo v10.0.8 software (Treestar). Hierarchical gating strategies were specified manually for each cell population of interest.

Airway hyper-responsiveness to methacholine

Airway hyper-responsiveness (AHR) was measured as described previously (13, 14) using the flexiVent small-animal ventilation system (SCIREQ). Briefly, mice were anaesthetized, tracheotomised, paralyzed, and connected to the ventilator. Methacholine (16-256 mg/mL in

saline) was aerosolized into the inspiratory stream, and lung resistance was measured after each dose.

Histological analysis

Lungs were fixed by inflation with 10% neutral buffered formalin, processed, and embedded in paraffin using standard protocols. 5-micron sections were stained with hematoxylin and eosin (H&E) and examined by light microscopy.

Preparation of lung and spleen cell suspensions

Lungs and spleens were digested with collagenase D (0.15 Wünsch U / mL) and DNAse I (0.1 mg/mL) (both from Roche Life Science) in phosphate-buffered saline, with 0.9 mM calcium chloride, 0.5 mM magnesium chloride hexahydrate, and 15 mM HEPES. Single-cell suspensions were resuspended in PBS without calcium or magnesium (for flow cytometric analyses) or complete medium consisting of RPMI 1640 (HyClone) supplemented with 10% fetal bovine serum (FBS), 2 mM L-glutamine, 100 U/mL penicillin, 100 µg/mL streptomycin, 15 mM HEPES, and 50 µM 2-mercaptoethanol for culture.

Treg adoptive transfer

In some experiments, pulmonary Treg were isolated from DT-depleted, IVIg-treated, and OVA-challenged mice by flow cytometric sorting, as detailed below. These cells were adoptively transferred by intratracheal infusion into recipient syngeneic mice (12), which were exposed to OVA or RW as above.

Co-culture experiments

CD11c+ DC purified by magnetic bead sorting (MACS, Miltenyi Biotec) from lungs of DT-treated and OVA-exposed mice were co-cultured at a 1:5 ratio with flow-sorted OT-II/Foxp3EGFP viable CD4+ Foxp3- splenic T cells, which have T cell receptors specific for the OT-II peptide of OVA (amino acids 323-339) in the context of MHC-II, and express EGFP in Foxp3-expressing cells.

Cultures were pulsed with 1 mg/mL OVA and maintained for 4 days, followed by stimulation with PMA (50 ng/mL) and ionomycin (500 ng/mL) (Sigma-Aldrich) in the presence of GolgiPlug (BD Biosciences) for the last 6 hours of culture (14).

Multiplex cytokine assays

Mouse TH1/TH2 Ultra-Sensitive Multiplex Kit from MSD was used to measure murine IFN-γ, IL-4, IL-5, IL-10, IL-12, and TNF-α in BAL according to the manufacturer's instructions. MSD plates were analyzed on the MSD 1250 Plate Imager. The concentrations of cytokines in test samples were determined by referencing their electrochemiluminescence responses against a standard curve generated from serially diluted calibrators.

ELISA

Total serum IgE and IL-13 in BAL were measured by ELISA (eBioscience) according to the manufacturer’s protocols.

Flow cytometric sorting of Treg

Treg from spleens of IVIg- or HSA-treated mice, with or without Treg depletion, were flow-sorted using a BD FACSAria III to isolate pure populations of IVIg-generated pTreg, mixed endogenous and IVIg-generated pTreg, and endogenous Treg. The flow gating strategy for the Treg sort was viable CD4+ CD25hi Foxp3+ cells (depicted in flow-cytometry supplemental Figure 1), as per the published gating strategy of d'Hennezel and Piccirillo (21, 22). Post-sort purity was verified to be 80-90%.

RNA extraction and processing

RNA was extracted from pooled flow-sorted Treg with TRIzol (Life Technologies) and cleaned with RNeasy Mini silica-gel membrane columns (Qiagen). RNA quality and concentration was assessed by Bioanalyzer microcapillary electrophoresis (Agilent). Samples used for microarray hybridization had 260/280 absorbance ratios >1.8 and RNA Integrity Numbers (RIN) > 7.0.

Gene expression microarray analyses

RNA samples were analyzed using Affymetrix Mouse Gene 2.0 ST microarrays, which contain probe sets for 41,345 unique mRNA sequences from the NCBI RefSeq database (release 51) and the Ensembl database (release 65): this provides genome-wide expression coverage for 26,515 genes. Preparatory cRNA synthesis and labeling (using the Affymetrix WT Pico kit), microarray hybridization reactions, and array scanning were performed according to standard protocols at the McGill University-Génome Québec Innovation Centre microarray core facility.

Microarray data processing and statistics

Gene expression data were subsequently processed using the Bioconductor packages *oligo* (23) for data read-in and normalization, and *limma* (24) for linear modeling and differential-expression statistics. Probe intensities were normalized across all arrays by the robust multi-array average (RMA) algorithm (25). Differential gene expression of IVIg-pTreg versus endogenous Treg (control group) was calculated by linear modeling of the contrast and empirical Bayes sample variance shrinkage, followed by moderated t-tests with false-discovery rate (FDR) correction (26). Results were expressed in terms of log(2) fold-change. Differentially expressed genes were defined as genes with log(2) fold-change greater than 2.

Quantitative RT-PCR confirmation of microarray results

To validate the gene array results using a second technique, RNA samples were assayed for expression of a selection of genes by quantitative RT-PCR. cDNA was generated from 100 ng of total RNA per sample using the iScript™ Reverse Transcription Supermix kit (Bio-Rad) and amplified using gene-specific primers for *Gzma* (forward, CCTGCAATGGGGATTCTGGC; reverse, GTATAGACACCAGGCCATCGG), *Gzmb* (forward, GACAACACTCTTGACGCTGG; reverse, GATGATCTCCCCTGCCTTTGT), and *Ifitm2* (forward, CAACATGCCCAGAGAGGTGT; reverse, CCCTAGACTTCACAGAGTAGGC). Primers were optimized by dilution standard curves for dynamic range and linearity. RT-PCR was performed on duplicate cDNA samples using the SYBR® Green PCR Master Mix on a 7500 Real-Time PCR System (Applied Biosystems). PCR products were

verified by melt-curve analysis for uniformity. Results were normalized using the *Gapdh* reference gene (forward, GCACAGTCAAGGCCGAGAAT, reverse, GCCTTCTCCATGGTGGTGAA) using the $2^{-\Delta\Delta Ct}$ method (27) and are presented as fold-change from control.

Gene list database analyses

To determine gene network interactions in our identified list of differentially-expressed genes, the selection was uploaded to the STRING (**S**earch **T**ool for the **R**etrieval of **I**nteracting **G**enes/Proteins) database (version 10.0) (28), which examines known relationships in between genes, building networks of predicted functional associations based on Gene Ontology (GO) annotations, pathways, and domains (29). The number of interactions present in our gene list was calculated by the STRING algorithm and compared to the expected number of interactions if the nodes were selected at random. A protein-protein interaction (PPI) enrichment P-value for the network was calculated, testing the likelihood that the number of interactions was higher than expected, along with a network clustering coefficient, which measured the connectedness of the network nodes.

To examine known gene functions in our identified list, differentially expressed genes were uploaded to the PANTHER (**P**rotein **AN**alysis **TH**rough **E**volutionary **R**elationships) classification system web database (30), which classifies genes based on curated ontology terms. Database hits were examined in the category of biological process using GO annotations and in the category of protein class using PANTHER accessions.

To examine functional gene clusters in our selection, the list of differentially-expressed genes was uploaded to the DAVID (**D**atabase for **A**nnotation, **V**isualization, and **I**ntegrated **D**iscovery) functional gene clustering algorithm (version 6.7) (31), which compares the uploaded gene list to a gene-gene similarity matrix of over 75,000 functional annotation terms, and generates a cluster map of functionally similar genes using fuzzy heuristic partitioning. Fisher's Exact test and Benjamini multiple comparisons corrections were used to test gene enrichment in annotation terms. Adjusted P-values less than 0.05 were considered statistically significant.

Statistics

Data analyses were performed using Prism 5 (GraphPad Software). One or two-way analysis of variance (ANOVA) with Tukey post-test was used to determine statistical differences compared to control groups. Data represent at least two independent experiments per result. $P<0.05$ was considered statistically significant.

Results

IVIg-generated pTreg are protective against OVA-induced AHR

We have demonstrated that IVIg induces conversion of $CD4^+$ $Foxp3^-$ T cells into $Foxp3^+$ Treg in pulmonary tissues (1). However, it is unknown if IVIg can induce suppressive Treg from non-Treg precursor $CD4^+Foxp3^-$ cells in the absence of other pre-existing Treg. The endogenous Treg population (pre-existing tTreg and pTreg) was depleted in OVA-sensitized DEREG mice by one dose of DT prior to IVIg treatment (Figure 1A). IVIg treatment generated $Foxp3^+$ Treg in the lungs of OVA-sensitized and challenged mice (Figure 1B, C) in the absence of endogenous Treg. IVIg required the presence of antigen in order to induce $Foxp3^+$ Treg (Figure 1B), suggesting a role for TCR stimulation in the peripheral induction of Treg. pTreg generated by IVIg were sufficient to attenuate AHR to methacholine (Figure 1F) and markedly improved lung histopathology (Figure 2 row II) in OVA-challenged mice. This suggests that IVIg-generated pTreg are sufficient to abrogate AHR in AAD.

IVIg-generated Treg have a unique phenotype

To further characterize the distinct IVIg-generated pTreg population, we examined Treg activation markers (2, 3) by flow cytometry of lung cells from animals depleted of endogenous Treg and treated with IVIg, as in Figure 1A. Both endogenous and IVIg-generated lung Treg displayed high expression levels of the membrane-bound form of TGF-β, latency-associated peptide (LAP) (Figure 1D), but IVIg-generated Treg expressed significantly lower levels of the

tTreg marker neuropilin-1 (Nrp1) (Figure 1E), suggesting that the IVIg-generated pTreg appear to be a phenotypically distinct pTreg population.

Fig. 1

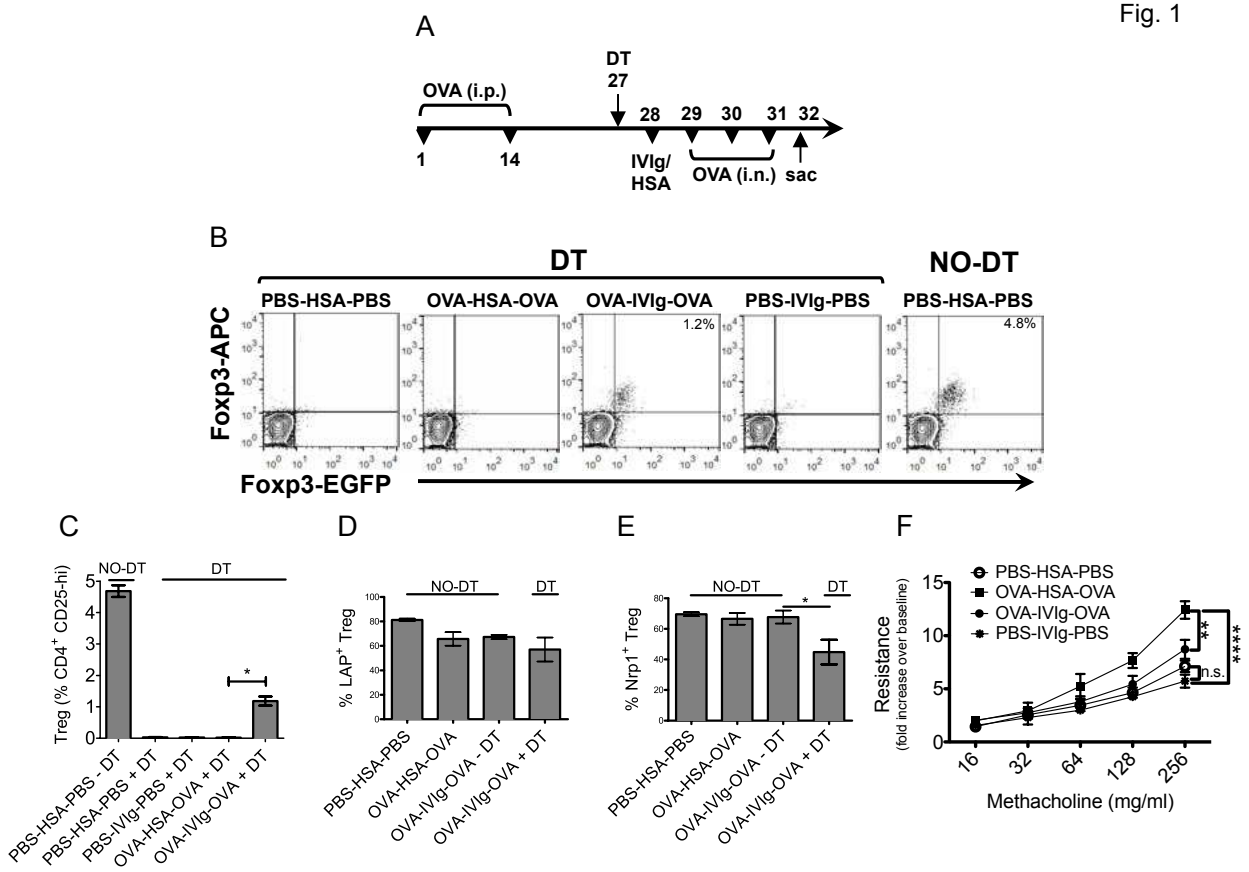

Figure 1. Peripheral induction of Treg by IVIg was sufficient to attenuate AHR.

A. Timeline of OVA sensitization, challenge, and depletion of endogenous Foxp3$^+$ Treg in DEREG mice. Mice were sensitized (i.p.) to OVA/alum on days 1 and 14, treated with IVIg or HSA on day 28, and challenged (i.n) with OVA on days 29, 30, and 31. Foxp3$^+$ Treg were depleted by one dose of (i.p) DT injection 24 hours prior to treatment (day 27).

B, C. Representative flow cytometric analysis (B) and bar graph (C) demonstrating efficient depletion of endogenous regulatory T cells in lungs upon DT injection prior to treatment. IVIg treatment of mice sensitized and challenged with OVA promoted the induction of Foxp3$^+$ Treg in

lung. *, P<0.05; ANOVA with Tukey post-hoc, n=4. Gating strategy: viable $CD4^+$ $CD25^{hi}$ cells were assessed for $Foxp3^{EGFP}$ expression and Foxp3-APC staining.

D, E. Bar graphs depicting the phenotype of IVIg-generated lung Treg: LAP (D) and Nrp1 (E) percentage expression were assessed on the viable $CD4^+$ CD25-high $Foxp3^+$ population. *, P<0.05; ANOVA with Tukey post-hoc, n=4. Gating strategy: viable $CD4^+$ $CD25^{hi}$ $Foxp3^+$ lymphocytes were analyzed for LAP and Nrp1 expression.

F. IVIg treatment of DT-depleted, OVA-challenged mice was able to attenuate methacholine-induced AHR. **, P<0.01, repeated-measures ANOVA with Tukey post-hoc, OVA-HSA-OVA + DT vs. OVA-IVIg-OVA + DT for peak methacholine response, n=6. ****, P< repeated-measures ANOVA with Tukey post-hoc, OVA-HSA-OVA + DT vs. PBS-HSA-PBS for peak methacholine response, n=6. n.s., no significant difference between PBS-HSA-PBS and PBS-IVIg-PBS groups, n=6.

Fig. 2

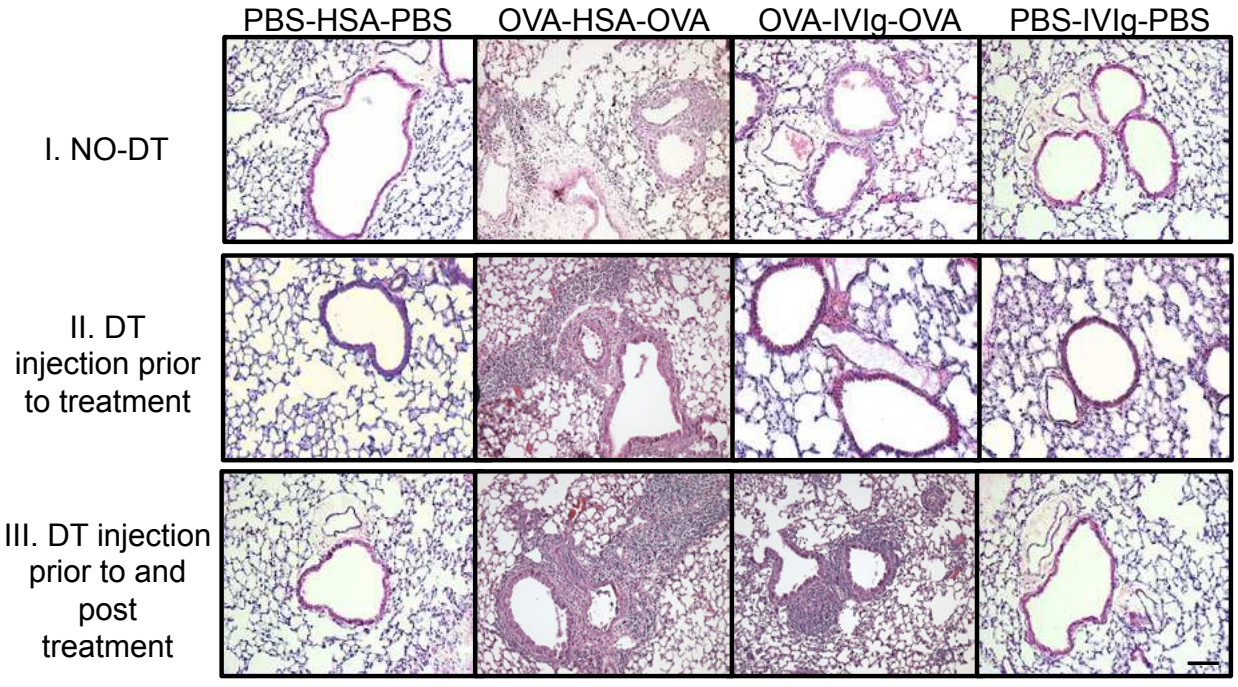

Figure 2. IVIg-generated Treg inhibited cellular influx in airways.

Representative photomicrographs of inflammation analyzed on H&E-stained lung sections (original magnification 200×; scale bar, 50 μm). IVIg treatment of OVA-sensitized and challenged mice alleviated airway inflammation compared to non-IVIg treated mice (row I). IVIg-generated pTreg, induced after endogenous Treg depletion prior to IVIg treatment, abrogated cellular influx to the lung in OVA-exposed animals (row II). Depletion of Treg prior to and during OVA challenge completely reversed the action of IVIg in preventing cellular influx to the lung (row III).

Treg are necessary for inhibition of airway inflammation

We have reported that IVIg inhibits antigen-driven airway inflammation and AHR in murine AAD, accompanied by induction of $Foxp3^+$ Treg in pulmonary tissues (1, 4). To determine if pTreg were necessary and sufficient for inhibition of allergen-induced AHR, we sensitized DEREG mice to OVA. We then selectively depleted $Foxp3^+$ Treg both prior to IVIg treatment and concurrent with OVA challenge by repeated injection of DT (Figure 3A, B, C). In OVA-exposed and challenged mice untreated with DT (NO-DT), IVIg increased the frequency of $Foxp3^+$ Treg in lung (Figure 3B, C) and both attenuated AHR (Figure 3E) and lowered the frequency of activated ($CD4^+CD25^+Foxp3^-$) non-Treg T cells in lung digests (Figure 3D). In contrast, complete depletion of Treg immediately prior to IVIg treatment and concurrent with OVA challenge eliminated IVIg-mediated reductions of activated $CD4^+$ T effector cells in the lungs (Figure 3D), and neither AHR (Figure 3E), nor pulmonary inflammation were diminished (Figure 2 row III). This strongly suggests that Treg are necessary for the protective effects of IVIg in AAD.

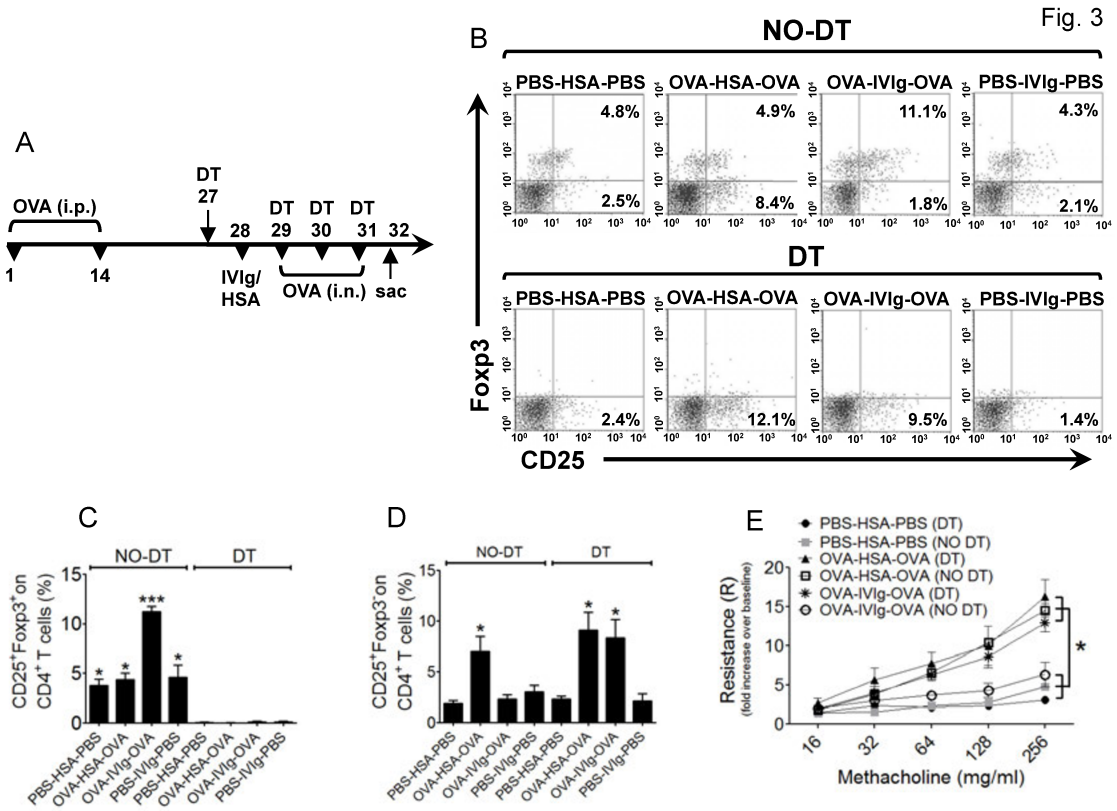

Figure 3. Repeated depletion of Foxp3$^+$ Treg abolishes the immunomodulatory action of IVIg in airway inflammation.

A. Timeline of OVA sensitization and challenge, IVIg treatment, and depletion of Treg in DEREG mice. Mice were sensitized (i.p) to OVA/alum on days 1 and 14, treated with IVIg or HSA on day 28, and challenged (i.n) with OVA on days 29, 30, and 31. Foxp3$^+$ Treg depletion was achieved with one dose of DT (i.p) 24 hours prior to IVIg/HSA treatment and 3 doses of DT concurrent with OVA challenge.

B, C. Representative flow cytometric dot plots (B) and frequency (C) of lung Treg. OVA-IVIg-OVA treatment of mice that were not Treg-depleted with DT induced a 2-fold increase in the frequency of Foxp3$^+$ Treg, comparing to the other control groups (B, upper panel). DT treatment led to complete depletion of Foxp3$^+$ Treg in all experimental groups (B, lower panel). ***, P<0.005; *, P<0.05; ANOVA with Tukey post-hoc, n=6. Gating strategy: viable CD4$^+$ lymphocytes were analyzed for CD25 and Foxp3 staining.

D. Frequency of $CD4^+$ $CD25^+$ $Foxp3^-$ activated T cells. Undepleted OVA-IVIg-OVA mice demonstrated significantly lower frequencies of activated non-Treg T cells in lungs compared to the OVA-HSA-OVA group. Depletion of Treg in mice reversed this effect of IVIg. *, $P<0.05$; ANOVA with Tukey post-hoc, n=6.

E. IVIg treatment of OVA-challenged mice attenuated methacholine-induced AHR, whereas Treg depletion reversed this effect **, $P<0.01$, repeated-measures ANOVA with Tukey post-hoc, PBS-HSA-PBS (DT, NO-DT) and OVA-IVIg-OVA (NO-DT) vs. other control groups for peak methacholine response, n=6.

Treg are required for inhibition of Th2 responses

The absence of pTreg also influenced systemic and intra-pulmonary inflammatory markers. Total and OVA-specific serum IgE was significantly lower after OVA challenge in IVIg-treated mice in the presence of pTreg, whereas mice depleted of Treg before and after antigen challenge exhibited highly elevated production of IgE in both IVIg-treated and non-treated OVA-immunized mice (Figure 4A). IVIg treatment diminished pro-inflammatory cytokines IL-4, IL-5, TNF-α and IFN-γ in the bronchoalveolar lavage (BAL) fluid, while Treg depletion completely reversed this effect. IL-10 was also significantly higher in the BAL of IVIg-treated mice in the presence of pTreg, whereas mice subjected to Treg depletion had attenuated IL-10 production (Figure 4B).

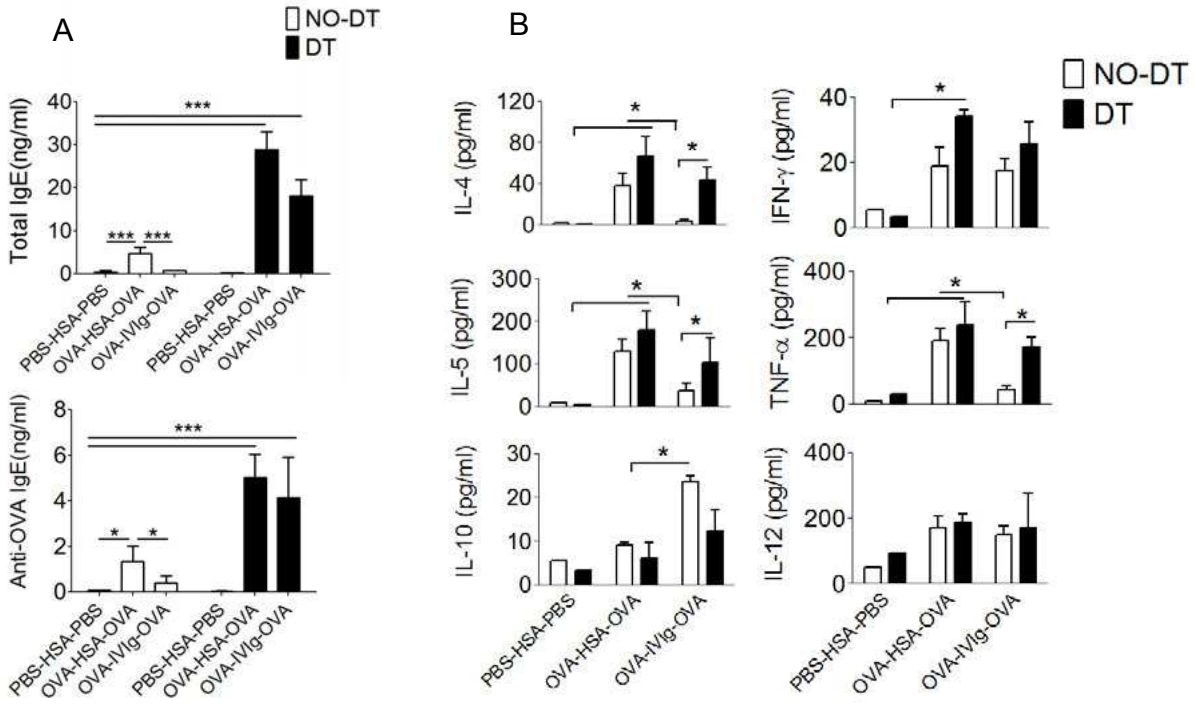

Figure 4. Modulation of pro-inflammatory mediators by IVIg was abrogated by repeated depletion of Foxp3^{+} Treg.

A. Total serum and OVA-specific IgE levels determined by ELISA 24 hours after the last challenge. IVIg treatment lowered the elevated serum IgE levels in non-DT-treated OVA-sensitized and challenged mice, whereas Treg depletion not only abrogated this effect but substantially increased the IgE levels in serum of both OVA-HSA-OVA and OVA-IVIg-OVA group, compared to non-DT-treated mice.

B. BAL cytokine level determined by multiplex assay 24 hours after the last challenge. IVIg significantly decreased BAL fluid IL-4, IL-5, TNF-α and IFN-γ levels in non-DT-treated OVA-exposed mice, compared to other control groups. Treg depletion prior to and during OVA challenge abrogated this effect. IL-10 was significantly higher in the BAL of non-Treg-depleted OVA-IVIg-OVA mice. ***, P<0.005; *, P<0.05; ANOVA with Tukey post-hoc, n=4.

IVIg-generated pTreg are antigen-specific

To investigate if antigen-specific pTreg were required for suppression of AHR, we utilized an adoptive transfer system (5) whereby IVIg-generated Treg were purified from the lungs of DEREG mice treated with one dose of DT prior to IVIg administration and OVA challenge. These cells were adoptively transferred to either OVA- or RW-sensitized syngeneic mice, one day prior to challenge, instead of IVIg treatment. Subsequently, recipient mice were challenged with their sensitizing antigen. pTreg transfer from OVA-exposed and IVIg-treated mice led to marked attenuation of AHR (Figure 5A), reduced total and OVA-specific serum IgE levels (Figure 5B, C), decreased IL-13 production in BAL (Figure 5D), and improved lung histopathology (Figure 5E). However, the transfer of OVA-specific pTreg into RW-sensitized and challenged mice did not inhibit AHR or other inflammatory parameters (Figure 5A-E). These data suggest that IVIg induces antigen-specific Treg, and that antigen specificity is an important function of Treg in decreasing AHR.

Fig. 5

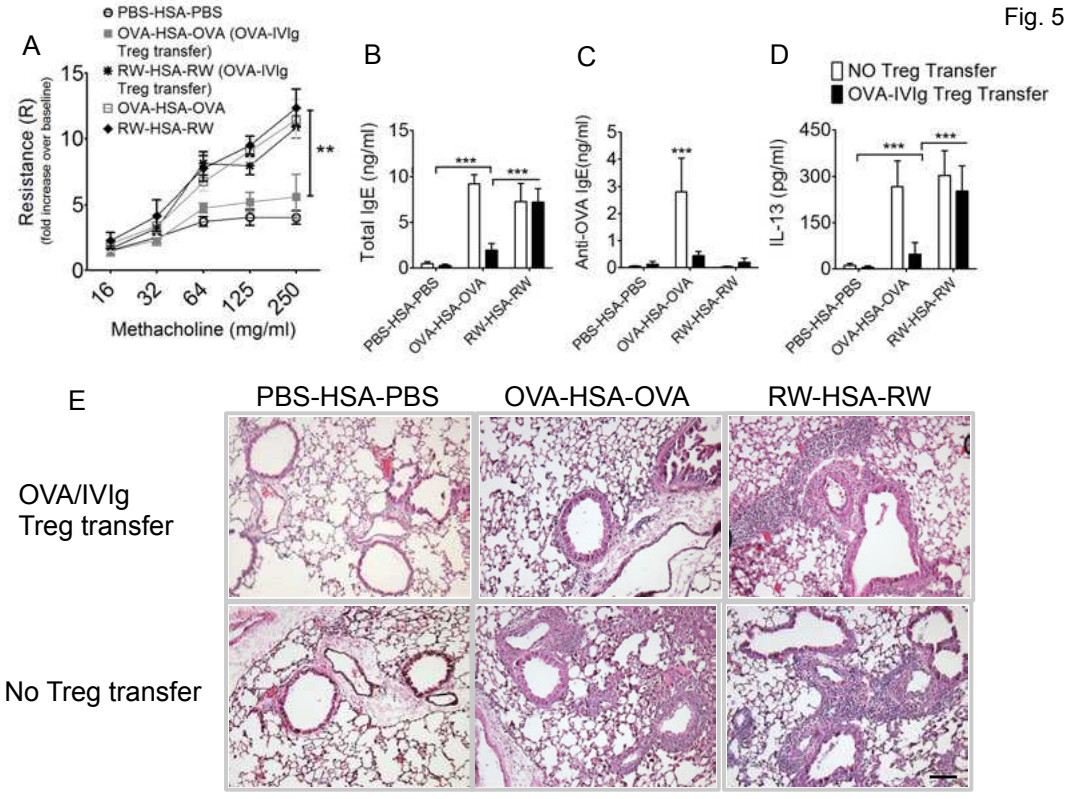

Figure 5. Adoptive transfer of OVA/IVIg-generated Treg suppressed pulmonary inflammation in an antigen-specific manner.

A. Adoptive transfer of pTreg obtained from OVA/IVIg-treated mice, in which endogenous Treg were depleted prior to IVIg treatment, to OVA-sensitized mice, attenuated methacholine-induced AHR after OVA challenge of the recipients, whereas OVA/IVIg pTreg were not protective in RW-exposed mice. **, P<0.01; repeated-measures ANOVA with Tukey post-hoc, negative control group and OVA-immunized pTreg recipients vs. other control groups for peak methacholine response, n=4.

B, C. Total serum IgE (B) and pulmonary IL-13 BAL levels (C) as determined by ELISA 24 hours after the last challenge. Adoptive transfer of IVIg-generated pTreg suppressed total IgE and IL-13 production in an antigen-specific manner. *, P<0.05; ANOVA with Tukey post-hoc, OVA-HSA-OVA vs. other control groups, n=4.

D. Representative photomicrographs of inflammation analyzed on H&E-stained lung sections (original magnification, 200×; scale bar, 50 μm.). OVA/IVIg pTreg adoptive transfer inhibited inflammatory cell influx in OVA-immunized, but not RW-immunized, animals.

IVIg modifies dendritic cells independent of the presence of Treg

Dendritic cells (DC) and Treg are known to interact and mutually modulate function (6). We have demonstrated that IVIg confers tolerogenic properties to $CD11c^+$ DC by decreasing their maturation and altering their cytokine production (1, 4). We questioned whether the regulatory effect of IVIg on DC required Treg. All endogenous and generated Treg were repeatedly depleted in DEREG mice sensitized and challenged with OVA. $CD11c^+$ DC were purified from the lungs of these mice, and their maturation status was determined by examining the expression of the co-stimulatory molecule CD80, as well as MHC class II (MHC-II). IVIg treatment decreased the expression of both CD80 and MHC-II in pulmonary DC, irrespective of the presence or absence of *in vivo* Treg (Figure 6A, B). Thus, Treg are not required for the IVIg-mediated downregulation of CD80 and MHC-II.

Fig. 6

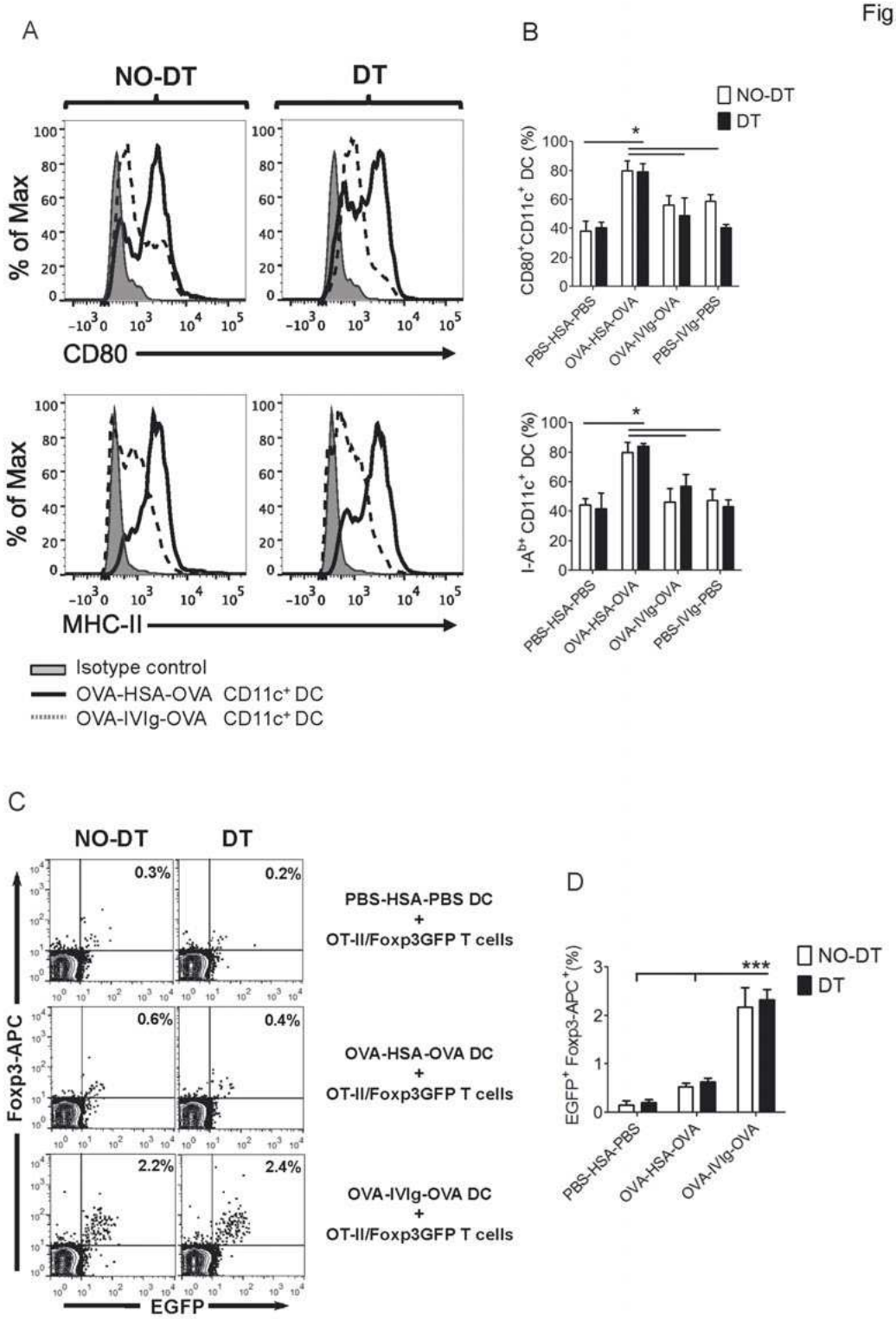

Figure 6. *In vivo* depletion of Treg did not alter the modulatory actions of IVIg on DC maturation or *ex vivo* Treg induction.

A, B. Representative flow cytometric analysis (A) and quantification (B) of CD80 and MHC-II expression on pulmonary $CD11c^+$ DC. IVIg treatment of OVA-exposed mice decreased the expression of CD80 and MHC-II on pulmonary $CD11c^+$ DC, with or without endogenous Treg depletion by DT. *, $P<0.05$; ANOVA with Tukey post-hoc, n=6. Gating strategy: viable $CD11c^+$ cells were analyzed for CD80 and MHC-II staining.

C, D. Lung $CD11c^+$ DC from Treg-depleted and non-Treg depleted mice were co-cultured with $CD4^+$ $Foxp3^-$ OT-II/$Foxp3^{EGFP}$ T cells in the presence of OVA for 4 days. Representative flow cytometry analysis (C) and quantification (D) of $Foxp3^{APC+\ EGFP+}$ Treg within total $CD4^+$ T cells, demonstrating that DC derived from OVA-IVIg-OVA mice, whether DT-treated or untreated, were both able to significantly expand OVA-specific $Foxp3^+$ Treg in co-culture, compared to other control groups. ***, $P<0.001$; ANOVA with Tukey post-hoc, n=6. Gating strategy: viable $CD4^+$ $CD25^{hi}$ cells were assessed for $Foxp3^{EGFP}$ expression and Foxp3-APC staining.

We have demonstrated that IVIg can modify $CD11c^+$ DC to induce Treg *ex vivo* (iTreg) in an antigen-specific manner. To determine if this required the presence of *in vivo* Treg, purified pulmonary $CD11c^+$ DC obtained from Treg depleted, IVIg-treated mice were co-cultured with OT-II/$Foxp3^{EGFP}$ $CD4^+$ T cells in the presence of OVA. OT-II/$Foxp3^{EGFP}$ cells cultured with $CD11c^+$ DC in the absence of IVIg, generated T effector cells which proliferated and produced Th2 and Th17 cytokines, with minimal induction of Treg (data not shown). In contrast, $CD11c^+$ DC from either DT- or non-DT-exposed mice treated with IVIg were equally able to induce $Foxp3^+$ iTreg *in vitro* (Figure 6C, D). This effect was associated with diminished Th1/Th2/Th17-type intracellular cytokine production by effector $CD4^+$ T cells in the co-culture (Figure 7A-D). IL-10 levels were significantly higher in co-cultures from IVIg-treated mice, compared to DC from non-treated animals. However, IL-10 production was attenuated in the absence of endogenous Treg (Figure 7E). Overall, these results suggest that IVIg induces tolerogenic changes in DC even in the absence of Treg.

Fig. 7

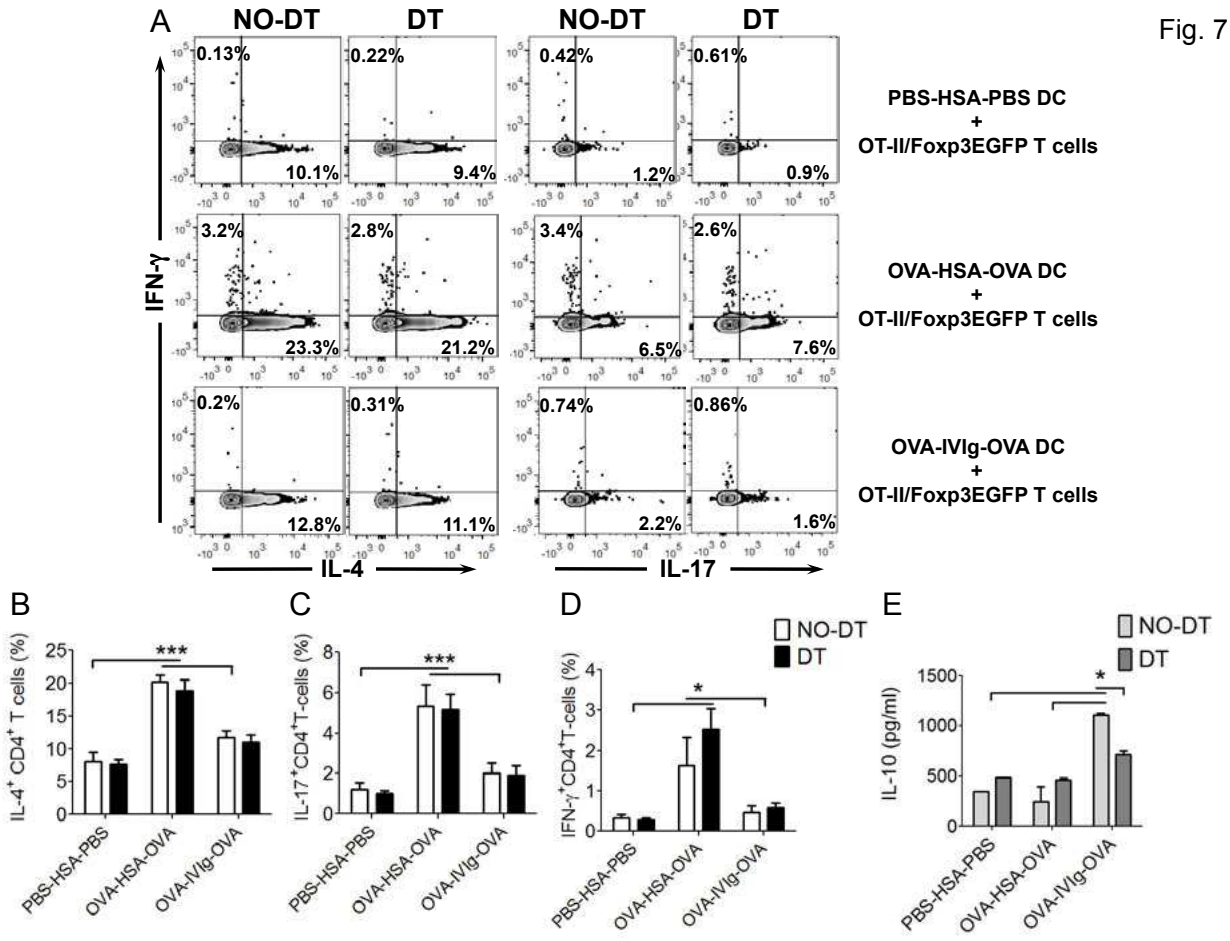

Figure 7. Depletion of endogenous Treg did not reverse the tolerogenic properties of IVIg-primed DC in regulation of cellular responses *ex vivo.*

$CD11c^+$ DC and OT-II/$Foxp3^{EGFP}$ $CD4^+$ T cells were purified, co-cultured, and stimulated with ionomycin/PMA in the presence of GlogiPlug. Intracellular IL-4, IL-17, and IFN-γ production were analyzed in $CD4^+$ T cells by flow cytometry.

A, B, C, D. Representative flow cytometric analyses (A) and quantification (B, C, D) of $IL\text{-}4^+$, $IL\text{-}17^+$, and $IFN\text{-}\gamma^+$ cells within $CD4^+$ T cells. ***, P<0.005; *,P<0.05; ANOVA with Tukey post-hoc, n=4. Gating strategy: viable $CD4^+$ lymphocytes were analyzed for intracellular cytokine staining.

E. IL-10 levels in co-culture supernatant, as determined by ELISA. OVA-IVIg-OVA DC from non-DT-treated mice increased IL-10 levels in co-culture compared to other groups. DC from OVA-IVIg-OVA mice treated with DT prior to and during OVA challenge were unable to induce IL-10 production in co-culture. *, P<0.05; ANOVA with Tukey post-hoc, n=4.

Differential gene expression of IVIg-generated pTreg

To investigate gene targets that were differentially expressed in pTreg generated by IVIg treatment, compared to endogenous Treg, we analyzed RNA from sorted Treg on gene-expression microarrays. Microarray data and MIAME (**M**inimum **I**nformation **A**bout a **M**icroarray **E**xperiment) compliance information is deposited in the National Center for Biotechnology Information Gene Expression Omnibus (GEO) database (GEO accession number GSE71811, accessible at http://www.ncbi.nlm.nih.gov/geo/query/acc.cgi?acc=GSE71811).

We found that 78 genes were differentially expressed by IVIg-generated pTreg, relative to endogenous Treg. We present the top 10 differentially expressed genes in Table I. Figure 8A depicts the log fold change as a function of mean log expression level (M-A plot). When comparing mixed (endogenous and IVIg-generated) Treg versus endogenous Treg alone, we detected similar patterns of differential gene expression (data not shown), reflecting gene expression from both endogenous and IVIg-generated Treg.

Gene expression data was confirmed by RT-qPCR for the genes *Gzma*, *Gzmb*, and *Ifitm2* (Figure 8E).

Gene Symbol	log(2)FC	Average Expression	t	P-Value	FDR P-value	B
Igkv10-96	4.219708628	8.168786494	2.31976789	0.038474312	0.247390427	-4.07776012
Gzmb	4.181552169	9.384794965	7.147125082	1.07E-05	0.004345594	3.756778046
Igk	4.01270105	7.019139998	3.940937957	0.001903012	0.042142496	-1.212521428
Hist1h2bk	3.116087063	7.878848707	4.664498275	0.000524374	0.020604625	0.038435769
Hist1h2ab	3.078058282	5.1489513	4.089289027	0.001453985	0.035997011	-0.951444191
Ighm	3.02809623	7.912686098	2.48994712	0.028161956	0.207180796	-3.789020284
Gm5593	3.008957503	7.092032121	5.340769276	0.000167017	0.012287079	1.145554211
Cdkn3	2.904471003	7.863296936	6.082340584	5.12E-05	0.007772727	2.27930145
1500009L16Rik	2.894095195	8.737148937	7.354114123	8.05E-06	0.004345594	4.024009575
Ifitm2	2.855573753	8.493691797	9.741504958	4.17E-07	0.002231589	6.687057179

Table I: Top 10 differentially expressed genes in IVIg-generated iTreg versus endogenous Treg.

Gene Symbol: official Mouse Genome Informatics Database abbreviation for gene

Log(2)FC: log(2)-fold-change for contrast

Average Expression: average log2-expression for the probe over all arrays and channels

t: moderated t-statistic

P-value: Raw P-value

FDR P-value: adjusted P-value using False Discovery Rate multiple comparisons correction.

B: log-odds that gene is differentially expressed

STRING database results

When examining our list of differentially-expressed genes, the STRING database calculated 63 network nodes, which represent genes with known protein-coding abilities, in the list. A simple numerical comparison between the calculated and expected number of "edges" - known relationships between genes – yields 810 edges for the network of differentially-expressed genes in IVIg-generated pTreg, as opposed to 33 expected edges, with an associated clustering coefficient of 0.898 and a PPI P-value >0.001. This strongly suggests that the network of gene products has significantly more interactions than expected, relative to a random set of similarly-sized proteins across the mouse genome. Thus, it is highly likely the proteins in the network are biologically linked as a group.

IVIg-generated pTreg have restored Granzyme A expression levels

To confirm the results of the gene array by an unrelated detection method, we examined the levels of intracellular GzmA protein expression by flow cytometry. Treg from negative-control animals displayed high GzmA MFI, which was lowered by OVA exposure. IVIg treatment increased GzmA expression levels to near baseline (Figure 8B). GzmB was undetectable by flow cytometry (data not shown).

IVIg-generated pTreg are a metabolically active population

We examined known gene function by *in silico* database analysis of our list of differentially expressed genes. PANTHER database hits for biological processes revealed that genes involved

in cellular and metabolic processes (including *Cdk1, Rrm2, Arhgap19*, *Anxa2*), biological regulation (including *Aurkb, Ccna2, Ccnb2, Ube2c, Gzma*), immune system processes (including *Igj, Il12rb2, Ccr5, Gzmb*), and apoptosis (*Birc5*) were enriched in our gene list (Figure 8C). Protein classes represented included cytoskeletal and nucleic-acid-binding proteins (including *Tpx2, Kif18b, Kif22, Kif23, Top2a, E2f8, Hist1h2bk, Hist1h1b*), enzyme modulators (including *Arhgap19, Arhgap11a, Ccnb2, Ccna2*), receptors and defense/immunity proteins (including *Il12rb2* and *Ccr5*) (Figure 8D).

DAVID functional annotation clustering yielded 23 clusters in total, 11 of which had statistically significant enrichments in annotation terms for cell cycle and cell division/mitosis (including *Cdk1, S100a6, Kif11, Prc1, Mki67, E2f8, Nuf2, Tpx2, Nusap1, Birc5, Cenpe, Aurkb, Cep55, Racgap1, Ube2c, Cdkn3, Esco2, Ncaph, Ccnb2, Plk1, Bub1, G,5593, H2afx, Ccna2*), cytoskeleton (including *Kif23, Kif22, Kif11, Prc1, Kif15, Tpx2, Nusap1, Gm5593, Kif18b, Birc5, Cenpe, Cep55, Aurkb, Racgap1, Anxa2*), chromosome/nucleosome (including *Hist1h2ab, Kif22, Mki67, Hist1h2bk, Hist1h1b, Hist1h1a, Nuf2, Bub1, H2afx, Hist1h2ak, Cenpe, Birc5, Aurkb, Top2a*), and histone (including *Hist1h2ab, Hist1h2bk, H2afx, Hist1h2ak*).

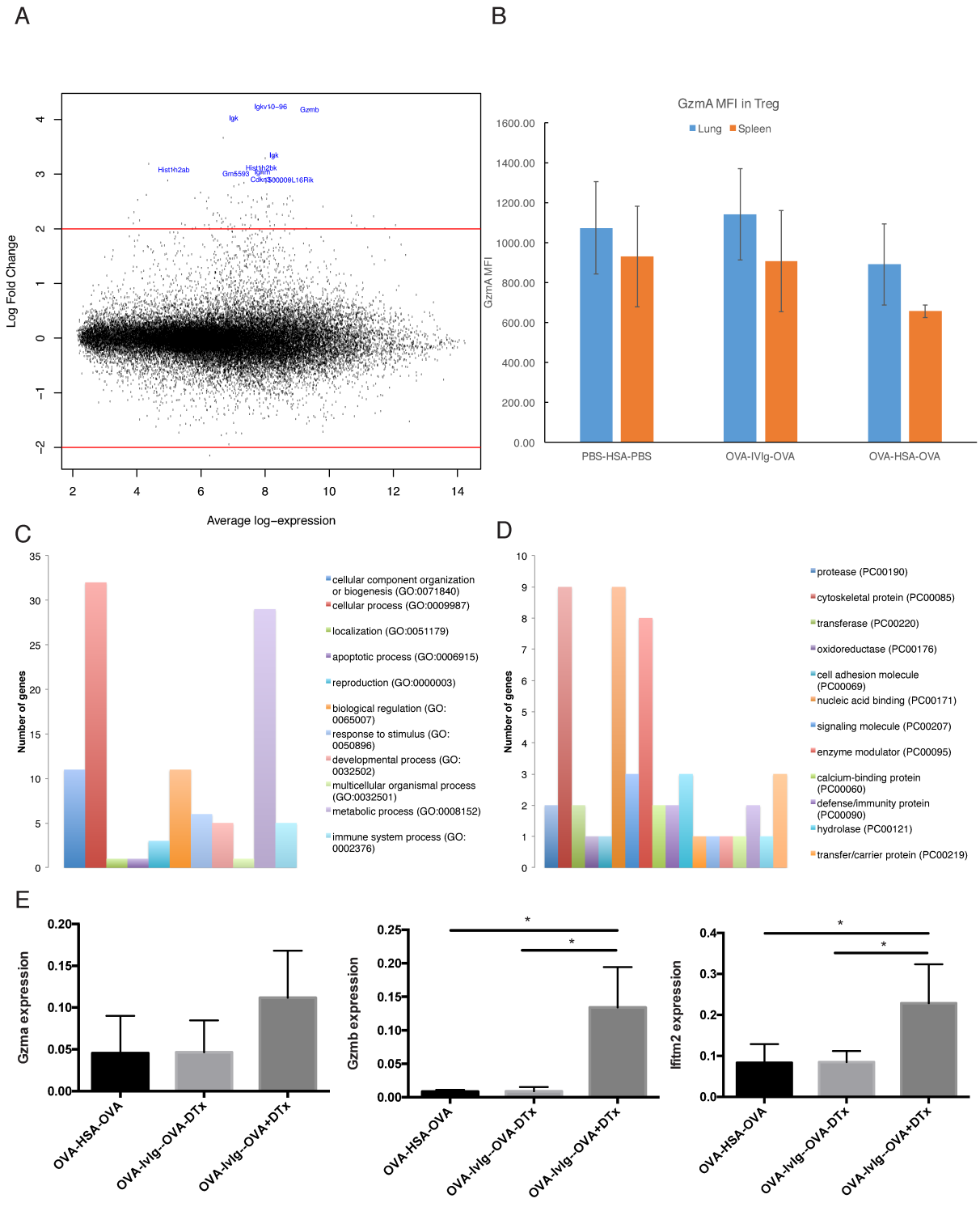

Figure 8. IVIg-generated Treg gene expression profiling suggests a metabolically active and plastic phenotype.

A. M-A (**M**inus log(2) fold change versus **A**verage log-expression) plot for the contrast of IVIg-generated pTreg versus endogenous Treg. Red lines indicate the threshold of 2-fold-change for differential gene expression. The 10 most differentially expressed genes are labeled with their NCBI gene symbol.

B. GzmA MFI in lung and spleen Treg (viable $CD4^+$ $CD25^{hi}$ $Foxp3^+$ cells) from sensitized, treated, and challenged animals.

C, D. PANTHER database search results. Annotation terms are plotted by number of genes per annotation term in the set of genes with log(2)FC>2. Individual genes can have multiple annotations. B, biological processes represented by GO annotations; C, protein classes represented by PANTHER annotations.

E. RT-qPCR confirmation of gene array results. Gene expression is presented as fold-change from control with normalization to *Gapdh* reference gene. *, P<0.05, ANOVA with Tukey post-hoc, n=4.

Discussion

IVIg-generated Treg

As an immune modulator, IVIg has multiple mechanisms of action (7). We have previously demonstrated that IVIg is able to modify DC-T-cell communication leading to induction of highly suppressive regulatory T-cells (1). We address here the distinctive nature of the pTreg induced by treatment of allergen-sensitized mice with IVIg. The present work is paralleled by a number of murine studies that have demonstrated functional pTreg *in vivo* (8). However, a particularly unique aspect of the system described here is the generation of a pure pTreg population, without endogenous Treg contamination. This allowed us to investigate differential expression of the various Treg compartments in a physiological setting of antigen-driven inflammation. It also allowed us to isolate sufficient antigen-specific pTreg generated *in vivo* for adoptive transfer experiments (9).

We have previously demonstrated (1, 4) that IVIg resolves antigen-induced airway inflammation and AHR in murine AAD via a mechanism associated with the peripheral induction of highly suppressive Foxp3$^+$ Treg and their homing to pulmonary tissues. This mechanism depended on modification of CD11c$^+$ DC and modulation of cytokine production. The most important finding of the present study was the requirement of Treg in IVIg-directed peripheral tolerance and protection against airway inflammation. pTreg were generated from naïve or mature CD4$^+$ effector T cells during T cell activation (10), and were effective in preventing the inappropriate immune responses to inhaled OVA, due to their antigen specificity and their compartmentalization capability (11).

Cellular phenotype

When examining specific IVIg-pTreg phenotypes, we determined that both IVIg-pTreg and endogenous Treg express high levels of LAP, a marker associated with enhanced suppressive activity. Chen et al (2) described a LAP-expressing Treg population that regulated the multiple sclerosis disease model experimental autoimmune encephalomyelitis (EAE) in a TGF-β-mediated fashion, and had greater suppressive ability than other Treg subsets. Similarly, Duan et al (12) found that LAP$^+$ Treg abolish both induction and effector phases of AAD in a model of antigen tolerance. Sun et al (13) suggest LAP as a marker for functional Treg in the context of cancer immunotherapy: this may provide an alternate biomarker for Treg induction in many disease states.

Conversely to LAP, we found that IVIg-pTreg had lower Nrp1 expression than endogenous Treg. Nrp1 has been recently described as a specific marker for tTreg (3), as opposed to canonical markers such as Foxp3, CD25, GITR, and CTLA-4. Weiss et al (14) found that Nrp1^{low} Treg were undetectable in thymus but enriched in the intestinal musoca, a major site of Treg induction. Interestingly, high Nrp1 expression correlated well with Helios expression, although Helios is found on subsets other than tTreg (15). Yadav et al (3) described Nrp1^{low} pTreg generated *in vitro* by CD3/CD28 stimulation or by antigen-loaded DC:T cell coculture, and *in vivo* by chronic antigen administration. Furthermore, Nrp1 levels remained stable regardless of activation state. Nrp1

has been implicated in sustaining interaction between DC and Treg and blocking effector T cell access (6). We speculate that pTreg, with low Nrp1 expression, are potentially more available to traffic to inflammatory tissue and suppress immune responses. This may explain our finding of greatly enhanced pTreg in pulmonary tissues from IVIg-treated mice (1).

Gene expression profile of IVIg-generated pTreg

When examining the gene expression profile of IVIg-generated pTreg, we determined that they represent a metabolically active, motile, and phenotypically plastic population, increasing the expression of genes associated with cell cycle, chromatin activity/histones, cytoskeleton, and apoptosis. This suggests several possible functions matching an active regulatory and phenotypically plastic phenotype, responding to inflammatory stimuli by modifying gene expression (16). The upregulated cytoskeleton-associated genes indicate that IVIg-generated pTreg are motile, homing to the inflammatory microenvironments in local and systemic tissues. The upregulated cell cycle/mitosis-associated and regulatory process genes reflect a potentially expanding population of functional regulatory cells. Furthermore, these cells are transcriptionally active, as evidenced by the upregulated genes associated with chromosome/nucleosome/histone. Beier et al (17) review *Foxp3* epigenetic modifications, and explain that methylation of the normally-demethylated *Foxp3* promoter TSDR (Treg-specific demethylated region) inhibits Treg function, while acetylation of TSDR promotes Treg function. They therefore suggest that histone deacetylaces (HDACs) are relevant targets for functional modulation. More specifically, Wang et al recently reported that HDAC3 modulates tTreg and pTreg development and function, and is essential for iTreg differentiation and suppressive function *in vitro* (18). Interestingly, we found that the *Foxp3* gene itself was not differentially expressed, with high average expression among all groups. Bin Dhuban et al (19) suggest that Foxp3 does not directly alter chromatin accessibility; rather, it modulates Treg transcriptional activity by binding to pre-established enhancers, such as the Foxo family of transcription factors.

We found that the second-highest differentially expressed gene in IVIg-generated pTreg was the serine protease granzyme B; granzyme A was also differentially expressed. This is consistent with

reported characterizations of Treg in other disease models. Velaga et al found that in a murine model of gastrointestinal graft-versus-host disease (GvHD), Treg require granzyme A to prevent GvHD, perhaps due to their increased migratory efficiency, as granzyme A cleaves extracellular matrix proteins (20). Using a murine model of respiratory syncytial virus (RSV) infection, Loebbermann et al (21) determined that Treg expressing granzyme B are required to suppress cellular infiltration into the lung in RSV infection; these cells degranulate after *in vitro* stimulation. They suggest that this requirement is likely due to the cytolytic action of granzyme B on virus-infected cells, and increased migratory ability due to decorin cleavage in the extracellular matrix, which facilitates Treg homing to inflammatory sites. This is another line of evidence that may explain our finding of pTreg enrichment in lung tissues of IVIg-treated antigen-exposed mice (1).

Dendritic cells and Treg induction

The requirement for DC in the induction of Treg in our model are in agreement with findings from other investigators, demonstrating the critical role of $CD11c^+$ DC in elaboration of peripheral T cell tolerance through induction of Treg (22, 23). IVIg induces downregulation of co-stimulatory molecules and modulates cytokine secretion by DC (24). Nonetheless, the induction of tolerogenic DC was necessary but not sufficient for inhibition of AAD if Treg were eliminated by successive DT injections. In addition to the AAD model, the implication of IVIg in induction and development of Treg has been demonstrated in experimental allergic encephalomyelitis (EAE) (25), systemic lupus erythematosus (26), vasculitis (27), immune thrombocytopenic purpura (28), and Kawasaki disease (29). Notably, the deficiency of $Foxp3^+$ Treg in patients with Kawasaki disease is associated with resistance to IVIg therapy (30). All of these findings indicate that Treg play an integral role in mediating the immune-modulatory effects of polyclonal IgG.

IgE and Treg

Interestingly, our data showed that the depletion of all endogenous Treg just prior to allergen challenge did not lead to marked exacerbation of airway pathology and AHR, despite a striking increase in total serum IgE levels. IgE is responsible for initiation of allergic reactions and is important for the development of persistent airway inflammation (31, 32). Consistent with our

findings, Baru et al (33) demonstrated that depletion of Foxp3$^+$ Treg during the course of allergen challenge did not lead to an aggravated allergic response, whereas Treg depletion in the priming phase of antigen-immunization resulted in exacerbation of allergic airway inflammation.

Conclusion

Taken together, our results show that IVIg generates a pure population of functional pTreg from non-Treg precursors. We demonstrate the absolute requirement for Foxp3+ Treg in the IVIg-mediated resolution of allergic airway inflammation, delineate the precise genetic signature and phenotype of this pure population of pTreg, and provide a rationale for potential application of IVIg in autoimmune and inflammatory conditions associated with Treg deficiencies. Further work will characterize the molecular mechanisms of pTreg function and DC tolerogenicity, along with Treg fate-mapping to delineate the precise timing and stability of the Treg regulatory response. These studies will provide a more profound understanding of the induction of regulatory function.

Author Contributions

AHM, GNK, and BDM designed the study. AHM, GNK, DX, MB, and MD performed the experiments and analyzed the data. AHM and GNK wrote the paper; GNK and BDM revised the paper. CAP and WM provided important critical comments. BDM supervised the research group and takes responsibility for the integrity of the work. All authors read and approved the final version of the manuscript.

Acknowledgements

We thank Camille Stegen of the McGill University flow cytometry core facility for her assistance with flow cytometric sorting. We thank the microarray core facility at the McGill University-Génome Québec Innovation Centre for their expertise and assistance with gene expression sample processing. We acknowledge infrastructure support from the Fonds de Recherche du Québec – Santé (FRQS). GNK is the recipient of a CIHR Canada Graduate Scholarships Doctoral

Research Award. CAP holds a CIHR Canada Research Chair. The authors declare that they have no competing interests.

References

1. Massoud AH, Guay J, Shalaby KH, Bjur E, Ablona A, Chan D, et al. Intravenous immunoglobulin attenuates airway inflammation through induction of forkhead box protein 3-positive regulatory T cells. *The Journal of allergy and clinical immunology* (2012) **129**(6):1656-65.e3. Epub 2012/05/09. doi: 10.1016/j.jaci.2012.02.050. PubMed PMID: 22564681.

2. Chen ML, Yan BS, Bando Y, Kuchroo VK, Weiner HL. Latency-associated peptide identifies a novel CD4+CD25+ regulatory T cell subset with TGFbeta-mediated function and enhanced suppression of experimental autoimmune encephalomyelitis. *Journal of immunology (Baltimore, Md : 1950)* (2008) **180**(11):7327-37. PubMed PMID: 18490732; PubMed Central PMCID: PMC2771858.

3. Yadav M, Louvet C, Davini D, Gardner JM, Martinez-Llordella M, Bailey-Bucktrout S, et al. Neuropilin-1 distinguishes natural and inducible regulatory T cells among regulatory T cell subsets in vivo. *The Journal of experimental medicine* (2012) **209**(10):1713-22, S1-19. doi: 10.1084/jem.20120822. PubMed PMID: 22966003; PubMed Central PMCID: PMC3457729.

4. Kaufman GN, Massoud AH, Audusseau S, Banville-Langelier AA, Wang Y, Guay J, et al. Intravenous immunoglobulin attenuates airway hyperresponsiveness in a murine model of allergic asthma. *Clinical and experimental allergy : journal of the British Society for Allergy and Clinical Immunology* (2011) **41**(5):718-28. Epub 2011/01/25. doi: 10.1111/j.1365-2222.2010.03663.x. PubMed PMID: 21255135.

5. Xu W, Lan Q, Chen M, Chen H, Zhu N, Zhou X, et al. Adoptive transfer of induced-Treg cells effectively attenuates murine airway allergic inflammation. *PloS one* (2012) **7**(7):e40314. Epub 2012/07/14. doi: 10.1371/journal.pone.0040314. PubMed PMID: 22792275; PubMed Central PMCID: PMCPmc3392250.

6. Kornete M, Piccirillo CA. Functional crosstalk between dendritic cells and Foxp3(+) regulatory T cells in the maintenance of immune tolerance. *Frontiers in immunology* (2012)

3:165. Epub 2012/06/28. doi: 10.3389/fimmu.2012.00165. PubMed PMID: 22737152; PubMed Central PMCID: PMCPmc3381230.

7. Kaufman GN, Massoud AH, Dembele M, Yona M, Piccirillo CA, Mazer BD. Induction of Regulatory T Cells by Intravenous Immunoglobulin: A Bridge between Adaptive and Innate Immunity. *Frontiers in immunology* (2015) **6**:469. doi: 10.3389/fimmu.2015.00469. PubMed PMID: 26441974; PubMed Central PMCID: PMCPMC4566032.

8. Schmitt EG, Williams CB. Generation and function of induced regulatory T cells. *Frontiers in immunology* (2013) **4**:152. doi: 10.3389/fimmu.2013.00152. PubMed PMID: 23801990; PubMed Central PMCID: PMC3685796.

9. Beres AJ, Drobyski WR. The role of regulatory T cells in the biology of graft versus host disease. *Frontiers in immunology* (2013) **4**:163. doi: 10.3389/fimmu.2013.00163. PubMed PMID: 23805140; PubMed Central PMCID: PMC3690651.

10. Chen W, Jin W, Hardegen N, Lei KJ, Li L, Marinos N, et al. Conversion of peripheral CD4+CD25- naive T cells to CD4+CD25+ regulatory T cells by TGF-beta induction of transcription factor Foxp3. *The Journal of experimental medicine* (2003) **198**(12):1875-86. Epub 2003/12/17. doi: 10.1084/jem.20030152. PubMed PMID: 14676299; PubMed Central PMCID: PMCPmc2194145.

11. Nguyen TL, Sullivan NL, Ebel M, Teague RM, DiPaolo RJ. Antigen-specific TGF-beta-induced regulatory T cells secrete chemokines, regulate T cell trafficking, and suppress ongoing autoimmunity. *Journal of immunology (Baltimore, Md : 1950)* (2011) **187**(4):1745-53. Epub 2011/07/13. doi: 10.4049/jimmunol.1004112. PubMed PMID: 21746962.

12. Duan W, So T, Mehta AK, Choi H, Croft M. Inducible CD4+LAP+Foxp3- regulatory T cells suppress allergic inflammation. *Journal of immunology (Baltimore, Md : 1950)* (2011) **187**(12):6499-507. doi: 10.4049/jimmunol.1101398. PubMed PMID: 22079987; PubMed Central PMCID: PMC3237738.

13. Sun J, Tang DN, Fu T, Sharma P. Identification of human regulatory T cells in the setting of T-cell activation and anti-CTLA-4 immunotherapy on the basis of expression of latency-associated peptide. *Cancer discovery* (2012) **2**(2):122-30. doi: 10.1158/2159-8290.CD-11-0236. PubMed PMID: 22585857.

14. Weiss JM, Bilate AM, Gobert M, Ding Y, Curotto de Lafaille MA, Parkhurst CN, et al. Neuropilin 1 is expressed on thymus-derived natural regulatory T cells, but not mucosa-generated induced Foxp3+ T reg cells. *The Journal of experimental medicine* (2012) **209**(10):1723-42, S1. doi: 10.1084/jem.20120914. PubMed PMID: 22966001; PubMed Central PMCID: PMC3457733.

15. Akimova T, Beier UH, Wang L, Levine MH, Hancock WW. Helios expression is a marker of T cell activation and proliferation. *PloS one* (2011) **6**(8):e24226. doi: 10.1371/journal.pone.0024226. PubMed PMID: 21918685; PubMed Central PMCID: PMC3168881.

16. Hori S. Lineage stability and phenotypic plasticity of Foxp3(+) regulatory T cells. *Immunological reviews* (2014) **259**(1):159-72. doi: 10.1111/imr.12175. PubMed PMID: 24712465.

17. Beier UH, Akimova T, Liu Y, Wang L, Hancock WW. Histone/protein deacetylases control Foxp3 expression and the heat shock response of T-regulatory cells. *Curr Opin Immunol* (2011) **23**(5):670-8. doi: 10.1016/j.coi.2011.07.002. PubMed PMID: 21798734; PubMed Central PMCID: PMCPMC3190028.

18. Wang L, Liu Y, Han R, Beier UH, Bhatti TR, Akimova T, et al. FOXP3+ regulatory T cell development and function require histone/protein deacetylase 3. *J Clin Invest* (2015) **125**(3):1111-23. doi: 10.1172/JCI77088. PubMed PMID: 25642770; PubMed Central PMCID: PMCPMC4362235.

19. Bin Dhuban K, Kornete M, E SM, Piccirillo CA. Functional dynamics of Foxp3(+) regulatory T cells in mice and humans. *Immunological reviews* (2014) **259**(1):140-58. doi: 10.1111/imr.12168. PubMed PMID: 24712464.

20. Velaga S, Ukena SN, Dringenberg U, Alter C, Pardo J, Kershaw O, et al. Granzyme A Is Required for Regulatory T-Cell Mediated Prevention of Gastrointestinal Graft-versus-Host Disease. *PloS one* (2015) **10**(4):e0124927. doi: 10.1371/journal.pone.0124927. PubMed PMID: 25928296; PubMed Central PMCID: PMCPMC4415808.

21. Loebbermann J, Thornton H, Durant L, Sparwasser T, Webster KE, Sprent J, et al. Regulatory T cells expressing granzyme B play a critical role in controlling lung inflammation

during acute viral infection. *Mucosal Immunol* (2012) **5**(2):161-72. doi: 10.1038/mi.2011.62. PubMed PMID: 22236998; PubMed Central PMCID: PMCPMC3282434.

22. Delgado M, Gonzalez-Rey E, Ganea D. Vasoactive intestinal peptide: the dendritic cell --> regulatory T cell axis. *Annals of the New York Academy of Sciences* (2006) **1070**:233-8. Epub 2006/08/05. doi: 10.1196/annals.1317.020. PubMed PMID: 16888172.

23. Sela U, Olds P, Park A, Schlesinger SJ, Steinman RM. Dendritic cells induce antigen-specific regulatory T cells that prevent graft versus host disease and persist in mice. *The Journal of experimental medicine* (2011) **208**(12):2489-96. Epub 2011/11/16. doi: 10.1084/jem.20110466. PubMed PMID: 22084406; PubMed Central PMCID: PMCPmc3256961.

24. Bayry J, Lacroix-Desmazes S, Carbonneil C, Misra N, Donkova V, Pashov A, et al. Inhibition of maturation and function of dendritic cells by intravenous immunoglobulin. *Blood* (2003) **101**(2):758-65. Epub 2002/10/24. doi: 10.1182/blood-2002-05-1447. PubMed PMID: 12393386.

25. Ephrem A, Chamat S, Miquel C, Fisson S, Mouthon L, Caligiuri G, et al. Expansion of CD4+CD25+ regulatory T cells by intravenous immunoglobulin: a critical factor in controlling experimental autoimmune encephalomyelitis. *Blood* (2008) **111**(2):715-22. Epub 2007/10/13. doi: 10.1182/blood-2007-03-079947. PubMed PMID: 17932250.

26. Costa N, Pires AE, Gabriel AM, Goulart LF, Pereira C, Leal B, et al. Broadened T-cell repertoire diversity in ivIg-treated SLE patients is also related to the individual status of regulatory T-cells. *Journal of clinical immunology* (2013) **33**(2):349-60. Epub 2012/10/16. doi: 10.1007/s10875-012-9816-7. PubMed PMID: 23064977.

27. Tsurikisawa N, Saito H, Oshikata C, Tsuburai T, Akiyama K. High-dose intravenous immunoglobulin treatment increases regulatory T cells in patients with eosinophilic granulomatosis with polyangiitis. *The Journal of rheumatology* (2012) **39**(5):1019-25. Epub 2012/04/03. doi: 10.3899/jrheum.110981. PubMed PMID: 22467925.

28. Aslam R, Hu Y, Gebremeskel S, Segel GB, Speck ER, Guo L, et al. Thymic retention of CD4+CD25+FoxP3+ T regulatory cells is associated with their peripheral deficiency and thrombocytopenia in a murine model of immune thrombocytopenia. *Blood* (2012) **120**(10):2127-32. Epub 2012/07/05. doi: 10.1182/blood-2012-02-413526. PubMed PMID: 22760780.

29. Olivito B, Taddio A, Simonini G, Massai C, Ciullini S, Gambineri E, et al. Defective FOXP3 expression in patients with acute Kawasaki disease and restoration by intravenous immunoglobulin therapy. *Clinical and experimental rheumatology* (2010) **28**(1 Suppl 57):93-7. Epub 2010/06/11. PubMed PMID: 20412712.

30. Hirabayashi Y, Takahashi Y, Xu Y, Akane K, Villalobos IB, Okuno Y, et al. Lack of CD4(+)CD25(+)FOXP3(+) regulatory T cells is associated with resistance to intravenous immunoglobulin therapy in patients with Kawasaki disease. *European journal of pediatrics* (2013) **172**(6):833-7. Epub 2013/01/24. doi: 10.1007/s00431-013-1937-3. PubMed PMID: 23340699.

31. Settipane RA. Advances in therapeutic immunomodulation of IgE-mediated respiratory disease. *Medicine and health, Rhode Island* (2008) **91**(6):187-90, 93-5. Epub 2008/07/10. PubMed PMID: 18610807.

32. Rabe KF, Calhoun WJ, Smith N, Jimenez P. Can anti-IgE therapy prevent airway remodeling in allergic asthma? *Allergy* (2011) **66**(9):1142-51. Epub 2011/06/08. doi: 10.1111/j.1398-9995.2011.02617.x. PubMed PMID: 21645010.

33. Baru AM, Ganesh V, Krishnaswamy JK, Hesse C, Untucht C, Glage S, et al. Absence of Foxp3+ regulatory T cells during allergen provocation does not exacerbate murine allergic airway inflammation. *PloS one* (2012) **7**(10):e47102. Epub 2012/10/17. doi: 10.1371/journal.pone.0047102. PubMed PMID: 23071726; PubMed Central PMCID: PMCPmc3468440.

Flow cytometry supplement

Panel	Antigen	Fluorochrome	Manufacturer	Clone
Treg	CD4	BV510	BioLegend	RM4-5
	CD25	PE	BioLegend	3C7
	Foxp3	APC	eBioscience	FJK-16s
	LAP	PerCP-Cy5.5	BioLegend	TW7-16B4
	Nrp-1	eFluor450	eBioscience	3DS304M
	GzmA	PerCP-eFluor710	eBioscience	GzA-3G8.5
	GzmB	PE-eFluor610	eBioscience	NGZB
DC	CD11c	PE-eFluor610	eBioscience	N418
	MHC-II	eFluor450	eBioscience	M5/114.15.2
	CD80	FITC	BD Pharmingen	16-10A1
	IL-4	PE	BioLegend	11B11
	IL-17	PerCP-Cy5.5	eBioscience	eBio17B7
	IFN-γ	APC	BioLegend	XMG1.2

Supplemental Table: Antibodies used for flow cytometric analyses.

Supplemental Figure 1: Treg sort gating strategy

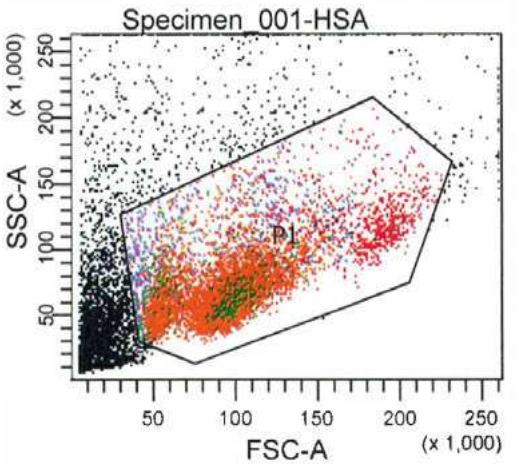

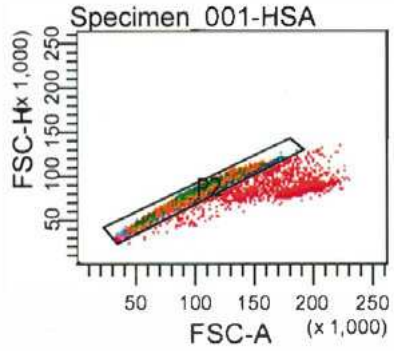

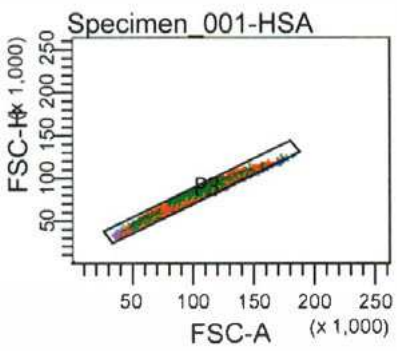

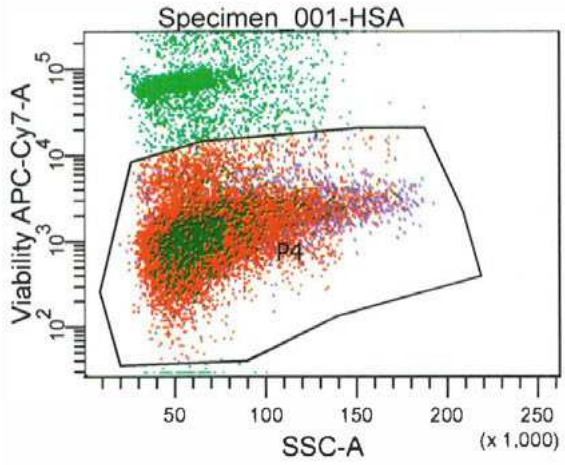

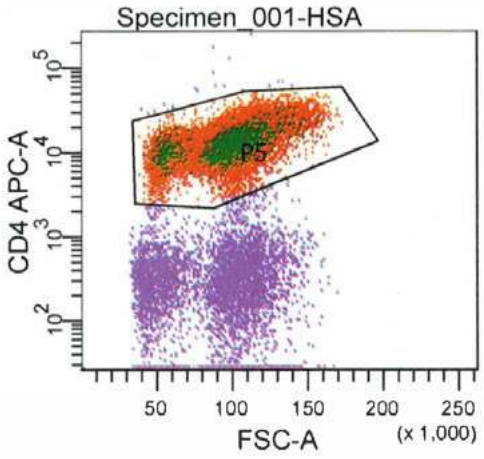

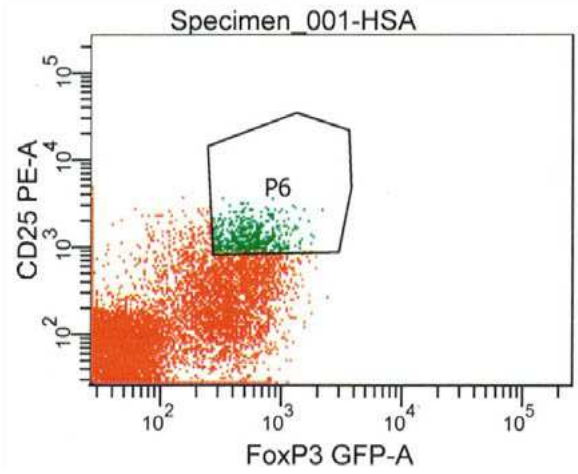

Tube: HSA

Population	#Events	%Parent	%Total
All Events	100,000	####	100.0
P1	81,212	81.2	81.2
P2	77,060	94.9	77.1
P3	76,680	99.5	76.7
P4	73,424	95.8	73.4
P5	68,225	92.9	68.2
P6	1,327	1.9	1.3

Chapter 5:

Gene expression analysis of Th2-stimulated human B cells

Gabriel N Kaufman

Rationale and Background

The author's doctoral research project centred around regulatory events in the immune system, primarily those related to IVIg treatment in the context of allergic and inflammatory disorders. The key cell types involved in this class of response are DC and T cells, as detailed in the Introduction to this thesis, and in the work discussed in the other research papers. With regard to the present study, the author's interest was piqued to examine regulatory pathways distinct from the DC:Treg axis, to broaden his understanding of immune-regulatory biology as a whole.

Our laboratory has a long-standing interest in immune-regulatory processes and B cell fundamental biology: increasingly, the regulatory potential of B cells is being demonstrated as crucial to clearance of inflammation and immunological tolerance (1). We therefore wished to study the events leading to B cell activation in the context of Th2-mediated allergic inflammation, and to determine what stimuli could lead to an immunosuppressive or regulatory phenotype.

The present work was performed in the context of a study originally designed to examine the effects of hydrocortisone treatment on activated B cells. However, as it was determined that hydrocortisone-treated activated B cells had no significantly changed gene expression patterns, relative to activated B cells alone (see discussion below), we focused instead on the search for novel molecules induced by activation of B cells in the initiation steps for class switching and IgE production. This allowed us to examine the transcriptome of activated B cells in a regulatory context, uncovering novel genes and pathways related to regulatory B cell activity.

This chapter discusses several expanded investigations performed by the author using some of the commonly accepted bioinformatics tools for gene expression analyses. The main body of work is currently published in *Frontiers in Immunology* (2), with the present author credited with third authorship on the paper. Tonsillar B cell isolation, cell cultures, and RNA extraction were performed by Salem Al-Tememi in 2005. Microarray sample preparation and array scanning was performed by McGill University and Génome Québec Innovation Centre staff under the auspices of their gene expression analysis services platform in May-June 2005. The present author performed the microarray data read-in from raw scan files, statistical analyses, and database searches, all in 2015-2016.

Introduction

B lymphocytes are crucial for the initiation and potentiation of allergic inflammation, by the production of IgE and the secretion of key cytokines that enhance allergic responses (3). Our laboratory has contributed towards the understanding of B cell autoregulation of Th2-mediated inflammation by demonstrating that human B cells secrete IL13 (4), a cytokine which promotes IgE isotype switching of B cells, upregulates CD23 and MHC class II expression, and inhibits pro-inflammatory cytokine/chemokine production. We also identified signaling pathways related to expression of the IL-13 receptor on human B cells (5).

In this context, we undertook to uncover novel molecules induced by activation of B cells via Th2 cytokines, the initiating steps for class switching and production of IgE. Using expression profiling of Th2-stimulated human tonsillar B-cells, we identified multiple genes that were previously known to influence IgE production, and a novel gene, Semaphorin 4C (*SEMA4C*) that had never before been described in immune biology.

Materials and Methods

Subject selection and ethics statement

Children between the ages of 3-12 requiring tonsillectomy or adenoidectomy were randomly recruited from the otolaryngology clinic at the Montreal Children's Hospital. as part of a study on

B cell responses to corticosteroids. At tonsillectomy, eligible children were not taking nasal or inhaled corticosteroids. All patient caregivers provided written informed consent. This research protocol was conducted in accordance with the WMA Declaration of Helsinki and was approved by the Research Ethics Board of the McGill University Health Centre.

Tonsillar B cell isolation

Human tonsils were minced and resuspended in wash medium: RPMI 1640 2% FBS with 2 mM L-Glutamine, 50 U/mL penicillin, 50 ug/mL streptomycin, 15 mM HEPES (all Hyclone) and 0.5 µg/mL amphotericin B (Life Technologies). The cells were overlaid on density-gradient separation medium (Lymphoprep, StemCell Technologies) and centrifuged to isolate the mononuclear cells. These cells were mixed with human red blood cells and B cells were purified using RosetteSep Human B Cell Enrichment Cocktail (StemCell Technologies).

B cell culture

B cells were cultured for 24 hours at 0.5 million cells/mL in complete medium (RPMI 1640 10% FBS with 2 mM L-glutamine, 50 U/mL penicillin, 50 µg/mL streptomycin, 1 mM sodium pyruvate and 15mM HEPES) in the presence or absence of 1 µg/mL anti-CD40 antibody purified from the G28-5 cell line (American Type Culture Collection) (6) and 100 U/mL recombinant human IL-4 (PeproTech), with or without 1 µM hydrocortisone (HC; Sigma-Aldrich).

RNA extraction and processing

RNA was extracted with TRIzol (Life Technologies) and cleaned with RNeasy Mini silica-gel membrane columns (Qiagen). RNA quality and concentration was assessed by Bioanalyzer microcapillary electrophoresis (Agilent). Samples used for microarray hybridization had 260/280 absorbance ratios >1.8 and RNA Integrity Numbers (RIN) >7.0.

Gene expression microarray analyses

RNA samples were analyzed using Affymetrix GeneChip Human Genome U133 Plus 2.0 microarrays, which contain probe sets for 54,675 unique gene-expression sequences from the

NCBI UniGene database, build 159: this provides genome-wide expression coverage for 24,442 genes. Preparatory cRNA synthesis and labeling, microarray hybridization reactions, and array scanning were performed according to standard protocols at the McGill University and Génome Québec Innovation Centre microarray core facility.

Microarray data statistical analyses

All data processing and statistical calculations were performed using the R statistical environment (7). Annotated data analysis scripts are provided in Appendix I. Gene expression data were processed using the Bioconductor packages *oligo* (8) for data read-in and normalization, and *limma* (9) for linear modeling and differential-expression statistics. Probe intensities were normalized across all arrays by the robust multi-array average (RMA) algorithm (10).

Differential gene expression of antiCD40/IL-4-treated B cells versus unstimulated B cells (control group) was calculated by linear modeling of the contrast and empirical Bayes sample variance shrinkage, followed by moderated t-tests with false-discovery rate (FDR) correction (11). Results were expressed in terms of log(2) fold-change. Differentially expressed genes were defined as genes with a log(2) fold-change greater than 2. FDR-corrected P-values less than 0.5 were considered statistically significant.

Gene list database analyses

To examine known gene functions in our identified gene list, 330 differentially expressed genes were selected, and uploaded to the PANTHER (**P**rotein **AN**alysis **TH**rough **E**volutionary **R**elationships) classification system web database (12), which classifies genes based on curated ontology terms. Database hits were examined in the category of biological process using Gene Ontology (GO) annotations (13) and in the category of protein class using PANTHER accessions. A binomial statistical representation test was performed to compare functional category

overrepresentation or underrepresentation in our gene list, relative to the reference list of the entire human genome.

To examine functional gene clusters in our selection, the list of differentially-expressed genes was uploaded to the DAVID (**D**atabase for **A**nnotation, **V**isualization, and **I**ntegrated **D**iscovery) functional gene clustering algorithm (version 6.7) (14), which compares the uploaded gene list to a gene-gene similarity matrix of over 75,000 functional annotation terms, and generates a cluster map of functionally similar genes using fuzzy heuristic partitioning. Fisher's Exact test and Benjamini multiple comparisons corrections were used to test gene enrichment in annotation terms. Adjusted P-values less than 0.05 were considered statistically significant.

To determine gene network interactions in our selection, the list of differentially-expressed genes was uploaded to the STRING (**S**earch **T**ool for the **R**etrieval of **I**nteracting **G**enes/Proteins) database (version 10.0) (15), which examines known relationships in between genes, building networks of predicted functional associations based on GO annotations, pathways, and domains. The number of interactions present in our gene list was calculated by the STRING algorithm and compared to the expected number of interactions if the nodes were selected at random from a set of similarly-sized protein products across the entire human genome. A protein-protein interaction (PPI) enrichment P-value for the network was calculated, testing the likelihood that the number of interactions was higher than expected, along with a network clustering coefficient, which measured the connectedness of the network nodes.

Enrichment analyses for GO biological processes and GO cellular components were performed and tested by comparing the associated count in the gene set to genome-wide background enrichment, with false-discovery rate (FDR) multiple comparison corrections. Adjusted P-values less than 0.05 were considered statistically significant.

Results

Stimulated B cells differentially express immune-system related genes

To investigate potential gene targets that were differentially expressed in human B cells following Th2-skewing conditions, we analyzed RNA from stimulated and unstimulated cells on gene-expression microarrays. Microarray data and MIAME (**M**inimum **I**nformation **A**bout a **M**icroarray **E**xperiment) compliance information was deposited in the Gene Expression Omnibus (GEO) database (GEO accession number GSE71810); the relevant metadata is included in Appendix III. Boxplots of raw and RMA-normalized data are depicted in Figure 1.

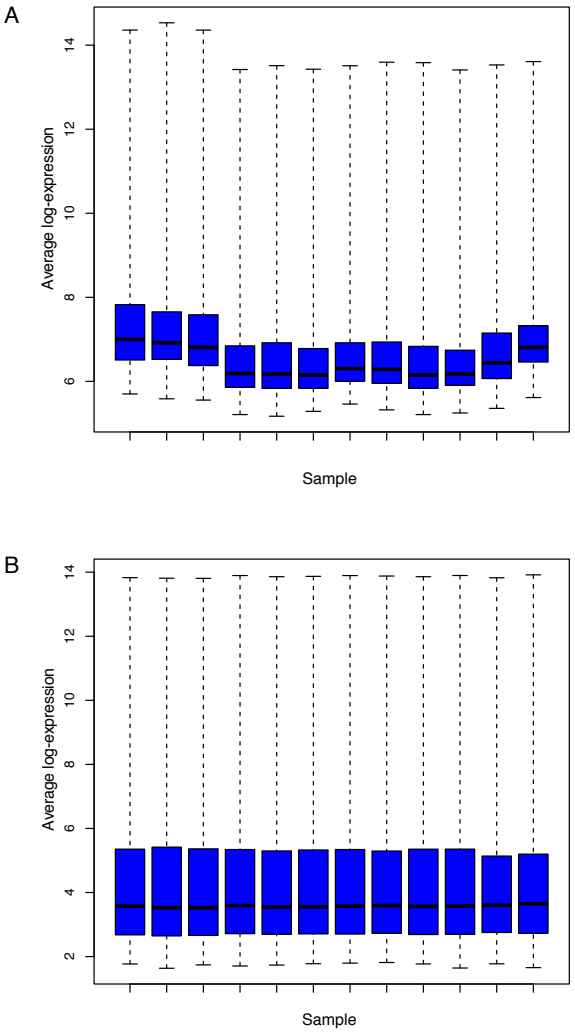

Figure 1. Boxplots of microarray expression levels before (A) and after (B) RMA normalization of expression data. Graphs are average log-expression for each sample, with median and interquartile ranges indicated.

Surprisingly, the original premise of this study, examining the effects of HC on antiCD40/IL-4-stimulated B cells, had to be rejected, as no significant differences in gene expression were found (Figure 2A). This suggests that HC alone does not significantly affect the gene expression profile of activated B cells at the 24-hour time point that was evaluated. We therefore chose to focus on the genes that were upregulated or downregulated by Th2-skewing treatment, relative to unstimulated cells (Figure 2B, Figure 2C, Table 1). Interestingly, when compared to control samples, cells stimulated with anti-CD40, IL-4, and HC for 24 hours displayed almost identical patterns of gene expression as cells stimulated with anti-CD40 and IL-4 (data not shown). Table 1 is a list of the top 10 differentially expressed genes for antiCD40/IL-4-treated B cells versus control.

Table 1: Differentially expressed genes in anti-CD40/IL4-treated B cells versus unstimulated cells.

Gene Symbol	Log(2)FC	Average Expression	t	P-value	FDR P-value	B
MAL	6.938443644	8.781046141	22.12378951	3.63E-11	2.84E-07	15.3252569
CCL17	6.105803764	7.680392611	16.5397378	1.11E-09	2.28E-06	12.50870126
IGH	5.935820046	7.673584573	12.06096389	4.14E-08	1.94E-05	9.187431123
LOC101928173	5.515918425	7.149173386	11.68877045	5.88E-08	2.39E-05	8.850838852
SEMA4C	5.21704198	7.547023138	21.29194618	5.71E-11	3.47E-07	14.97365834
TBC1D9	-5.036190035	5.841642242	-15.44879776	2.45E-09	3.26E-06	11.80732796
CYP26A1	4.930913543	7.459197163	7.998347059	3.54E-06	0.000373054	4.810661778
BATF3	4.918258573	7.085415104	22.83952642	2.49E-11	2.27E-07	15.61211466
TFPI2	4.822924251	5.491276439	16.39571399	1.23E-09	2.31E-06	12.41949125
NFIL3	4.719930309	6.618679958	37.8227258	5.99E-14	3.27E-09	19.4033636

Gene Symbol: Official Mouse Genome Informatics abbreviation for gene name.

Log(2)FC: log(2)-fold-change for contrast

Average Expression: average log2-expression for the probe over all arrays and channels

t: moderated t-statistic

P-value: Raw P-value

FDR P-value: adjusted P-value using False Discovery Rate multiple comparisons correction.

B: log-odds that gene is differentially expressed

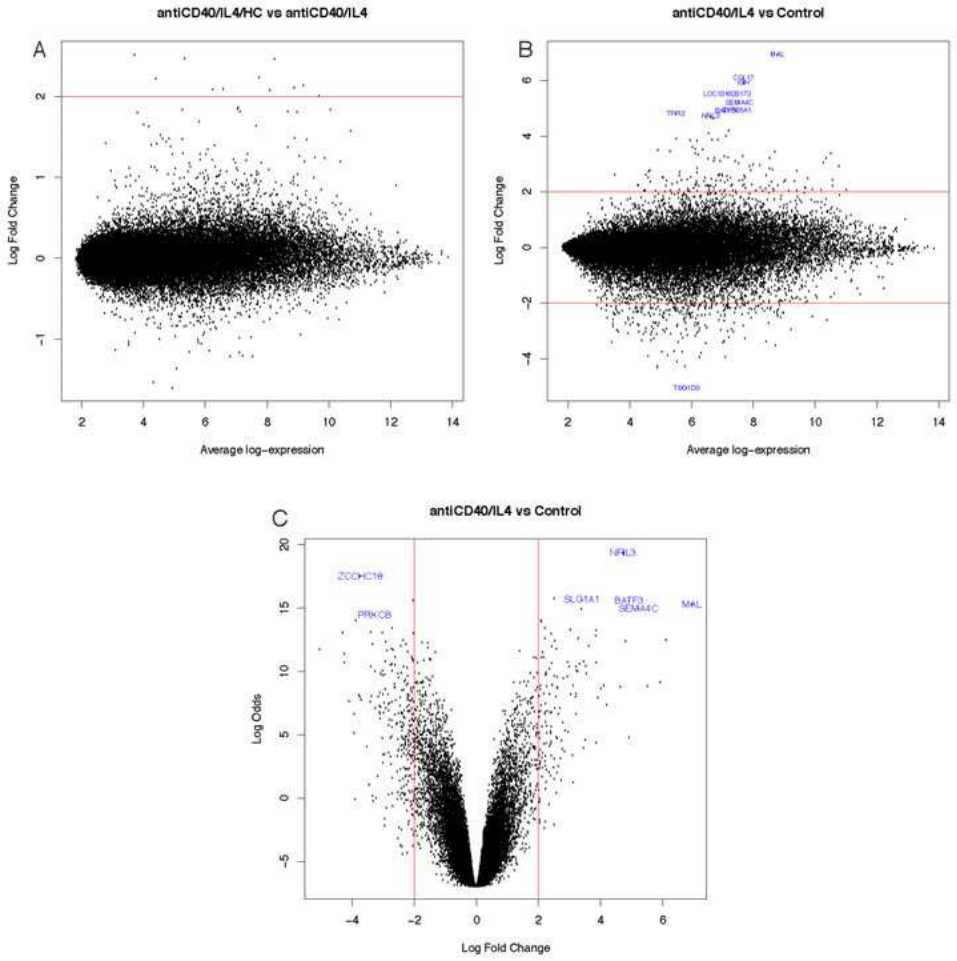

Figure 2. M-A (**M**inus log(2) fold change versus **A**verage log-expression) plots for the contrast of antiCD40/IL-4/HC versus antiCD40/IL-4 stimulated B cells (A) and antiCD40/IL-4 versus unstimulated B cells (B). (C) is a volcano plot, which depicts the log(2) fold-change versus the log-odds of differential gene expression for the contrast of antiCD40-IL-4 versus unstimulated B cells. The genes that are most highly differentially expressed are plotted farther to the left and right sides, while the most highly statistically significantly changed genes are plotted nearer the top of

the plot. For all plots, red lines indicate the threshold of log(2) fold-change for differential gene expression. The 10 most differentially expressed genes are labeled with their NCBI gene symbol.

PANTHER database results

We examined known gene function by *in silico* database analysis of our list of differentially expressed genes. PANTHER database hits for biological process revealed that genes involved in cellular processes, metabolic processes, and immune system processes were highly enriched in our gene list (Figure 3A). Protein classes represented include receptors, nucleic acid binding proteins, and immunity proteins (Figure 3B). Statistically overrepresented biological processes included immune system processes (GO:0002376, Fold-enrichment 2.66, P-value 8.79E-09), immune responses (GO:0006955, Fold- enrichment 2.94, P-value 4.03E-05), biological regulation (GO:0065007, Fold-enrichment 1.28, P-value 5.48E-03), among others. Statistically overrepresented cellular components included external side of plasma membrane (GO:0009897, Fold-enrichment 4.3, P-value 0.03830), among others.

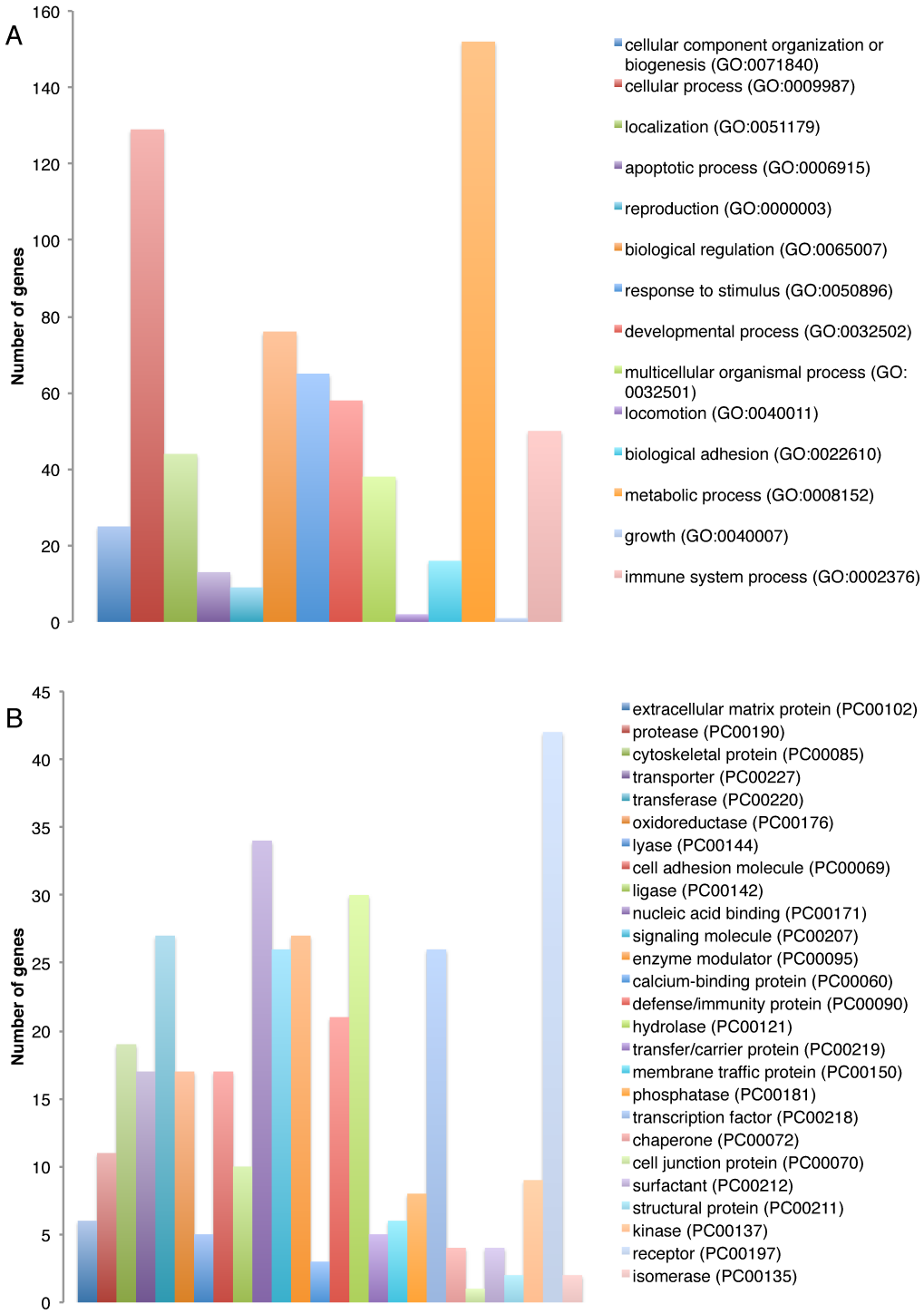

Figure 3. PANTHER database search results. Annotation terms are plotted by number of genes in the set of genes with log(2)FC>2. A, biological processes represented by GO annotations; B, protein classes represented by PANTHER annotations.

Functional annotation clustering

DAVID functional annotation clustering yielded 93 clusters in total, 6 of which had statistically significant enrichments (Appendix II) in annotation terms for immune-system functionally relevant annotations such as cell activation (Fold enrichment 4.110687951, Benjamini adjusted P-value 0.011821747; genes including *GAPT, EGR1, ICAM1, IL6, IL21R, TGFBR2, IL7R, SLAMF1, CD9, CD80, CXCR4, NDRG1, AICDA, FAS, LCP1*), leukocyte activation (Fold enrichment 4.225062464, Benjamini adjusted P-value 0.027278134; genes including *GAPT, EGR1, ICAM1, CD80, CXCR4, IL21R, TGFBR2, NDRG1, AICDA, FAS, IL7R, SLAMF1, LCP1*), immunoglobulin domain (Fold-enrichment 3.038139924, Benjamini adjusted P-value 0.022937931; genes including *ICAM1, BTNL9, IL6ST, VPREB3, FCRL2, FCRL1, PALLD, FCRL5, SLAMF1, FCRL4, FCGR2B, CD80, CD58, IGSF3, PECAM1, SEMA4C, FAIM3*), and membrane (Fold-enrichment 1.369494019, Benjamini adjusted P-value 0.034805415; genes including *SEMA4C, ADCY1, ICAM1, CCR6, TGFBR2, FAIM3, CLEC4A, MAL, IL21R*) among others.

STRING database results

When examining our list of differentially-expressed genes, the STRING database calculated 242 nodes, which represent genes with known protein-coding abilities, in the list. When clustered together, a network view is produced (Figure 4). A simple numerical comparison between the calculated and expected number of “edges” - known relationships between genes – yields 281 edges for the network of differentially-expressed genes in antiCD40/IL-4-treated human B cells, as opposed to 68 expected edges from baseline transcriptome background across the entire human genome, with an associated PPI P-value >0.001. This strongly suggests that the network of gene products has significantly more interactions than expected, relative to a random set of similarly-sized proteins across the human genome. Thus, it is likely the proteins in the network are biologically linked, as a group.

When we examine the functional enrichment present in the network in terms of GO biological processes, we see highly significant enrichments for immune system processes (61 genes, FDR 3.93e-10), cell surface receptor signaling pathways (47 genes, FDR 0.000262), and cell activation

(27 genes, FDR 3.43e-06), to sample a few. Furthermore, when GO cellular components are examined, we see highly significant enrichments for external side of plasma membrane (13 genes, FDR 0.00329), integral component of membrane (89 genes, FDR 0.00892), intrinsic component of membrane (91 genes, FDR 0.00892), membrane part (99 genes, FDR 0.0109), among others.

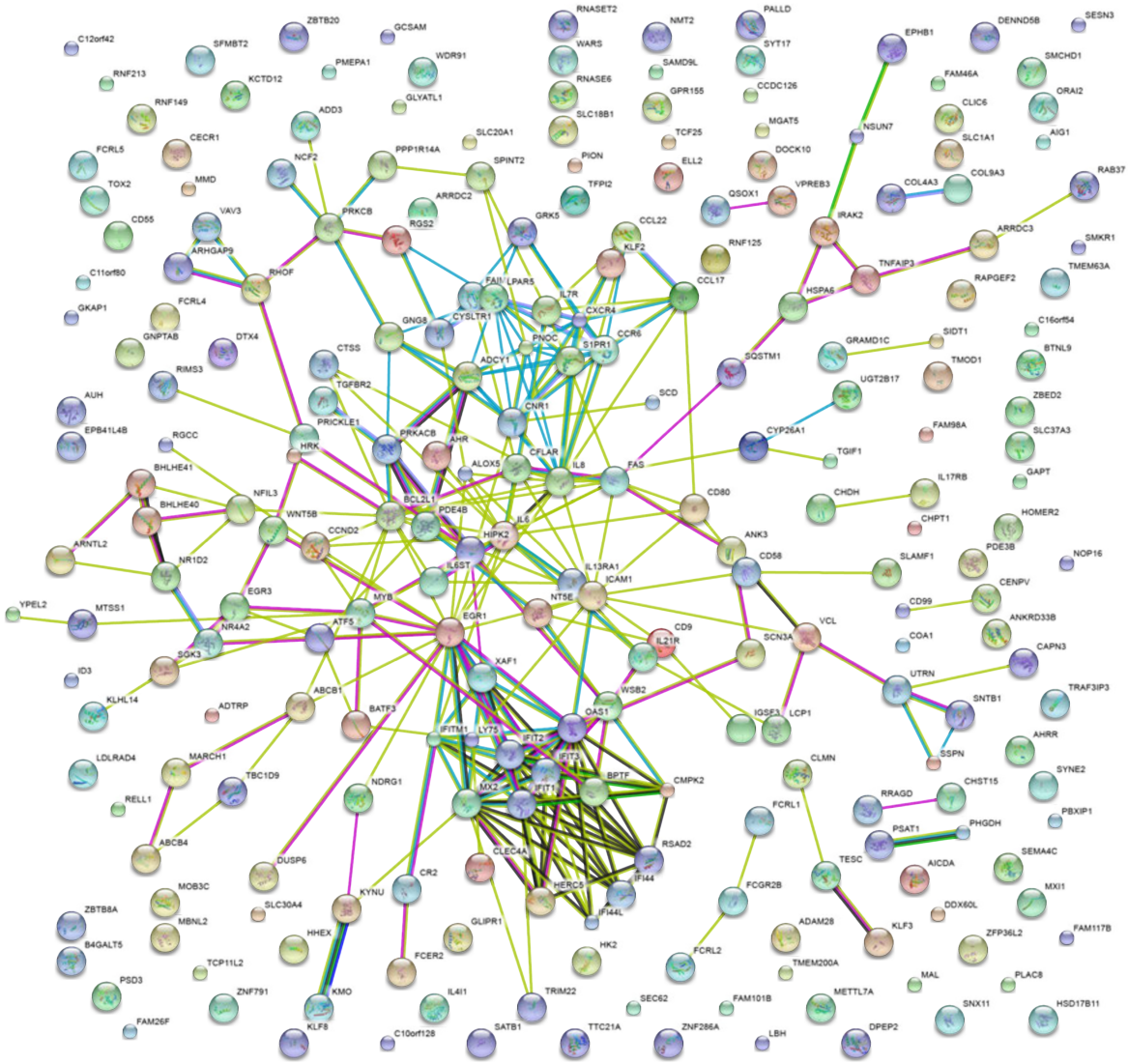

Figure 4. STRING network. Visual summary of interaction network for the list of differentially-expressed genes. Nodes represent proteins and edges represent predicted functional associations between given proteins. Line colour indicates the class of interaction evidence: red line, fusion; green line, neighborhood; blue lines, coocurrence; purple, experimental; yellow, textmining; light

blue, database; black, coexpression. Physical distance between nodes along an edge has no meaning.

Discussion

Our results are somewhat surprising, given that HC had no discernible effect on gene transcription in activated B cells after 24 hours. The present work does not exclude the possibility that HC-affected gene transcription occurred in a shorter time period: clinically, steroids begin to show effects at 6 hours' post-administration, which implies a fairly rapid pharmacokinetic profile. However, gene transcription due to continuous *in vitro* stimulus often persists for some time; furthermore, antiCD40/IL-4 treatment alone did yield patterns of differential gene expression. It would therefore be interesting to examine the expression profile of cells treated with HC alone.

It is long established that CD40 and IL4 stimulation of B cells leads to increased mRNA expression, functional gene transcription, and IgE secretion (16, 17). *In vivo*, this process is initiated by naïve T (Th0) cells being driven by paracrine IL-4 from antigen-presenting cells – typically myeloid DC in regional lymph nodes –to differentiate into Th2 cells, which then secrete IL-4 and IL-13. These cytokines ligate their receptors on B cells, activating the JAK/STAT pathway and phosphorylating the STAT6 transcription factor, which translocates to the nucleus and induces transcription of genes associated with immunoglobulin class switching and cell activation (18). Concurrent with this cytokine stimulation, T cell CD40 ligand (CD40L, also known as CD154) interacts with CD40 on B cells, driving antibody heavy-chain class switching to IgE (19). This process is simulated *in vitro* with anti-CD40 signalling antibody treatment.

The vast majority of genes and categories that we determined were differentially regulated by Th2-skewed B cell activation are indeed related to immune system processes and cell activation or metabolism. Our results provide a network view of the initial stages of B cell activation, and reveal that Th2-skewed B cells, in addition to activating known immunostimulatory pathways and

processes, also activate pathways implicated in immunoregulation and dampening of the inflammatory response.

Interestingly, one of the most highly upregulated genes that we found was the axonal guidance molecule *SEMA4C* (Figure 1B, Table 1). This finding is particularly novel, since – to our knowledge – there is no data or reports implicating SEMA4C in immune biology, particularly in B cells. Our laboratory has performed extensive characterization of this protein's novel functions in the immune system in both human *in vitro* and mouse *in vivo* model systems over the last 5 years – since the microarray data was originally acquired – with two manuscripts presently (August 2016) submitted for consideration. Briefly, this work suggests that SEMA4C appears to be a marker for memory B cells, and is part of the immune synapse that develops as B cells mature. Furthermore, SEMA4C appears to play a role in B cell regulatory function, impacting Th2 responses in allergic airways disease.

Ironically, the present author ended up performing the raw data analysis, which provided the fundamental impetus for this work, towards the end of the finalization of the SEMA4C papers! The original data was half-analyzed, neglected due to a collaborator's departure from McGill to the Ontario Institute for Cancer Research / University of Toronto, lost, and then retrieved from Genome Quebec's archive servers by the present author, and analyzed as a side project to his main thesis work on gene expression profiling of mouse regulatory T cells. The author wishes to acknowledge the tremendous help of Daniel Vincent, microarray platform manager at Genome Quebec, for his efforts in relocating the raw scan files and the associated sample-conditions matrix!

References

1. Rosser EC, Mauri C. Regulatory B cells: origin, phenotype, and function. *Immunity* (2015) **42**(4):607-12. doi: 10.1016/j.immuni.2015.04.005. PubMed PMID: 25902480.

2. Xue D, Desjardins M, Kaufman GN, Béland M, Al-Tememi S, Ahmed E, et al. Semaphorin 4C: A Novel Component of B-Cell Polarization in Th2 Driven Immune Responses. *Frontiers in Immunology* (2016) **7**:558. doi: 10.3389/fimmu.2016.00558.

3. Oettgen HC, Geha RS. IgE regulation and roles in asthma pathogenesis. *J Allergy Clin Immunol* (2001) **107**(3):429-40. doi: 10.1067/mai.2001.113759. PubMed PMID: 11240941.

4. Hajoui O, Janani R, Tulic M, Joubert P, Ronis T, Hamid Q, et al. Synthesis of IL-13 by human B lymphocytes: regulation and role in IgE production. *J Allergy Clin Immunol* (2004) **114**(3):657-63. doi: 10.1016/j.jaci.2004.05.034. PubMed PMID: 15356573.

5. Hajoui O, Zheng H, Guay J, Letuve S, Fawaz LM, Mazer BD. Regulation of IL-13 receptor alpha 1 expression and signaling on human tonsillar B-lymphocyte subsets. *J Allergy Clin Immunol* (2007) **120**(6):1425-32. doi: 10.1016/j.jaci.2007.07.011. PubMed PMID: 17761275.

6. Clark EA, Ledbetter JA. Activation of human B cells mediated through two distinct cell surface differentiation antigens, Bp35 and Bp50. *Proc Natl Acad Sci U S A* (1986) **83**(12):4494-8. PubMed PMID: 3487090; PubMed Central PMCID: PMC323760.

7. R Core Team. *R: A language and environment for statistical computing.* Vienna, Austria: R Foundation for Statistical Computing (2016).

8. Carvalho BS, Irizarry RA. A framework for oligonucleotide microarray preprocessing. *Bioinformatics* (2010) **26**(19):2363-7. Epub 2010/08/07. doi: 10.1093/bioinformatics/btq431. PubMed PMID: 20688976; PubMed Central PMCID: PMCPMC2944196.

9. Ritchie ME, Phipson B, Wu D, Hu Y, Law CW, Shi W, et al. limma powers differential expression analyses for RNA-sequencing and microarray studies. *Nucleic Acids Res* (2015) **43**(7):e47. Epub 2015/01/22. doi: 10.1093/nar/gkv007. PubMed PMID: 25605792; PubMed Central PMCID: PMCPMC4402510.

10. Irizarry RA, Hobbs B, Collin F, Beazer-Barclay YD, Antonellis KJ, Scherf U, et al. Exploration, normalization, and summaries of high density oligonucleotide array probe level data. *Biostatistics* (2003) **4**(2):249-64. Epub 2003/08/20. doi: 10.1093/biostatistics/4.2.249. PubMed PMID: 12925520.

11. Smyth GK. Linear models and empirical bayes methods for assessing differential expression in microarray experiments. *Stat Appl Genet Mol Biol* (2004) **3**:Article3. Epub 2006/05/02. doi: 10.2202/1544-6115.1027. PubMed PMID: 16646809.

12. Mi H, Muruganujan A, Casagrande JT, Thomas PD. Large-scale gene function analysis with the PANTHER classification system. *Nat Protocols* (2013) **8**(8):1551-66. doi: 10.1038/nprot.2013.092.

13. Gene Ontology Consortium. Gene Ontology annotations and resources. *Nucleic Acids Res* (2013) **41**(Database issue):D530-5. doi: 10.1093/nar/gks1050. PubMed PMID: 23161678; PubMed Central PMCID: PMCPMC3531070.

14. Huang DW, Sherman BT, Lempicki RA. Systematic and integrative analysis of large gene lists using DAVID bioinformatics resources. *Nat Protocols* (2008) **4**(1):44-57. doi: 10.1038/nprot.2008.211.

15. Szklarczyk D, Franceschini A, Wyder S, Forslund K, Heller D, Huerta-Cepas J, et al. STRING v10: protein-protein interaction networks, integrated over the tree of life. *Nucleic Acids Res* (2015) **43**(Database issue):D447-52. doi: 10.1093/nar/gku1003. PubMed PMID: 25352553; PubMed Central PMCID: PMCPMC4383874.

16. Gascan H, Gauchat JF, Aversa G, Van Vlasselaer P, de Vries JE. Anti-CD40 monoclonal antibodies or CD4+ T cell clones and IL-4 induce IgG4 and IgE switching in purified human B cells via different signaling pathways. *J Immunol* (1991) **147**(1):8-13. PubMed PMID: 1711085.

17. Spriggs MK, Armitage RJ, Strockbine L, Clifford KN, Macduff BM, Sato TA, et al. Recombinant human CD40 ligand stimulates B cell proliferation and immunoglobulin E secretion. *J Exp Med* (1992) **176**(6):1543-50. PubMed PMID: 1281209; PubMed Central PMCID: PMCPMC2119450.

18. Goenka S, Kaplan MH. Transcriptional regulation by STAT6. *Immunol Res* (2011) **50**(1):87-96. doi: 10.1007/s12026-011-8205-2. PubMed PMID: 21442426; PubMed Central PMCID: PMCPMC3107597.

19. Gould HJ, Sutton BJ. IgE in allergy and asthma today. *Nat Rev Immunol* (2008) **8**(3):205-17. doi: 10.1038/nri2273. PubMed PMID: 18301424.

Chapter 5 Appendix I - Annotated R code for microarray bioinformatics analysis

```
## Affymetrix Human Genome U133 Plus 2.0 data processing ##
## Raw data read, normalization, and differential gene expression ##

## REFERENCES

## Processing Affymetrix Gene Expression Arrays ##
## Chris Benner, Salk Institute ##
## http://homer.salk.edu/homer/basicTutorial/affymetrix.html ##
## Mouse Gene 2.0 ST array instructions ##



## Analyze your own microarray data in R/Bioconductor ##
## BioInformatics Training and Services Wiki, Vlaams Instituut voor Biotechnologie, Flanders, BE
 ##
# http://wiki.bits.vib.be/index.php/Analyze_your_own_microarray_data_in_R/Bioconductor #

# set the working directory
setwd("/Users/kaufman_home/Documents/Mazer-lab-files/data/Human-B-cell_microarray/HC-
 project_2005/CEL_raw-data-files")

# Load the oligo library
library(oligo)

# List all CEL files in directory, create list object
celFiles <- list.celfiles()
```

```
## Read in the pertinent set of CEL files:
# (Control, antiCD40.IL4, antiCD40.IL4.HC)
# Read in the CEL files using the read.celfiles() parser
affyRaw <-
 read.celfiles("YF050531H133P06.CEL","YF050531H133P12.CEL","YF050531H133P13.CEL","YF0
 50620H133P01.CEL","YF050620H133P07.CEL","YF050620H133P08.CEL","YF050620H133P09.C
 EL","YF050620H133P15.CEL","YF050620H133P16.CEL","YF050620H133P17.CEL","YF050620H1
 33P23.CEL","YF050620H133P24.CEL")

## specific platform design info package for Human Genome U133 Plus 2.0 arrays is
 'pd.hg.u133.plus.2' - should load automatically

# Normalize data across all arrays
eSet <- rma(affyRaw) ## Uses RMA

## Annotate normalized expression set data with gene symbol and Entrez GeneID

# Load array-specific annotation library
library(hgu133plus2.db) # for Human Genome U133 Plus 2.0 arrays

## load annotation package
library(annotate)

## assign ID values
ID <- featureNames(eSet)
GeneSymbol <- getSYMBOL(ID,"hgu133plus2.db")
EntrezGeneID <-getEG(ID, "hgu133plus2.db")
fData(eSet) <- data.frame(ID=ID,GeneSymbol=GeneSymbol, EntrezGeneID = EntrezGeneID)
```

```
# Assign index names to normalized CEL files
## create conditions list
sample.condition <- c("Control_1", "antiCD40.IL4_1", "antiCD40.IL4.HC_1", "Control_2",
 "antiCD40.IL4_2", "antiCD40.IL4.HC_2", "Control_3", "antiCD40.IL4_3", "antiCD40.IL4.HC_3",
 "Control_4", "antiCD40.IL4_4", "antiCD40.IL4.HC_4")

# tag CEL files with labels
ph <- eSet@phenoData
ph@data[,1] <- sample.condition

# condition labels
ph@data[,2] = c("Control", "antiCD40.IL4", "antiCD40.IL4.HC", "Control", "antiCD40.IL4",
 "antiCD40.IL4.HC", "Control", "antiCD40.IL4", "antiCD40.IL4.HC", "Control", "antiCD40.IL4",
 "antiCD40.IL4.HC")
colnames(ph@data)[2]="group"

#Display new phenoData list with index and group
ph@data

########################################
###### Identification of differentially expressed genes
## load required package limma
library(limma)
## identify experimental groups
groups <- ph@data$group
## assign factor groupings
f <- factor(groups,levels = c("Control", "antiCD40.IL4", "antiCD40.IL4.HC"))

## Define design matrix
```

```
design = model.matrix(~ 0 + f)
colnames(design)=c("Control", "antiCD40.IL4", "antiCD40.IL4.HC")

## fit normalized data to design matrix
data.fit = lmFit(eSet,design)

## define contrast matrix
contrast.matrix <- makeContrasts(antiCD40.IL4_vs_Control = antiCD40.IL4 - Control,
 antiCD40.IL4.HC_vs_Control = antiCD40.IL4.HC - Control, antiCD40.IL4.HC_vs_antiCD40.IL4 =
 antiCD40.IL4.HC - antiCD40.IL4 , levels = design)

# Second linear model fit
data.fit.con <- contrasts.fit(data.fit,contrast.matrix)

## Empirical Bayes sample variance shrinkage
data.fit.eb <- eBayes(data.fit.con)

## Microarray QC
# Boxplots of individual arrays
# boxplot of raw data
pdf(file = "Boxplot_raw-data.pdf", title = "Boxplot - Affy raw data")
boxplot(affyRaw, col="blue")
dev.off()

# boxplot of RMA-normalized data
pdf(file = "Boxplot_RMA-normalized-data.pdf", title = "Boxplot - RMA-normalized data")
boxplot(eSet, col="blue")
dev.off()
```

```
################################
#### TopTable t-testing with false discovery rate multiple-comparisons p-value adjustment #
## Sorted by log(Fold-Change)

## antiCD40.IL4_vs_Control
Top.Table1 <- topTable(data.fit.eb, coef = "antiCD40.IL4_vs_Control", adjust.method = "fdr",
 sort.by = "logFC", number = Inf)

## antiCD40.IL4.HC_vs_Control
Top.Table2 <- topTable(data.fit.eb, coef = "antiCD40.IL4.HC_vs_Control", adjust.method = "fdr",
 sort.by = "logFC", number = Inf)

## antiCD40.IL4.HC_vs_antiCD40.IL4
Top.Table3 <- topTable(data.fit.eb, coef = "antiCD40.IL4.HC_vs_antiCD40.IL4", adjust.method =
 "fdr", sort.by = "logFC", number = Inf)

## Can also make a larger topTable with first 1000, 5000, 10000 differentially-expressed genes
## Can also sort by adjusted p-value

# Write tab-delimited text file of Empirical Bayes TopTable with fdr p-value adjustment #

## IVIg-iTreg versus endogenous Treg
write.table(Top.Table1, file = "topTable1_antiCD40-IL4_vs_Control.txt", sep = "\t")
## IVIg-iTreg versus n_iTreg
write.table(Top.Table2, file = "topTable2_antiCD40-IL4-HC_vs_Control.txt", sep = "\t")
## n_iTreg versus endogenous Treg
write.table(Top.Table3, file = "topTable3_antiCD40-IL4-HC_vs_antiCD40-IL4.txt", sep = "\t")
```

```
##############################
## Volcano plots of comparisons
## antiCD40.IL4_vs_Control
pdf(file = "VolcanoPlot_antiCD40-IL4_vs_Control.pdf")
volcanoplot(data.fit.eb, coef = "antiCD40.IL4_vs_Control", highlight = 10, names = GeneSymbol,
 xlab="Log Fold ", ylab = "Log Odds", main = "antiCD40/IL4 vs Control")
# add red lines at -2 and +2-fold-s
abline(v = c(-2, 2), col = 2)
dev.off()

##############################

# MA plots of comparisons

# antiCD40.IL4_vs_Control

pdf(file = "MAplot_antiCD40-IL4_vs_Control.pdf", title = "M-A plot - antiCD40-IL4 vs control")
plotMA(data.fit.eb, coef = 1, xlab = "Average log-expression", ylab = "Log Fold Change", main =
 "antiCD40/IL4 vs Control")

# add red lines at -2 and 2-fold-changes
abline(h = c(-2, 2), col = 2)

# Label top 10 differentally-expressed genes from relevant Top.Table

x1 <- Top.Table1$AveExpr
y1 <- Top.Table1$logFC
G1 <- Top.Table1$GeneSymbol
text(x1[1:10], y1[1:10], labels=G1[1:10], cex = 0.6, col = "blue")
```

```
dev.off()


# antiCD40.IL4.HC_vs_Control

pdf(file = "MAplot_antiCD40-IL4-HC_vs_Control.pdf", title = "M-A plot - antiCD40-IL4-HC vs
 control")
plotMA(data.fit.eb, coef = 2, xlab = "Average log-expression", ylab = "Log Fold Change", main =
 "antiCD40/IL4/HC vs Control")

# add red lines at -2 and 2-fold-changes
abline(h = c(-2, 2), col = 2)

# Label top 10 differentally-expressed genes from relevant Top.Table

x2 <- Top.Table2$AveExpr
y2 <- Top.Table2$logFC
G2 <- Top.Table2$GeneSymbol
text(x2[1:10], y2[1:10], labels=G2[1:10], cex = 0.6, col = "blue")

dev.off()



# antiCD40.IL4.HC_vs_antiCD40.IL4

pdf(file = "MAplot_antiCD40-IL4-HC_vs_antiCD40-IL4.pdf", title = "M-A plot - antiCD40-IL4-HC
 vs antiCD40-IL4")
```

```
plotMA(data.fit.eb, coef = 3, xlab = "Average log-expression", ylab = "Log Fold Change", main =
 "antiCD40/IL4/HC vs antiCD40/IL4")

# add red lines at -2 and 2-fold-changes
abline(h = c(-2, 2), col = 2)

# Label top 10 differentally-expressed genes from relevant Top.Table

x3 <- Top.Table3$AveExpr
y3 <- Top.Table2$logFC
G3 <- Top.Table2$GeneSymbol
text(x2[1:10], y2[1:10], labels=G2[1:10], cex = 0.6, col = "blue")

dev.off()
```

Chapter 5 Appendix II – DAVID results

DAVID functional annotation clustering of differentially expressed genes in anti-CD40/IL4-treated B cells versus unstimulated cells. Statistically significant enrichment terms presented.

Enrichment score: geometric mean (in -log scale) of member's Fisher's Exact test P-values in the annotation cluster
Category: Annotation parent source for ontology terms
Term: Individual enriched ontology terms associated with gene list
Count: number of genes in list that match annotation term
%: Number of genes involved in given term divided by total number of input genes
PValue: from Fisher's Exact test for gene enrichment in annotation terms
Genes: Genes from gene list that are grouped under a specific ontology
List Total: number of genes in gene list mapped to any term in this ontology
Pop Hits (Population hits): number of genes with this GO term on the whole array
Pop Total (Population total): number of genes on the background list mapped to any term in this ontology
Fold Enrichment: ratio of enrichment proportion over background enrichment
Benjamini: Multiple-comparisons corrected P-value for Fisher's Exact test

Annotation Cluster 1	Enrichment Score: 3.735842674274605									
Category	Term	Count	%	PValue	Genes	List Total	Pop Hits	Pop Total	Fold Enrichment	Benjamini
GOTERM_BP_FAT	GO:0001775~cell activation	15	0.69124424	1.68E-05	GAPT, EGR1, ICAM1, IL6, IL21R,	172	287	13528	4.110687951	0.011821747

					TGFBR2, IL7R, SLAMF1, CD9, CD80, CXCR4, NDRG1, AICDA, FAS, LCP1					
GOTERM_BP_FAT	GO:0045321~leukocyte activation	13	0.599078341	5.86E-05	GAPT, EGR1, ICAM1, CD80, CXCR4, IL21R, TGFBR2, NDRG1, AICDA, FAS, IL7R, SLAMF1, LCP1	172	242	13528	4.225062464	0.027278134
Annotation Cluster 2	Enrichment Score: 3.2581721163950075									
Category	Term	Count	%	PValue	Genes	List Total	Pop Hits	Pop Total	Fold Enrichment	Benjamini
GOTERM_CC_FAT	GO:0044459~plasma membrane	49	2.258064516	2.18E-05	SLC20A1, SCN3A,	157	2203	12782	1.810842771	0.002010974

	part				IL6ST, UTRN, VCL, IL17RB, GNG8, S1PR1, CXCR4, ANK3, SNTB1, CLEC4A, FAS, RAPGEF2, IL13RA1, SLC1A1, RHOF, ICAM1, NCF2, PSD3, SSPN, CCR6, CD80, FAIM3, ADD3, LCP1, CYSLTR1, FCER2, MMD, RSAD2, BCL2L1,					

					IL7R, EPHB1, RIMS3, CD9, CNR1, LY75, IL6, TGFBR2, ABCB1, MAL, SLAMF1, HOMER2, ABCB4, CD55, SYNE2, CD58, SYT17, KCTD12					
Annotation Cluster 3	Enrichment Score: 2.456826371375816									
Category	Term	Count	%	PValue	Genes	List Total	Pop Hits	Pop Total	Fold Enrichment	Benjamini
GOTERM_CC_FAT	GO:0005886~plasma membrane	72	3.31797235	1.62E-05	ADCY1, SLC20A1, SCN3A, IL6ST, UTRN, FCRL2,	157	3777	12782	1.551974826	0.002988078

					FCRL1, FCRL5, RELL1, FCRL4, IL17RB, VCL, GNG8, S1PR1, ANK3, SPINT2, CXCR4, CLEC4A, SNTB1, FAS, IL13RA1, RAPGEF2, SLC1A1, RHOF, NT5E, GAPT, ICAM1, NCF2, PSD3, SSPN, PRKCB, CCR6, LPAR5, CD80, CLIC6,					

					FAIM3, ADD3, PMEPA1, LCP1, CYSLTR1, IFITM1, FCER2, MMD, RSAD2, BCL2L1, IL7R, EPHB1, RIMS3, CD9, CNR1, NDRG1, LY75, ADAM28, TESC, IL6, CR2, VAV3, TGFBR2, MAL, ABCB1, SLAMF1, HOMER2, ABCB4, CD55, SYNE2, FCGR2B,					

					PECAM1, CD58, GRK5, ALOX5, SYT17, KCTD12					
SP_PIR_KEYWORDS	membrane	102	4.700460829	1.24E-04	ADCY1, SCN3A, IL6ST, UTRN, PDE3B, SIDT1, RELL1, VCL, IL17RB, GNG8, S1PR1, CLEC4A, FAS, RNF149, RAPGEF2, AIG1, TMEM200A, PSD3, CYP26A1, SSPN, METTL7A, CHPT1, CCR6,	229	6256	19235	1.369494019	0.034805415

					LPAR5, IGSF3, MGAT5, ADD3, ORAI2, IFITM1, CYSLTR1, FCER2, MMD, TMEM63A, KMO, BCL2L1, EPHB1, AHRR, CNR1, SLC30A4, NDRG1, B4GALT5, ADAM28, GPR155, SCD, TGFBR2, ABCB1, SLAMF1, HOMER2, ABCB4, CD55, SYNE2, PRICKLE1,					

					CD58, TRAF3IP3, SYT17, SLC20A1, IL21R, FCRL2, FCRL1, FCRL5, FCRL4, SPINT2, CXCR4, SNTB1, CHST15, DENND5B, IL13RA1, SLC1A1, RHOF, NT5E, DPEP2, GAPT, ICAM1, BTNL9, CLMN, PRKCB, UGT2B17, CD80, CLIC6, SEMA4C, FAIM3,					

					C16ORF54, GRAMD1C, PMEPA1, LCP1, SLC37A3, HK2, RSAD2, IL7R, SEC62, CD9, GNPTAB, GLIPR1, QSOX1, LY75, CR2, MAL, C10ORF128, FCGR2B, PECAM1, ALOX5, FAM26F					
GOTERM_CC_FAT	GO:0031224~intrinsic to membrane	87	4.00921659	0.001336974	ADCY1, SCN3A, SLC20A1, IL6ST, IL21R, FCRL2, FCRL1, PDE3B,	157	5485	12782	1.291343502	0.040411697

					SIDT1, FCRL5, RELL1, FCRL4, IL17RB, S1PR1, SPINT2, CXCR4, CLEC4A, RNF149, FAS, CHST15, IL13RA1, RAPGEF2, DENND5B, NT5E, SLC1A1, DPEP2, GAPT, ICAM1, BTNL9, NCF2, CLMN, AIG1, TMEM200A, SSPN, CHPT1, UGT2B17, CCR6,					

					CD80, LPAR5, IGSF3, CLIC6, SEMA4C, FAIM3, C16ORF54, GRAMD1C, MGAT5, PMEPA1, ORAI2, CYSLTR1, IFITM1, FCER2, SLC37A3, TMEM63A, MMD, KMO, BCL2L1, IL7R, SEC62, EPHB1, CD9, GNPTAB, GLIPR1, CNR1, SLC30A4, QSOX1,					

					B4GALT5, LY75, ADAM28, GPR155, IL6, CR2, SCD, TGFBR2, MAL, ABCB1, C10ORF128, SLAMF1, ABCB4, CD55, SYNE2, FCGR2B, CD58, PECAM1, TRAF3IP3, SYT17, FAM26F, KCTD12					
Annotation Cluster 4	Enrichment Score: 2.4524974699793276									
Category	Term	Count	%	PValue	Genes	List Total	Pop Hits	Pop Total	Fold Enrichment	Benjamini
SP_PIR_KEYWOR	Immunoglobulin	17	0.783410138	1.63E-04	ICAM1,	229	470	1923	3.03813992	0.02293793

DS	domain				BTNL9, IL6ST, VPREB3, FCRL2, FCRL1, PALLD, FCRL5, SLAMF1, FCRL4, FCGR2B, CD80, CD58, IGSF3, PECAM1, SEMA4C, FAIM3			5	4	1
Annotation Cluster 10	Enrichment Score: 1.7699373586313218									
Category	Term	Count	%	PValue	Genes	List Total	Pop Hits	Pop Total	Fold Enrichment	Benjamini
GOTERM_CC_FAT	GO:0000267~cell fraction	26	1.198156682	0.001408228	KYNU, SCN3A, CYSLTR1, UTRN, FCRL2, MMD, PDE3B,	157	1083	12782	1.954537702	0.036558662

					OAS1, WARS, SPINT2, ANK3, PDE4B, FAS, NT5E, SLC1A1, PSD3, CYP26A1, ABCB1, MAL, CHPT1, ABCB4, UGT2B17, CD55, GRK5, ALOX5, DUSP6					
Annotation Cluster 17	Enrichment Score: 1.259995679823867									
Category	Term	Count	%	PValue	Genes	List Total	Pop Hits	Pop Total	Fold Enrichment	Benjamini
GOTERM_CC_FAT	GO:0009897~external side of plasma membrane	10	0.460829493	2.36E-04	LY75, ICAM1, S1PR1, CD80, IL6ST,	157	170	12782	4.789059573	0.014436526

					FCER2, TGFBR2, FAS, IL7R, SLAMF1					
GOTERM_CC_FAT	GO:0009986~cell surface	13	0.599078341	0.00115152	LY75, IRAK2, ICAM1, S1PR1, CD80, IL6ST, FCER2, TGFBR2, ABCB1, FAS, IL7R, SLAMF1, IL17RB	157	348	12782	3.041328062	0.041734879

Scope: Self Format: HTML Amount: Quick GEO accession: GSE71810 GO

Series GSE71810

Query DataSets for GSE71810

Status	Public on Feb 15, 2016
Title	Gene expression data from human tonsillar B lymphocytes
Organism	Homo sapiens
Experiment type	Expression profiling by array
Summary	B lymphocytes are important mediators of adaptive immunity. They drive naïve T cells to different T-helper profiles. Th2 responses are implicated in allergic reactions. The goal of this study was to characterize the gene expression profile of B cells under Th2-skewing conditions.
Overall design	B lymphocytes were isolated from human tonsils and cultured for 24 hours under Th2-skewing stimulation (anti-CD40 and IL4 treatment) or with no stimulation. RNA was isolated from 4 biological replicates for each condition. 8 samples in total were hybridized to Affymetrix gene expression microarrays. variable: treatment: antiCD40-IL4: antiCD40-IL4_1, antiCD40-IL4_2, antiCD40-IL4_3, antiCD40-IL4_4 variable: treatment: unstimulated: Control_1, Control_2, Control3, Control_4 repeat: biological replicate: antiCD40-IL4_1, antiCD40-IL4_2, antiCD40-IL4_3, antiCD40-IL4_4 repeat: biological replicate: Control_1, Control_2, Control3, Control_4
Contributor(s)	Kaufman GN, Al-Tememi S, Mazer BD
Citation missing	*Has this study been published? Please login to update or notify GEO.*
Submission date	Aug 06, 2015
Last update date	Mar 18, 2016
Contact name	Bruce David Mazer
E-mail	bruce.mazer@mcgill.ca
Organization name	RI-MUHC
Department	RESP
Street address	1001 boul. Décarie
City	Montreal
State/province	Quebec
ZIP/Postal code	H4A 3J1
Country	Canada
Platforms (1)	GPL570 [HG-U133_Plus_2] Affymetrix Human Genome U133 Plus 2.0 Array
Samples (8)	GSM1846236 Control_bio-rep-1 GSM1846237 antiCD40-IL4_bio-rep-1 GSM1846238 Control_bio-rep-2

GSM1846239 antiCD40-IL4_bio-rep-2

GSM1846240 Control_bio-rep-3

GSM1846241 antiCD40-IL4_bio-rep-3

GSM1846242 Control_bio-rep-4

GSM1846243 antiCD40-IL4_bio-rep-4

Relations

BioProject PRJNA292116

Analyze with GEO2R

Download family	Format
SOFT formatted family file(s)	SOFT
MINiML formatted family file(s)	MINiML
Series Matrix File(s)	TXT

Supplementary file	Size	Download	File type/resource
GSE71810_RAW.tar	60.1 Mb	(http)(custom)	TAR (of CEL)

Raw data provided as supplementary file

Processed data included within Sample table

Chapter 6: General Conclusions

Gabriel N Kaufman

The first salient research findings of the author's PhD project were that IVIg requires the inhibitory Fc gamma receptor IIb on dendritic cells to abrogate allergic airways disease and to induce regulatory T cells (Chapter 3). To our knowledge, this is the first demonstration of a mechanism of action for IVIg in an allergen-driven inflammatory disease model, which correlates well with the available data from autoimmune disease models. Future research directions would include examining correlates of this work in human cells *in vitro*, and by using humanized FcγR mice (1). These approaches will provide further insights into the cellular and molecular mechanisms involved in the anti-inflammatory actions of IVIg in allergic disease, and to potentially generalize these findings to develop novel therapeutic mechanisms for antigen-driven inflammatory diseases. The goals would be to understand the phenotype of tolerogenic dendritic cells, how to modulate this phenotype pharmacologically, and to eventually explore cell-based therapeutic options. For example, dendritic cells could be derived from patient peripheral mononuclear blood cells, tolerized *in vitro*, and infused into the patient in order to control inflammatory disease. Dendritic cells (either *ex vivo* derived or cell lines) could also be used *in vitro* as read-outs for high-throughput screening assays, monitoring their phenotypic changes towards tolerogenicity after candidate-molecule treatment.

It must be noted that while *in vitro* tolerized Treg adoptive transfer may be a therapeutic approach to consider, the requirement for higher cell numbers than dendritic cell adoptive transfer, along with the concerns regarding Treg stability, make this author less comfortable adopting such a strategy without further characterization of the Treg response and timing.

As a product derived from human blood plasma, IVIg is a scarce resource, is quite costly to produce, and carries the (low but impossible to eliminate) risk of blood-borne pathogen transmission. Furthermore, there are at least 150 off-label uses of IVIg reported in the literature, with varying qualities of evidence supporting these uses (2). Clarifying the precise mechanisms of immunomodulation will allow for more "best-evidence" guidance development for current

and future clinical use, providing therapeutic approaches with the highest chances of success for clinical indications that represent potential targets for IVIg's mechanisms of action.

Understanding the molecular mechanisms of IVIg-mediated immune tolerance will also allow for the exploration of substitute therapeutic options. A major research priority of Canadian Blood Services (which the author benefitted from first-hand, in the form of a graduate studentship with a stated goal to contribute to the following!) is the development of replacement therapeutics for IVIg that achieve the same molecular mechanistic effects and clinical phenotype. Of particular interest to the author's laboratory is the family of Treg epitope peptides or Tregitopes (EpiVax Inc.), which are short peptides containing at least one 9-mer frame per peptide that has *in silico* predicted high-affinity binding to four or more MHC-II alleles (3). Initially, Tregitopes were described as derived from the IgG molecule Fc and Fab regions; currently, EpiVax is validating Tregitopes derived from collagen, albumin, and other proteins. The mechanisms of actions of Tregitopes parallel IVIg (4); work is presently ongoing in collaboration with EpiVax to examine whether Tregitopes induce an antigen-specific Treg response.

The second major finding of the author's PhD work was that IVIg requires regulatory T cells for resolution of allergic airway inflammation, generating a pool of phenotypically distinct peripheral Treg population from non-Treg precursors. This work provides a rationale for potential application of IVIg for induction of Treg in autoimmune and inflammatory conditions associated with diminished Treg. Further work should characterize the molecular mechanisms of pTreg function and DC tolerogenicity, allowing a more profound understanding of the induction of regulatory function. We are interested in delineating the functional cross-talk between DC and Treg, examining the precise signals from tolerogenic DC to naïve effector T cells and establishing how these signals are delivered, whether by cell-cell contact, exosome transfer, cytokine release, or (most likely) by some combination of these methods.

An additional goal for future work would be to determine the timing of the Treg response, or how long is Treg tolerance maintained after IVIg treatment. Two approaches to test the stability

of IVIg-generated Treg were suggested to the present author by his former colleague (Amir H Massoud, personal communication). The first would be to use a Treg fate mapping approach, using transgenic mice that give different fluorescent signals based on gain and subsequent loss of Foxp3 expression (reviewed in (5)); this would allow tracking of current Treg versus ex-Treg levels. The second approach would be to expand on our Treg sorting technique to perform epigenetic analysis on IVIg-derived Tregs to examine the level of Foxp3 intron 1 conserved noncoding sequence 2 (CNS2) region methylation, which would provide an index of Foxp3 gene silencing and loss of Treg function (6).

In (peripherally) related work, we determined that B cells, when stimulated under Th2-skewing conditions, induce Semaphorin 4C, previously not known to be expressed or functional in immune biology, which appears to play an integral role in immune-synapse formation and impacts Th2 responses in allergic airways disease (7). The work undertaken since that discovery has been to characterize the roles of Semaphorin 4C in the formation of the immune synapse, along with its contribution to regulatory B cell activity using *in vivo* knockout mouse approaches (8). The major findings of that study were that Sema4C is required for optimal cytokine production from regulatory B cells, and that interaction between Sema4C and its ligand plexin B2 are likely required for regulation of cytokine production by activated B cells. The next steps would be to characterize the signalling pathways associated with Semaphorin 4C in the context of regulatory cell responses, with an eye to potential therapeutic targets. These studies will provide directions towards defining master-switch molecules that govern regulatory B cell development.

References

1. Smith P, DiLillo DJ, Bournazos S, Li F, Ravetch JV. Mouse model recapitulating human Fcgamma receptor structural and functional diversity. *Proc Natl Acad Sci U S A* (2012) **109**(16):6181-6. doi: 10.1073/pnas.1203954109. PubMed PMID: 22474370; PubMed Central PMCID: PMCPMC3341029.

2. Leong H, Stachnik J, Bonk ME, Matuszewski KA. Unlabeled uses of intravenous immune globulin. *Am J Health Syst Pharm* (2008) **65**(19):1815-24. doi: 10.2146/ajhp070582. PubMed PMID: 18796422.

3. De Groot AS, Moise L, McMurry JA, Wambre E, Van Overtvelt L, Moingeon P, et al. Activation of natural regulatory T cells by IgG Fc-derived peptide "Tregitopes". *Blood* (2008) **112**(8):3303-11. doi: 10.1182/blood-2008-02-138073.

4. Cousens LP, Tassone R, Mazer BD, Ramachandiran V, Scott DW, De Groot AS. Tregitope update: Mechanism of action parallels IVIg. *Autoimmunity Reviews* (2013) **12**(3):436-43. doi: 10.1016/j.autrev.2012.08.017.

5. Sawant DV, Vignali DA. Once a Treg, always a Treg? *Immunol Rev* (2014) **259**(1):173-91. doi: 10.1111/imr.12173. PubMed PMID: 24712466; PubMed Central PMCID: PMCPMC4008876.

6. Morikawa H, Ohkura N, Vandenbon A, Itoh M, Nagao-Sato S, Kawaji H, et al. Differential roles of epigenetic changes and Foxp3 expression in regulatory T cell-specific transcriptional regulation. *Proc Natl Acad Sci U S A* (2014) **111**(14):5289-94. doi: 10.1073/pnas.1312717110. PubMed PMID: 24706905; PubMed Central PMCID: PMCPMC3986152.

7. Xue D, Desjardins M, Kaufman GN, Béland M, Al-Tememi S, Ahmed E, et al. Semaphorin 4C: A Novel Component of B-Cell Polarization in Th2 Driven Immune Responses. *Frontiers in Immunology* (2016) **7**:558. doi: 10.3389/fimmu.2016.00558.

8. Xue D, Kaufman GN, Dembele M, Béland M, Massoud AH, Mindt BC, et al. Semaphorin 4C Protects against Allergic Inflammation: Requirement of Regulatory CD138+ Plasma Cells. *Journal of Immunology* (2016). Epub 2016 Nov 23. doi: 10.4049/jimmunol.1600831. PubMed PMID: 27881703.

Excursus:

Mathematical models of the respiratory system

Gabriel N Kaufman

The following chapter provides an expanded discussion of the mathematical underpinning for much of the flexiVent™ (SCIREQ) respiratory physiology results presented by the author in the two research articles of the thesis. Furthermore, the author has extensive experience with respiratory physiology modelling and measurement, dating back to his summer internships at the Meakins-Christie Laboratories over the course of his BSc in the years 2003-2004. This paper is a basic overview of common mathematical models of respiratory system mechanics. It presents a brief introduction to mathematical modelling of the respiratory system and discusses some of the most common mechanical function models currently employed by researchers, with equations, parameter descriptions, and schematic figures.

Introduction

The respiratory system

The respiratory system is one of the most complex physiological systems in the body. Requiring precision organization and synchronization with the circulatory system, it must function flawlessly to ensure a steady supply of oxygen to the brain and body. Disruption of oxygenation for more than four minutes can lead to irreversible brain damage. Furthermore, many pathophysiological processes disrupt normal respiratory behaviour. It is therefore crucial to understand the precise nature of respiratory system functioning, and one of the most powerful approaches to do so is by mathematical modelling.

Why mathematical modelling?

The general rationale behind mathematical modelling of the respiratory system is quite simple: many parameters that are essential for the understanding of respiratory function are often unnameable to direct measurement, and can only be derived through inferential calculation

based on a mathematical model. Therefore, mathematical models can be employed to investigate numerous areas of respiratory physiology.

Types of mathematical models

Mathematical models of the respiratory system can take many different forms, depending on the desired application of the model. This also influences the class or type of model, in that the model parameters are chosen depending on the particular system or systems of interest. Models can be grouped functionally: the various classes depend on the topics of investigation, which can include anatomical understanding of the respiratory system, pulmonary/circulatory integration control, the neural respiratory control system, steady-state and stress adaptations of the breathing cycle, respiratory chemistry, gas flow, and pulmonary mechanics (to name but a few). There may be considerable overlap in between classes, due to the interrelatedness of the parameters (1).

Data reduction refers to the description of a series of data by a mathematical model, such that the model can then substitute for the entire data set: for example, a mathematical formula can be postulated to represent a series of breathing rates over time. It can also be used to examine trends, such as in repeated measures analysis, where a variable is measured repeatedly in a cohort of subjects over a study period. Hypothesis testing, in the context of respiratory systems modelling, is the use of a sophisticated mathematical model to answer questions about pulmonary physiology, by incorporating model terms that represent physiological subsystems or particular mechanisms of interest. This is also known as forward modelling. Parameter derivation, or the estimation of respiratory parameters not directly measurable, is perhaps the most basic use of mathematical modelling, and will be discussed in detail in the context of models of mechanical function of the respiratory system in the section on mechanical function modelling.

A clinically relevant extension of parameter derivation is that the calculated variables can be used for diagnostic purposes in the clinical monitoring of health and disease. For example, respiratory

system resistance, derived from airway flow and pressure measurements, is used to classify patients' asthmatic responses to inhaled bronchoconstrictors. Dose-response modelling is where a mathematical model of respiratory function includes a drug dose parameter, and dose-response curves are predicted from the model using probability theory. The interested reader is referred to two prototypical case studies: Whiting et al. (2) predicted the change in forced vital capacity following the administration of a bronchodilator to patients with chronic bronchitis, and Morris et al. (3) designed an inhalational anaesthesia delivery system that relies on mathematical expressions for anaesthetic transport, patient breathing, and blood gas pressures in order to optimize anaesthetic dose.

The use of mathematical models for pedagogical purposes is to allow students to appreciate the inter-relatedness of all the various parameters of respiratory homeostasis, and to allow them to understand what happens when one or more of these parameters is perturbed by external forces (stress, disease, exercise, etc.). This can be practically realized when the model is programmed as a computer simulation of respiratory function, such as the MacPuf model described by Dickinson (4), which has been used as a training aide for anaesthesiology and respiratory residents.

Mechanical function modelling

Because of their relevance to this author's research, he has chosen to focus this brief overview on the mathematical models that describe the mechanics of the respiratory apparatus. This class of respiratory system modelling arises from the need to investigate the dynamic mechanical properties of the respiratory system as a whole in human patients and experimental animals, where the only measurement strategies available, without relatively invasive procedures, are the measurements of flow and pressure at the airway opening. Computational and mathematical modelling is then used to extract information from these data in order to inform the investigator about the behaviour of the various components of the respiratory apparatus, and the different lung regions under investigation (5). More specifically, the measured data is inputted into a

mathematical representation of the mechanical properties of the lung, and the derived parameters of interest are then calculated. This is referred to as inverse modelling or system identification.

Model descriptions

Single-compartment model

The most basic model of lung mechanics is the single-compartment model, which defines the entire respiratory system as a single unit with homogeneous ventilation, with a single airway (Figure 1). First proposed in 1950 by Otis et al. (6), this model is defined by designating the elastance or recoil of the lung compartment, and the resistance of the single airway, as a function of total transpulmonary pressure, giving the following linear relation

$$P_{tp} = R\dot{V} + EV + P_0$$

where the measured parameters P_{tp} (total transpulmonary pressure), $\dot{V}$ (flow at airway opening), and V (lung volume) are related to the resistance R and elastance E; P_0 is the pressure across the lungs at the functional residual capacity (FRC) (7, 8). Multiple linear regression is used to fit the data to the model, and a coefficient of determination or correlation is then reported along with the derived parameters. (From this author's personal experience, a correlation coefficient of 0.8 or better is considered to be an acceptable model fit.)

[To digress: lung volume V is often obtained by integrating the flow measurement $\dot{V}$ over time, such that

$$\int_t \dot{V} = V$$

or by whole-body plethysmography, so that residual volume can be accurately measured.

Another strategy is to estimate volume based on subject weight, or body mass index, by comparing to databases of standard values (9).]

Due to its relative intuitiveness and simplicity, this model is widely used for investigations where a particular parameter, usually pulmonary flow resistance R, is reported as an outcome measure for an induced experimental condition such as allergic asthma. This author (10) has measured airway hyper-responsiveness, quantified by R during methacholine challenge, in Balb/c mice rendered allergic to ovalbumin using the flexiVent low-frequency forced oscillation technique (11).

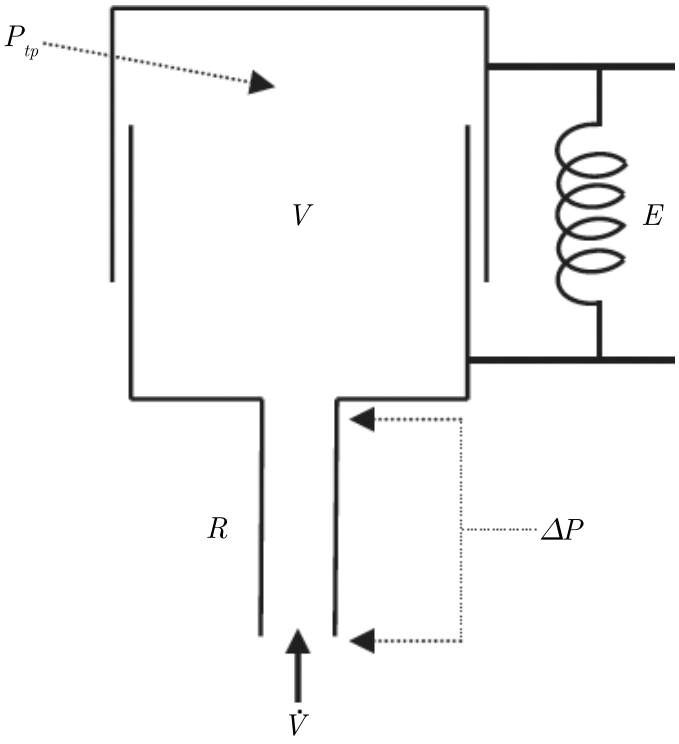

Figure 1: Single-compartment model of the lung. The compartment is a distensible unit with spring constant E, and the airway resistance is designated as R. The transpulmonary pressure P_{tp} is related to the volume V, and the pressure difference ΔP is related to the flow $\dot{V}$. Modified from Bates, *Lung Mechanics*, Figure 3.1 (12).

This model has been criticized as being “a gross oversimplification of reality” (5). It does not adequately model stress adaptation of breathing, nor does it allow for the quantification of any differential ventilation of different lung regions (13). Furthermore, it does not allow for frequency-dependent changes in compliance, which is the ease of expansion of the lungs and chest wall (mathematically, compliance is the reciprocal of elastance) (12). This has led investigators to propose more complex models of respiratory mechanics, which we discuss below.

Two-compartment models

According to Bates and Suki (5), there are three two-compartment models that can be viewed as extensions of the single-compartment model. All of them have an advantage over the single-compartment model in that they can describe the frequency dependence of resistance and elastance at physiological breathing frequencies, because they incorporate parameters representing both fast-acting and slow-acting tissue components into their equations of motion. Furthermore, they can account for stress adaptations of breathing in response to exercise or pathology.

The two-compartment models can be further subdivided into two types: the gas-redistribution models, and the viscoelastic model. We discuss them below in their chronological order of appearance in the literature. All of them assume that different lung regions are not ventilated identically, and therefore assign more spaces, and more parameters, to differentiate between the various anatomical regions. This reality makes the equations governing the systems much more complicated (and less intuitive, for this author!) than the single-compartment model.

As shown by Similowski and Bates (14), all three of the two-compartment models obey the same form of second-order differential equation. That is, the parameters described are exactly the same for all three models. Therefore, it is impossible to choose the best of them based on modelling information and parameter measurements alone. Bates et al. (15) and Ludwig et al.

(16) used the alveolar capsule technique, which measures alveolar pressure, in anaesthetized dogs to determine that the model of Mount best describes normal respiratory mechanics at resting breathing frequencies.

[To digress: the alveolar capsule technique was first used by Sasaki et al. (17) in 1977. It consists of a small pressure transducer inside a capsule that is glued to the pleural surface, which is then carefully punctured. This allows the direct measurement of alveolar pressure by the pressure transducer. Practically speaking, several capsules are often affixed on different regions of the lung, and the resulting alveolar pressures averaged, in order to account for ventilator differences among the various lung regions. This can be used to investigate various physiological and pathological paradigms of respiration, such as bronchoconstriction (18).]

Viscoelastic model

The viscoelastic model, first proposed by Mount in 1955 (19), is somewhat of a compromise between a single-compartment and a two-compartment model. It defines the respiratory system as a single unit with homogeneous ventilation, with a single airway. The tissue resistance, however, is represented by a collection of three elements: a dashpot and two springs (referred to collectively as a Kelvin body). Thus, the viscoelastic model is considered a two-compartment model from a mathematical viewpoint, due to the two influences on the state at any given time: the extension of the dashpot, and the volume in the alveolar compartment. (In more mathematical terms, the relevant equation of motion is a second-order differential equation.) The first spring represents the static elastic properties of the lung, i.e. the inherent stretchability of the tissue, while the series combination of the second spring and the dashpot (referred to as a Maxwell body) represents the viscoelastic behaviour of the lung, which accounts for both shear and strain forces exerted on the lung during breathing (Figure 2).

The complete equation of motion for the viscolelastic model, as derived by Bates et al. (20), is

$$R_t\dot{P}(t) + E_2P(t) = R_{aw}R_t\ddot{V}(t) + (E_1R_t + E_2R_{aw} + E_2R_t)\dot{V}_t + E_1E_2V(t)$$

where $P(t)$ and $V(t)$ refer to the pressure and volume across the airway opening as functions of time, R_{aw} is the airway resistance, E_1 is the spring constant of the first spring of the Kelvin body, E_2 is the spring constant of the second spring of the Maxwell body, and $R(t)$ is the dashpot resistance of the Maxwell body. (Time derivatives are indicated by dot notation: one dot means the first derivative, and two dots means the second derivative. Thus, $\dot{V}$ represents flow, or the rate of change of volume V, and $\ddot{V}$ would represent the acceleration or deceleration of the flow, or the rate of change of flow $\dot{V}$.) As we discuss below in the subsubsection on the constant-phase model, the viscoelastic model has been extended as the constant-phase model of lung mechanics, with a different set of parameters and tissue mechanics assumptions.

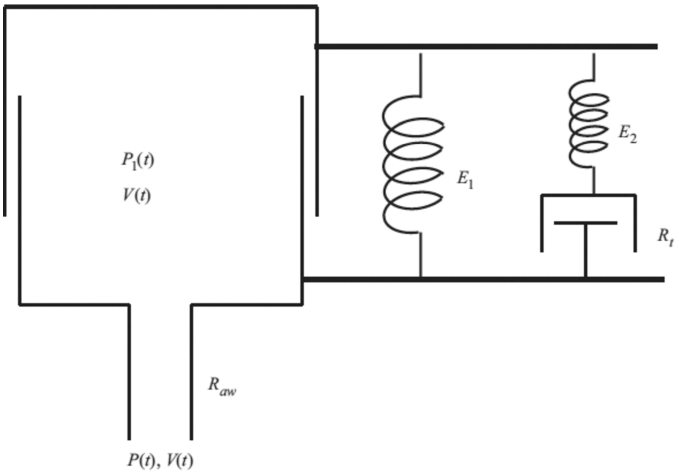

Figure 2: Viscoelastic model of the lung. R_{aw} represents airway resistance. The lung tissues are described by a Kelvin body with three elements: E_1, E_2, and R_t. From Bates, *Lung Mechanics*, Figure 7.5 (12).

Parallel model

First proposed in 1956 by Otis et al. (13), the parallel two-compartment model attempts to address some of the limitations of the single-compartment model. This model defines the respiratory system as two parallel compartments, supplied by a common airway which connects the two compartments at a branch point, the only point of interaction between them. Each unit has its own resistance, elastance, and compliance (Figure 3). The advantage of this model over the single-compartment model is that it can explain the decrease in compliance seen with increased ventilatory frequency, due to the differing time constants of the two compartments in this situation. This allows for the compartmentalization and analysis of ventilation heterogeneity among different anatomical regions.

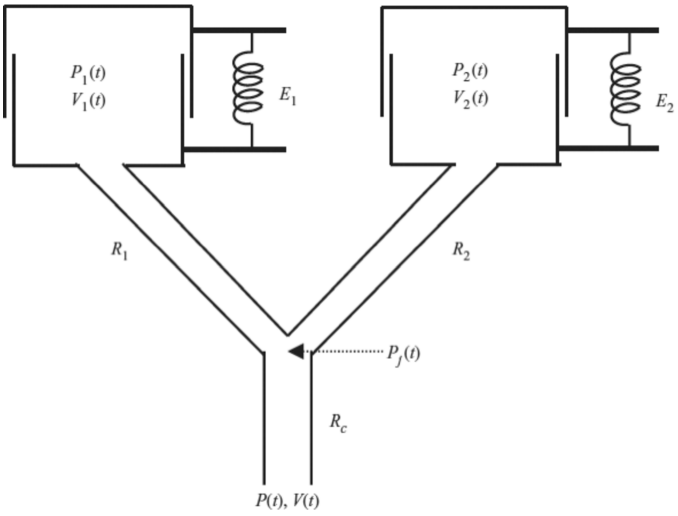

Figure 3: Parallel two-compartment model of the lung. Each compartment has its own pressure, volume, resistance, and elastance. The conducting airway resistance is designated R_c and the pressure at the branch point, as a function of time, is designated $P_j(t)$. From Bates, *Lung Mechanics*, Figure 7.2 (12).

The complete equation of motion for the parallel two-compartment model, as derived by Bates et al. (7), is

$$(R_1 + R_2)\dot{P}(t) + (E_1 + E_2)P(t) = [R_1R_2 + R_c(R_1 + R_2)]\ddot{V}(t) + [(R_2+R_c)E_1 + (R_1 + R_2)E_2]\dot{V}(t) + E_1E_2V$$

where R_c is the resistance of the common airway, R_1 and R_2 are the respective compartment resistances, E_1 and E_2 are the respective compartment spring constants which represent the elastance, and $P(t)$ and $V(t)$ are the pressure and volume at the airway opening. (We use the standard dot notation for time derivatives as above.)

Series model

In 1969, Mead (21) proposed a different two-compartment model, where the proximal and distal airways are represented by two compartments connected in series, and are supplied by a common airway in front of the proximal compartment (Figure 4). The first compartment represents the central airways, which are distensible, and the second compartment represents the lung periphery, which is uniformly ventilated. This model can also predict the frequency-dependent decrease in compliance seen with increased ventilation, which is a stress adaptation. The advantage of this model over the parallel two-compartment model is that it can accurately reflect the differences between proximal and distal lung regions.

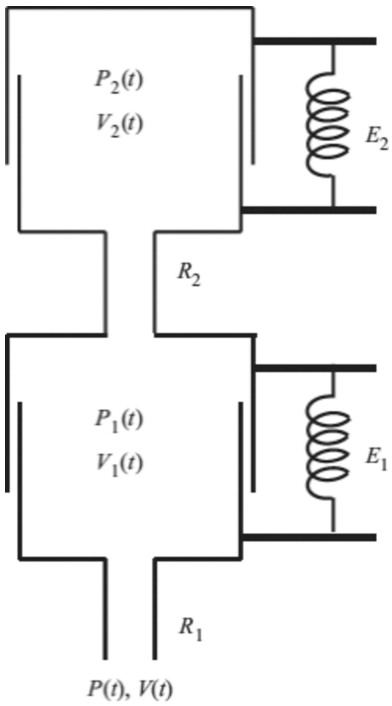

Figure 4: Series two-compartment model of the lung. Each compartment has its own pressure, volume, resistance, and elastance. From Bates, *Lung Mechanics*, Figure 7.3 (12).

The complete equation of motion for the series two-compartment model, as derived by Bates et al. (7), is

$$R_2\dot{P}(t) + (E_1 + E_2)P(t) = R_1R_2\ddot{V}(t) + (E_1R_2 + E_2R_1 + R_1E_1)\dot{V}(t) + E_1E_2V(t)$$

with model parameters R_1 and R_2 representing the respective compartment resistances, E_1 and E_2 representing the compartmental spring constants, and $P(t)$ and $V(t)$ reflecting the measured pressure and volume at the airway opening. (We use the standard dot notation for time derivatives as above.)

Constant-phase model

The viscoelastic model, as discussed above, predicts that a sudden change in the length of lung tissue will cause an exponential stress adaptation. However, biomechanics experiments have shown that physical stretching of strips of lung tissue actually results in a power-function stress adaptation. Furthermore, the ratio of time-varying pressure and flow, or impedance, of lung tissue has a magnitude that varied inversely with frequency (22). Therefore, resistance and elastance of lung tissues are likely fundamentally linked at a structural level (23). These biomechanical considerations motivated Hantos et al. (24) to test measurements of lung impedance derived from Mount's viscoelastic model against a constant-phase model of lung function built on a model first proposed by Hildebrandt (25) in 1970. Hantos et al. (24) measured mechanical impedance in open-chest dogs at known volume oscillations and transpulmonary pressured, and calculated the tissue impedance according to the two models. They reported that the constant-phase model was more reliable in fitting the data obtained and in parameter robustness.

The constant-phase model assigns a frequency-independent ratio to the elastic and dissipative components of the tissue impedance, such that the equation of the constant-phase model is the Fourier transform (12) of the equation of motion for the viscoelastic model, giving

$$Z_L(f) = R_N + i2\pi f I + \frac{G - iH}{(2\pi f)^{\alpha}}$$

where R_N is the Newtonian flow resistance of the airway tree (26), I is the inertance of the gas in the central airways, G is the tissue damping or viscous energy dissipated into the tissues, and H is the tissue elasticity or the energy stored in the tissues (Figure 5). G and H are related via the parameter α, which is defined by the relation

$$\alpha = \frac{2}{\pi}\tan^{-1}\left(\frac{H}{G}\right)$$

where iterative estimation of α, starting at 1, is then used to obtain estimates for R_N, I, G, and H, using multiple linear regression. That is, initial estimates are used to calculate a new estimate of α, which in turn is used to provide new estimates for R_N, I, G, and H. This iterative scheme converges to several significant figures within four or five iterations (12).

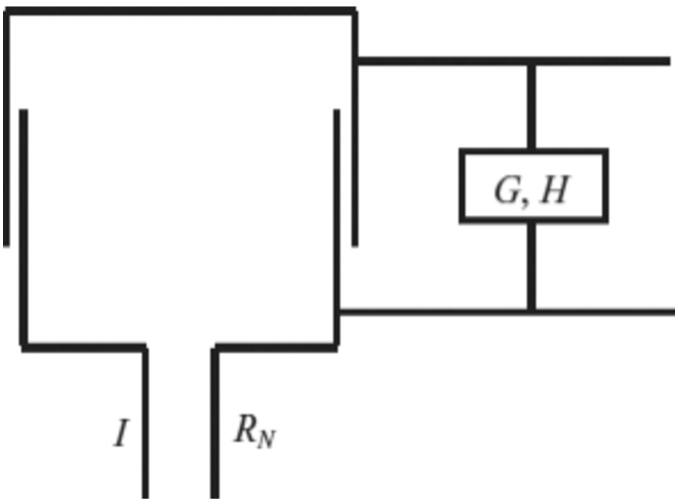

Figure 5: Constant-phase model of the lung. R_N is a Newtonian flow resistance, I is gas inertance, and G and H are parameters that describe constant-phase tissue impedance. From Bates, *Lung Mechanics*, Figure 10.2 (12).

Interpreting the parameters of the constant-phase model is perhaps more difficult than with the other models discussed: while R_N and I reflect airway diameter, G, and H are more difficult to pin down, given that it is sometimes unclear how to relate them to a concrete physiological reality. According to Bates (12), there are two possible interpretations that may be invoked, depending on context: either that changes in G and H represent changes in the intrinsic

rheological properties of the lung, or that they represent indices of alveolar collapse or airway closure. Lutchen et al. (27) suggested that the ratio of G/H, defined as hysteresivity by Fredberg and Stamenovic (23), can reflect airway constriction heterogeneity, in that increases in the G/H ratio probably indicate the amount of airway closure, as opposed to an actual increase in lung tissue mechanical resistance.

The constant-phase model allows for the relatively simple compartmentalization of lung mechanics into central airway components (R_N and I), and peripheral tissue components (G and H). However, measuring these parameters accurately requires the application of forced flow oscillations to the airway opening, a technique that is best performed in anaesthetized and paralyzed experimental animals. (To measure them in conscious humans would require voluntary apnea, an uncomfortable, albeit not impossible, measurement strategy for the subject.) For this reason, the constant-phase model has become the equation of choice for investigating the pulmonary mechanics of small and medium-sized animals, e.g. from mouse to primate. Nonetheless, it is not without controversy: due to the difficulty in interpreting changes in the parameters of this model and relating them to pathophysiology, there has been some debate as to the utility of reporting these parameters in physiological studies (28). This author posits that an additional factor that may explain the reluctance of some researchers to use this model is the additional mathematical complexity that it requires in terms of calculation and interpretation.

Conclusions

While investigating the various types of mathematical models of lung function, this author was struck by the diversity of potential applications for these models, as well as the relative abundance of potential models to represent physiological reality. In his limited readings, he has found that parameters that are most often reported in the literature are derived from the single-compartment model or the constant-phase model. From this, he concludes that the choice of model, and the interpretation of modelling data, depends enormously on what is required for

the purposes of the investigation. In sum, each investigator must carefully consider what they need to extract from the model, and choose accordingly. This can only be done by understanding the theoretical and mathematical underpinnings of the models available.

References

1. Carson E, Murray-Smith D. Ch. 1: The conceptual basis of modelling the respiratory system. In: Cramp D, Carson E, editors. *The respiratory system*. Measurement in Medicine Series. **Vol. 2**. Croom Helm; (1988).

2. Whiting B, Kelman AW, Struthers AD. Prediction of response to theophylline in chronic bronchitis. *Br J Clin Pharmacol* (1984) **17**(1):1-8. PubMed PMID: 6691882; PubMed Central PMCID: PMCPMC1463311.

3. Morris P, Tatnall ML, Montgomery FJ. Controlled anaesthesia: a clinical evaluation of an approach using patient characteristics identified during uptake. *Br J Anaesth* (1983) **55**(11):1065-75. PubMed PMID: 6357255.

4. Dickinson CJ. *A computer model of human respiration : ventilation, blood gas transport and exchange, hydrogen ion regulation : for teaching, research and clinical use, "MacPuf"*. Baltimore: University Park Press (1977).

5. Bates J, Suki B. Assessment of peripheral lung mechanics. *Respir Physiol Neurobiol* (2008) **163**(1-3):54-63. doi: 10.1016/j.resp.2008.03.012.

6. Otis A, Fenn W, Rahn H. Mechanics of breathing in man. *J Appl Physiol* (1950) **2**(11):592-607.

7. Bates J, Baconnier P, Milic-Emili J. A theoretical analysis of interrupter technique for measuring respiratory mechanics. *J Appl Physiol* (1988) **64**(5):2204-14.

8. Bates J, Rossi A, Milic-Emili J. Analysis of the behavior of the respiratory system with constant inspiratory flow. *J Appl Physiol* (1985) **58**(6):1840-8.

9. Bates J. Ch. 54: Measurement Techniques in Respiratory Mechanics,. In: Hamid Q, Shannon J, Martin J, editors. *Physiologic Basis of Respiratory Disease*. BC Decker; (2005).

10. Kaufman G, Massoud A, Audusseau S, Banville-Langelier A, Wang Y, Guay J, et al. Intravenous immunoglobulin attenuates airway hyperresponsiveness in a murine model of allergic asthma. *Clin Exp Allergy* (2011) **41**(5):718-28. doi: 10.1111/j.1365-2222.2010.03663.x.

11. Schuessler T, Bates J. A computer-controlled research ventilator for small animals: design and evaluation. *IEEE Trans Biomed Eng* (1995) **42**(9):860-6. doi: 10.1109/10.412653.

12. Bates J. *Lung Mechanics: An Inverse Modeling Approach*. Cambridge, UK;: Cambridge University Press (2009).

13. Otis A, McKerrow C, Bartlett R, Mead J, McIlroy M, Selver-Stone N, et al. Mechanical factors in distribution of pulmonary ventilation. *J Appl Physiol* (1956) **8**(4):427-43.

14. Similowski T, Bates J. Two-compartment modelling of respiratory system mechanics at low frequencies: gas redistribution or tissue rheology? *Eur Respir J* (1991) **4**(3):353-8.

15. Bates J, Ludwig M, Sly P, Brown K, Martin J, Fredberg J. Interrupter resistance elucidated by alveolar pressure measurement in open-chest normal dogs. *J Appl Physiol* (1988) **65**(1):408-14.

16. Ludwig M, Romero P, Sly P, Fredberg J, Bates J. Interpretation of interrupter resistance after histamine-induced constriction in the dog. *J Appl Physiol* (1990) **68**(4):1651-6.

17. Sasaki H, Takishima T, Sasaki T. Influence of lung parenchyma on dynamic bronchial collapsibility of excised dog lungs. *J Appl Physiol* (1977) **42**(5):699-705.

18. Lauzon A, Dechman G, Bates J. On the use of the alveolar capsule technique to study bronchoconstriction. *Respir Physiol* (1995) **99**(1):139-46.

19. Mount L. The ventilation flow-resistance and compliance of rat lungs. *J Physiol* (1955) **127**(1):157-67.

20. Bates J, Brown K, Kochi T. Respiratory mechanics in the normal dog determined by expiratory flow interruption. *J Appl Physiol* (1989) **67**(6):2276-85.

21. Mead J. Contribution of compliance of airways to frequency-dependent behavior of lungs. *J Appl Physiol* (1969) **26**(5):670-3.

22. Bates J, Maksym G, Navajas D, Suki B. Lung tissue rheology and 1/f noise. *Ann Biomed Eng* (1994) **22**(6):674-81.

23. Fredberg J, Stamenovic D. On the imperfect elasticity of lung tissue. *J Appl Physiol* (1989) **67**(6):2408-19.

24. Hantos Z, Daróczy B, Csendes T, Suki B, Nagy S. Modeling of low-frequency pulmonary impedance in dogs. *J Appl Physiol* (1990) **68**(3):849-60.

25. Hildebrandt J. Pressure-volume data of cat lung interpreted by a plastoelastic, linear viscoelastic model. *J Appl Physiol* (1970) **28**(3):365-72.

26. Tomioka S, Bates J, Irvin C. Airway and tissue mechanics in a murine model of asthma: alveolar capsule vs. forced oscillations. *J Appl Physiol* (2002) **93**(1):263-70. doi: 10.1152/japplphysiol.01129.2001.

27. Lutchen K, Hantos Z, Peták F, Adamicza A, Suki B. Airway inhomogeneities contribute to apparent lung tissue mechanics during constriction. *J Appl Physiol* (1996) **80**(5):1841-9.

28. Bates J, Mitzner W. Point:Counterpoint: lung impedance measurements are/are not more useful than simpler measurements of lung function in animal models of pulmonary disease. *J Appl Physiol* (2007) **103**(5):1900-1; discussion 4. doi: 10.1152/japplphysiol.00369.2007.